Nonlinear Response of Dipolar Systems to Superimposed AC and DC Bias Fields

Nijun Wei

Thesis submitted to the University of Dublin

for the degree of Doctor of Philosophy

Department of Electronic and Electrical Engineering

Trinity College Dublin

2016

Declaration

I declare that this thesis has not been submitted as an exercise for a degree at this or any other university and it is entirely my own work.

I agree to deposit this thesis in the University's open access institutional repository or allow the library to do so on my behalf, subject to Irish Copyright Legislation and Trinity College Library conditions of use and acknowledgement.

List of Publications:

[1] W.T. Coffey, Y.P. Kalmykov, and N. Wei, Nonlinear normal and anomalous response of non-interacting electric and magnetic dipoles subjected to strong AC and DC bias fields, *Nonlinear Dyn.* **80**, 1861-1867 (2015).

[2] N. Wei, P.-M. Déjardin, Y.P. Kalmykov, and W.T. Coffey, External dc bias-field effects in the nonlinear ac stationary response of dipolar particles in a mean-field potential, *Phys. Rev. E*. **93**, 042208 (2016).

[3] N. Wei, D. Byrne, W.T. Coffey, Y.P. Kalmykov, and S.V. Titov, Nonlinear frequency-dependent effects in the dc magnetization of uniaxial magnetic nanoparticles in superimposed strong alternating current and direct current fields, *J. Appl. Phys*. **116**, 173903 (2014).

Signed:

Date:

Acknowledgement

I would like to thank my supervisors Professor William T. Coffey and Professor Yuri Kalmykov for their professional guidance in my research work. I am grateful to P. M. Déjardin for his hospitality and his patient explanations. I wish to thank Declan Byrne and William Dowling for helpful suggestions on my thesis writing. I would also like to thank Teresa, Paul, Cormac and other colleagues in the Department of Electronic and Electrical Engineering for those chats we had when I felt upset, and especially my old friends, Qian, Lei and Nanxi for their company and encouragements. I want to thank my family for supporting me through all the years of education. Finally, I thank Ambassade de France en Irlande for research visits to Perpignan and the Irish Government and Trinity College Dublin for funding this work.

Abstract

The main purpose of this thesis is to study the nonlinear ac stationary response of dipolar systems to superimposed ac and dc bias fields via the rotational Brownian motion model. In this way we investigate (i) the nonlinear dielectric and Kerr effect ac stationary responses of noninteracting permanent electric dipoles and the analogous nonlinear magnetic relaxation of noninteracting magnetic dipoles in ferrofluids, (ii) the nonlinear dielectric and dynamic Kerr effect of a system of permanent dipoles in a uniaxial mean field potential, and (iii) the frequency-dependent dc component of the magnetization of noninteracting magnetic nanoparticles possessing simple uniaxial anisotropy. A new effective matrix method of calculation of the nonlinear ac stationary responses of dipolar systems for arbitrary dc field strength via perturbation theory in the ac field is developed for a uniaxial mean field potential. Furthermore, accurate analytic equations for nonlinear dynamic susceptibilities, allowing one to qualitatively understand the main features of the nonlinear ac stationary response of dipolar systems, are also derived using the two-mode approximation. Two distinct dispersion regions appear in the dc components of the polarization and birefringence of electric dipoles and the dc component of the magnetization for magnetic dipoles at low- and mid-frequencies, corresponding to slow overbarrier and fast intrawell relaxation modes, respectively. Such frequency-dependent behaviour allows one to estimate the longest relaxation time via the half-width of the low-frequency spectra of the dynamic susceptibility. In the nonaxially symmetric case, a third high-frequency resonant dispersion in the dc component of the magnetization appears, accompanied by parametric resonance behaviour due to excitation of transverse resonance modes with characteristic frequencies close to the precession frequency. It is also shown how the results obtained can be generalized to anomalous relaxation via the fractional rotational diffusion equation. Possible experimental verifications of theoretical predictions in polar dielectrics and ferrofluids, are discussed.

Contents

List of Symbols

$\mathbf{A}$	Time-independent five-diagonal system matrix, cf. Eq. (4.17).
$A(\delta)$	Depopulation factor, cf. Eq. (5.28).
a	Diameter of a particle.
a_n, c_n, d_n, g_n	Coefficients of five-term differential-recurrence relation (2.37).
α	Dimensionless damping constant, $\alpha = \eta\gamma M_S$.
$\mathbf{B}$	Two-diagonal matrix, cf. Eq. (4.17).
β	Inverse thermal energy $\beta = (kT)^{-1}$ for electric dipoles, or inverse thermal energy density $\beta = v/(kT)$ for magnetic dipoles.
$\mathbf{C}_n(\omega)$	Column vector of $F_{-k}^{n}(\omega)$ in Eq. (2.44) or of $\mathbf{c}_n^k(\omega)$ in Eq. (2.90).
$C_{a,\alpha,b,\beta}^{c,r}$	Clebsch-Gordan coefficients.
$\mathbf{c}_n(t)$	Column vectors of $\langle Y_{l,m}(\vartheta,\varphi)\rangle(t)$, cf. Eq. (2.82).
$\mathbf{c}_n^k(\omega)$	Column vectors of $c_{n,m}^k(\omega)$, cf. Eq. (2.86).
$c_{n,m}^k(\omega)$	Coefficients of $Y_{n,m}(t)$ expanded as a Fourier series in time, cf. Eq. (2.85).
$\mathbf{c}^{(m)}(t)$	Column vectors of $f_n^{(m)}$ in Eq. (4.16).
c_k^n	Coefficients of $\Phi_{n1}(t)$ expressed in an infinity of relaxation modes, cf. Eq. (4.31).
$\chi_{nk}(\omega)$	Complex susceptibilities.
$\chi_{HN}(\omega)$	Havriliak-Negami complex susceptibility.
$\chi_{CC}(\omega)$	Cole-Cole complex susceptibility.

$\chi_{CC}(\omega)$	Cole- Davidson complex susceptibility.
$\chi_D(\omega)$	Debye complex susceptibility.
$\chi_0(\xi,\xi_0,\omega)$	DC magnetization of ferrofluid.
χ_{nk}, $\chi_{nk}(0)$, χ_S	Static susceptibilities, see Section 2.7.
D_R, k'	Proportionality constant, cf. Eqs. (2.12) and (2.56).
${}_{-\infty}D_t^{\alpha}$	Riemann-Liouville fractional derivative, cf. Eq. (2.135).
$d\Omega$	Solid angle on the unit sphere, $d\Omega = \sin\vartheta d\vartheta d\varphi$.
Δ_{nk}, τ_W^{nk}	Parameters of the two-mode approximation, cf. Eqs. (2.125) and (2.126).
$\delta_{n,m}$	Kronecker's delta, equal to 1 if m=n and to 0 otherwise.
$\mathbf{E}(t)$	External electric field.
$E_{\alpha}(z)$	Mittag-Leffler function, cf. Eq. (2.136).
$\mathbf{e}_r, \mathbf{e}_{\vartheta}, \mathbf{e}_{\varphi}$	Unit vectors in the direction of r, ϑ, φ increasing, see Fig. 2.1.
$e_{l,m,l',m'}$	Coefficients in the general differential-recurrence relation (2.73).
erfi(z)	Error function of imaginary argument.
$F_{-k}^{n}(\omega)$	Fourier amplitudes of $f_n(t)$ expanded as a Fourier series in time, cf. Eq. (2.40).
$F_{n,k}^{(m)}(\omega)$	Fourier amplitudes of $f_n(t)$ approximated by a Fourier series in time via the perturbation approach, e.g., Eq. (4.36).
$f_n(t)$	Statistical moment for ac stationary response in 2D rotational diffusion model, $f_n(t) = \langle P_n \rangle(t)$.
$f_n^{(m)}$	m order solution of $f_n(t)$, $f_n^{(m)} \propto \xi^m$, e.g., Eq. (4.8).

$f_{n,off}^{(1)}(t)$	Linear step-off solution of $f_n(t)$, cf. Eq. (2.108).
$f_{l,m}(t)$	Time-dependent coefficients of $\Psi(\vartheta,\varphi,t)$ expanded in spherical harmonics, c.f. Eq. (2.60).
$\overline{f_n}(\omega)$	Average of $f_n(t)$ over a period of the ac field, cf. Eq. (4.70).
$G(t)$	Green function (the unit impulse response) , cf. Eq. (2.111).
$\mathbf{H}(t)$	External magnetic field including ac and dc components.
$\mathbf{H}_0$	External dc bias magnetic field.
$\mathbf{H}$	External ac magnetic field vector.
$\mathbf{h}$	Unit vector in the direction of the magnetic field.
h	Dimensionless dc field parameter, $h=\xi_0/(2\sigma)$.
η	Phenomenological damping parameter (viscosity).
$\mathbf{I}$	Identity matrix of infinite dimension.
I	Moment of inertia of the sphere.
$\mathbf{J}$	Probability current, $\mathbf{J}=\mathbf{J}_d+\mathbf{J}_{diff}$.
$\mathbf{J}_d$	Drift current density, $\mathbf{J}_d=W\dot{\mathbf{u}}$.
$\mathbf{J}_{diff}$	Diffusion probability current, $\mathbf{J}_{diff}=-k'\partial_{\mathbf{u}}W$.
J_ϑ, J_φ	Components of $\mathbf{J}$ in the coordinate system of $\mathbf{e}_r, \mathbf{e}_\vartheta, \mathbf{e}_\varphi$.
$K(t)$	Kerr effect response, cf. Eq. (3.11).
K	Anisotropy constant.
k	Boltzmann constant.
L_{FP}	Fokker-Planck operator, cf. Eq. (2.57).
$\hat{L}_Z, \hat{L}_\pm, \hat{L}^2$	Angular momentum operators.

$\boldsymbol{\lambda}(t)$	White noise driving torque, cf. Eq. (2.3).
λ_k	Eigenvalues of L_{FP} (λ_1 is the smallest non-vanishing one).
λ	Ratio of ac and dc field strength, $\lambda = E / E_0$.
$\mathbf{M}$, $\mathbf{M}(t)$	Magnetic dipole moment (function), ~10^4–10^5 μ_B.
M_S	Saturation magnetization.
M_0	Equilibrium solution for $M_\xi(\omega)$, cf. Eq. (5.12).
$\overline{M_\xi}$	DC magnetization for assemblies, cf. Eq. (5.30).
$M_\xi(\omega)$	DC component of the magnetization $m(t)$, cf. Eq. (5.11).
$M_H(t)$	Magnetization of ferrofluid, cf. Eq. (3.32).
$m(t)$	Stationary solution for the magnetization, cf. Eq. (5.4).
$m_1^k(\omega)$	Fourier amplitudes of $m(t)$ expanded as a Fourier series in time, cf. Eq. (5.9).
N_0	Number of particles per unit volume.
$\boldsymbol{\mu}$, $\boldsymbol{\mu}(t)$	Electric dipole moment (function), $\sim 0-11\,D$.
μ_0	Permeability of free space, $\mu_0 = 4\pi\cdot 10^{-7}\,\mathrm{JA^{-2}m^{-1}}$
$\mathbf{O}$	Zero matrix of infinite dimension.
$P(t)$	Electric polarization response, cf. Eq. (3.10).
$P_n(\cos\vartheta)$	Legendre polynomial.
$\langle P_n\rangle(t), \langle P_n(\cos\vartheta)\rangle(t)$	Expectation value of $P_n(\cos\vartheta)$, cf. Eq. (2.34).
$\boldsymbol{\Phi}_2^{(2)}(\omega)$, $\boldsymbol{\Phi}_1^{(3)}(\omega)$	Matrices used in Eqs. (4.19) - (4.21).
$\Phi_{km}(t)$	Normalized equilibrium correlation functions, cf. Eq. (2.109).

$\boldsymbol{\varphi}_1^{(1)}(\omega)$, $\boldsymbol{\varphi}_0^{(2)}(\omega)$	Column vectors of Eqs. (4.19) - (4.21).
Ψ	Wave function in quantum mechanics.
ψ	Angle between the external field and easy axis, see Fig. 5.1.
$\mathbf{Q}_n^{\pm}, \mathbf{Q}_n$	Matrices of statistical moments in three-term matrix recurrence relation, e.g., Eq. (2.44)
$\mathbf{q}_n$, $\mathbf{q}_n^{\pm}$, $\mathbf{p}_n$, $\mathbf{p}_n^{\pm}$	Supermatrix coefficients of the differential-recurrence relation (2.81).
r, ϑ, φ	Radial, polar and azimuthal angle coordinates of the spherical polar coordinate system (Fig. 2.1).
Γ_i^{IHD}	Kramers escape rates in the intermediate-to-high damping (IHD) limit.
γ	Gyromagnetic ratio.
$\gamma_1, \gamma_2, \gamma_3$	Direction cosines of $\mathbf{h}$.
$\mathbf{S}_n(\omega)$	Function rendering $\mathbf{C}_n(\omega)$ in terms of the next lowest order one, $\mathbf{C}_n(\omega) = \mathbf{S}_n(\omega)\mathbf{Q}_n^{-}(\omega)\mathbf{C}_{n-1}(\omega)$.
S_i	Action calculated at the saddle point of the *i*th well.
σ	Dimensionless inverse temperature parameter, $\sigma = \beta K$.
ς	Viscous drag coefficient.
T	Absolute temperature.
τ_D	Debye relaxation (free diffusion) time, $\tau_D = \varsigma / (2kT)$.
τ_N	Free diffusion time of the magnetization, $\sim 10^{-11} - 10^{-8}$ s.
τ_{ND}	Free diffusion time of ferrofluid.
τ_n^{eff}	Effective relaxation time, cf. Eq. (2.117).
τ_n	Integral relaxation time, cf. Eq. (2.116).
Θ	Angle between the vectors $\mathbf{M}$ and $\mathbf{H}$.

$\mathbf{u}$	Unit vector along the dipole moment.
u_X, u_Y, u_Z	Direction cosines of $\mathbf{u}$.
V	Potential energy of electric dipole, or free energy density of magnetic dipole.
V_-, V_+	Half sided sums of V, Eq. (2.71).
V_t	Time-dependent potential.
ΔV	Potential barrier, $\beta\Delta V = \sigma(1-\xi_0/2\sigma)^2$.
$v_{r,s}$	Coefficients of the Fourier series expansion of V, cf. Eq. (2.74).
$W_0(\vartheta,\varphi)$	Equilibrium Boltzmann distribution.
$W(\vartheta,\varphi,t)$	Distribution function of 3D rotational diffusion.
$W(\vartheta,t)$	Distribution function of 2D rotational diffusion.
$\boldsymbol{\omega}(t)$	Angular velocity.
ω_1, ω_2	Characteristic frequencies of relaxation modes, cf. Eq. (5.26).
ω_{pr}	Precessional frequency.
$\omega_{\max}$	Frequency of the low-frequency peak in the spectra of the imaginary part of the susceptibility, see, for example, Fig. 4.2.
$\Delta\omega$	Half-width of the spectra of the real part of the susceptibility, see Fig. 4.2.
$\mathbf{X}_{2n}$, $\mathbf{X}^t_{2n}$ etc.	Matrix elements of $\mathbf{q}_n$, $\mathbf{q}^{\pm}_n$, $\mathbf{p}_n$, $\mathbf{p}^{\pm}_n$, cf. Eq. (2.83).
$X_{nk}(\omega)$	Normalized complex susceptibilities, $X_{nk}(\omega) = \chi_{nk}(\omega)/\chi_{nk}$.
$x_{l,m}$, $y_{l,m}$, etc	Static coefficients in the differential-recurrence relation (2.80).
$x^t_{l,m}$, $y^t_{l,m}$, etc	Dynamic coefficients in the differential-recurrence relation (2.80).

$\xi(t)$	Dimensionless external field parameter.
ξ_0	Dimensionless strength of the external dc electric field $\xi_0 = \mu E_0 / (kT)$ or magnetic field $\xi_0 = \nu \mu_0 M_S H_0 / (kT)$.
ξ	Dimensionless strength of the external ac electric field $\xi_0 = \mu E / (kT)$ or magnetic field $\xi = \nu \mu_0 M_S H / (kT)$.
ξ_1	Small dimensionless probing applied field strength.
$\mathbf{Y}$, $\mathbf{Z}_n$	Submatrices of $\mathbf{Q}_n^{\pm}, \mathbf{Q}_n$, cf. Eq. (2.46).
$Y_{l,m}(\vartheta,\varphi)$	Spherical harmonics.
$Y_{n,m}(t)$, $\langle Y_{l,m} \rangle(t)$, $\langle Y_{l,m}(\vartheta,\varphi) \rangle(t)$	Statistical moment, i.e., expectation value of $Y_{l,m}(\vartheta,\varphi)$, cf. Eq. (2.67).
Z	Partition function, cf. Eq. (2.101).
Δ	Laplacian on the surface of the unit sphere, cf. Eq. (2.18).
∇	Gradient on the surface of the unit sphere, cf. Eq. (2.17).
$\nabla \cdot$	Divergence on the surface of the unit sphere, cf. Eq. (2.13).
$\langle \ \rangle_0$	Equilibrium ensemble spatial average, cf. Eq. (2.34).

1 Introduction

When studying the nonlinear effects of polar dielectrics subjected to an ac driving force, one of the most interesting cases is where a strong ac force and a strong dc bias force are applied simultaneously. If we compare this situation to a system [1-3] where (a) a strong ac force is applied alone or (b) a strong dc bias force is applied alongside a weak ac force, we can observe new effects due to the entanglement of the nonlinear ac and dc responses. Many of these new effects are of particular interest as they depend on the frequency of the driving ac field. In this thesis I considered these nonlinear effects on the ac stationary response in three systems: (i) noninteracting electric/magnetic dipoles; (ii) permanent electric dipoles in the mean field potential; and (iii) magnetic nanoparticles. The approach developed is then generalized to treat anomalous relaxation for disordered materials and complex liquids.

In a dipolar system consisting of an assembly of electrically noninteracting particles with permanent electric moment $\boldsymbol{\mu}$ in a time-varying external electric field $\mathbf{E}(t)$, the torque due to the external field tends to align the particles in the direction of the applied field, thus causing the system to become polarized. The polarization $\mathbf{P}(t)$ in dielectrics is usually delayed with respect to the time-varying electric field, resulting in dielectric relaxation which is measured relative to the mean dipole moment in the direction of the electric field [1],

$$P_E(t) \sim \langle \boldsymbol{\mu} \cdot \mathbf{E} \rangle(t) / E = \mu \langle \cos \vartheta \rangle(t), \tag{1.1}$$

i.e., the expectation value $\langle P_1(\cos\vartheta)\rangle(t)$ of the first Legendre polynomial $P_1(\cos\vartheta)$ (ϑ being the polar angle of the electric dipole moment vector $\boldsymbol{\mu}$ of the molecule). Dielectric relaxation of electric dipoles in a time-varying electric field is analogous to magnetic relaxation of magnetic dipoles $\mathbf{M}$ in a time-varying magnetic field $\mathbf{H}(t)$, where the mean moment is then in the direction of the magnetic field of $\langle \mathbf{M} \cdot \mathbf{H} \rangle(t) / H = M_S \langle \cos \vartheta \rangle(t)$ [4], i.e., also $\sim \langle P_1(\cos\vartheta)\rangle(t)$. Furthermore, when a dipolar system comprised of polar and anisotropically polarizable particles is acted on by an external electric field **E**, it becomes birefringent, acquiring the same properties as a uniaxial crystal. The

birefringence can be described by the electric birefringence function $K(t)$ which is defined using the expectation value of the second Legendre polynomial $\langle P_2(\cos\vartheta)\rangle(t)$ as [1]

$$K(t) \sim E^2\left(\alpha_{\parallel}^0 - \alpha_{\perp}^0\right)\langle P_2(\cos\vartheta)\rangle(t) \tag{1.2}$$

where $\alpha_{\parallel}^0$ and $\alpha_{\perp}^0$ are the components of the optical polarizability due to the electric field (optical frequency) of the light beam passing through the liquid medium. This electro-optical (Kerr) effect is a purely nonlinear phenomenon. Related nonlinear phenomena include nonlinear dielectric relaxation of polar liquids and nematic liquid crystals and nonlinear magnetic relaxation of ferrofluids (colloidal suspension of magnetic nanoparticles). The theories describing all these nonlinear phenomena, regardless of the physical system being considered, usually have been based on very similar mathematical approaches (Langevin equation [1] and/or Fokker-Planck equation [5]) involving the rotational Brownian motion of a rigid body in an external potential.

The starting point for analysing nonlinear dielectric relaxation and Kerr effect phenomena in dipolar systems is usually either the Langevin equation or the corresponding Fokker-Planck equation for the noninertial rotational diffusion model in the mean field potential when inertial effect are neglected. The Fokker-Planck equation (also called the Smoluchowski equation), directly derived from the Langevin equation, describes the time evolution of the orientational distribution function of a particle on a unit sphere. Here, we shall use the Fokker-Planck equation approach (see Chapter 2 for details). The Fokker-Planck equation for the probability distribution function $W(\vartheta,\varphi,t)$ of orientations of Brownian particles can be written down in a general form as [1]

$$\begin{aligned}\frac{\partial W}{\partial t} = {} & D\left[\frac{1}{\sin\vartheta}\frac{\partial}{\partial\vartheta}\left(\sin\vartheta\frac{\partial W}{\partial\vartheta}\right)+\frac{1}{\sin^2\vartheta}\frac{\partial^2 W}{\partial\varphi^2}\right] \\ & +\frac{D}{kT}\left[\frac{1}{\sin\vartheta}\frac{\partial}{\partial\vartheta}\left(\sin\vartheta W\frac{\partial V}{\partial\vartheta}\right)+\frac{1}{\sin^2\vartheta}\frac{\partial}{\partial\varphi}\left(W\frac{\partial V}{\partial\varphi}\right)\right],\end{aligned} \tag{1.3}$$

where ϑ and φ are the polar and azimuthal angles in Fig. 2.1, respectively, V is the mean field potential, D is the rotational diffusion coefficient, k is the Boltzmann constant, and T is the absolute temperature. Equation (1.3) can then be used to calculate the response of noninteracting electric or magnetic dipoles if V in Eq. (1.3) only considers the potential due to an external field $\mathbf{E}(t)$, for example,

$$V(\vartheta,t) = -\mu E(t)\sin\vartheta . \tag{1.4}$$

Equation (1.3) can also be used to evaluate the dielectric response of permanent electric dipoles in the mean field potential if V is composed of a mean-field potential part and a field dependent part, for example,

$$V(\vartheta,t) = -K\cos^2\vartheta - \mu E(t)\sin\vartheta . \tag{1.5}$$

Now, the theory of dielectric relaxation of polar fluids bears a close resemblance to the theory of magnetic relaxation of single domain ferromagnetic particles as formulated by Brown [6]. Fine single domain ferromagnetic particles possessing internal magnetocrystalline anisotropy potential, which, by their very nature, have several equilibrium states with potential barriers between them, exhibit *unstable magnetization behaviour* due to thermal agitation, causing superparamagnetism and magnetic viscosity. When the barrier energy is comparable to the thermal energy, a change in field will lead to a change in magnetization due to the large magnetic dipole moment (lagging, however, behind the field change) analogous to the solid state-like (Arrhenius) Debye relaxation process in polar dielectric solids over a potential barrier. Brown's major contribution to this theory was the derivation of the Fokker-Planck equation for the distribution function of the particle magnetic moment orientations on the unit sphere:

$$\begin{aligned}\frac{\partial W}{\partial t} = \frac{1}{2\tau_{\mathrm{N}}\sin\vartheta}\Bigg\{&\left[\frac{\partial}{\partial\vartheta}\left(\sin\vartheta\frac{\partial W}{\partial\vartheta}\right)+\frac{1}{\sin\vartheta}\frac{\partial^2 W}{\partial\varphi^2}\right]\\ &-\frac{v}{\alpha kT}\left[\frac{\partial}{\partial\vartheta}\left(W\frac{\partial V}{\partial\varphi}\right)-\frac{\partial}{\partial\varphi}\left(W\frac{\partial V}{\partial\vartheta}\right)\right]\\ &+\frac{v}{kT}\frac{\partial}{\partial\vartheta}\left[\sin\vartheta W\frac{\partial V}{\partial\vartheta}+\frac{1}{\sin\vartheta}\frac{\partial}{\partial\varphi}\left(W\frac{\partial V}{\partial\varphi}\right)\right]\Bigg\},\end{aligned} \tag{1.6}$$

where V is now the particle free energy per unit volume, τ_N is the free diffusion relaxation time, $\beta = v/(kT)$, v is the volume of the particle, and α is the damping coefficient. When $\alpha\to\infty$ with $\tau_{\mathrm{N}} = \mathrm{const}$, i.e., ignoring the gyromagnetic term, Brown's Fokker–Planck equation (1.6) has the same mathematical form as the *noninertial* rotational diffusion equation, Eq. (1.3).

To treat the longitudinal relaxation in axially symmetric potentials $V(\vartheta,t)$ where the azimuthal angle dependence may be ignored (see, e.g., Eq.(2.19) below), both Eqs. (1.3) and (1.6) can be written as a single-variable rotational diffusion equation. Then, their

solutions may be expanded as a series of Legendre polynomials $P_n(\cos\vartheta)$ (see Eq. (2.23) below). In the general case where the azimuthal angle φ must also be considered, solutions of Eqs. (1.3) and (1.6) may be presented as a series of spherical harmonics, $Y_{n,m}(\vartheta,\varphi)$ (see e.g., Eqs. (2.59) and (2.60) below). After substituting the general solutions into the diffusion equations, Eqs. (1.3) and (1.6), the problem is reduced to the solution of an infinite hierarchy of differential-recurrence relations of the expectation values of the Legendre polynomials $\langle P_n(\cos\vartheta)\rangle(t)$ (or spherical harmonics $\langle Y_{n,m}(\vartheta,\varphi)\rangle(t)$), which can be solved by using the matrix continued fraction method (see Chapter 2 for details). As we have seen above, the physical quantities of interests describing the ac stationary response of dielectric and Kerr effect relaxation are the electric polarization function, $\sim\langle P_1(\cos\vartheta)\rangle(t)$, and the electric birefringence function, $\sim\langle P_2(\cos\vartheta)\rangle(t)$, respectively.

To review the previous treatments of the nonlinear dielectric and magnetic relaxation in dipolar systems, we start with Debye's theory of dielectric relaxation of polar molecules using two distinct models of the phenomenon [7]. In the first of the two models, the rotation of a polar molecule in a liquid composed of noninteracting polar molecules is treated as a type of Brownian motion [7] (e.g., Eq. (1.4)). This theory can be used to predict the dispersion and absorption of microwave (GHz) radiation by polar fluids and is the principle underlying the microwave oven as the dipoles cannot keep in phase with the fast field. The phase lag results in heating as energy is interchanged with the bath. Put more precisely, the energy of the dipoles is dissipated via friction due to the bath, which may be regarded as a collection of harmonic oscillators. Debye also considered a second *solid state-like* mechanism of relaxation which mainly pertains to relaxation in solids, whereby a dipole can stay either of two directions (i.e., parallel or antiparallel to the applied field) and reverse its direction by crossing over a potential barrier due to thermal agitation which is modelled by Brownian motion (e.g., Eq. (1.5)). The relaxation time (the time to cross the barrier from one orientation to the other) is an Arrhenius process and is thus exponentially long [8]. This discrete orientation model was used much later by Néel in order to calculate the relaxation time of the magnetization of fine single-domain ferromagnetic particles [9]. His calculation is a famous generalization of the Debye theory to treat the overbarrier relaxation process via the rotational Brownian motion of a rodlike particle in an external mean field uniaxial potential, commonly called the Maier-Saupe potential (cf. Eq. (1.5)).

Now, in this liquid state-like Debye model (cf. Eq. (1.4)), when the stimulus due to the field is much smaller than the thermal energy, the linear ac response term is sufficient to determine the relaxation process, as demonstrated by Debye [7]. Much later, the Debye calculation was extended by Coffey and Paranjape [2] to include terms cubic in the applied field via perturbation theory. In all cases of nonlinear response, no unique response function exists as it always depends on the precise form of the stimulus, unlike the linear response. They studied the response to (i) a strong ac field and (ii) a *weak* ac field combined with a *strong* dc bias field. The results of the first case have been compared with nonlinear response measurements by De Smet *et al*. [10] and Jadżyn *et al*. [11] and agree with these experiments. Additionally, the perturbation calculation for the strong ac field was verified by Déjardin and Kalmykov [12] by solving the differential-recurrence relation generated by the rotational Smoluchowski equation [1] using matrix continued fractions in the frequency domain (see Section 2.3). They also used this method to consider the strong ac and dc fields case [13]. In the case (ii) of a weak ac field combined with a strong dc bias field, the ac field was supposed so weak that terms in its square and higher are omitted. Subsequently, Déjardin *et al*. [14] extended this perturbation calculation to include the nonlinear ac terms. Similar results may pertain to the magnetization response under the influence of strong ac and dc bias fields of a *blocked* ferrofluid composed of a colloidal suspension of single domain ferromagnetic particles. Here, the solid state-like or Néel [4] magnetization relaxation (cf. the second Debye model) mechanism over the internal magnetocrystalline anisotropy-Zeeman energy barriers inside the particle due to magnetic Brownian motion is *frozen* so that only the liquid state-like Brownian mechanical motion remains. We remark that the nonlinear relaxation effect is easier to observe experimentally in the ferrofluid because of the large magnetic moment, $10^4 \sim 10^5 \mu_B$, of single domain particles compared to that of polar molecules. This behaviour was experimentally detected by Fannin *et al*. [15] for a strong ac magnetic field.

The perturbation method for calculating the nonlinear response of noninteracting dipoles (e.g., Eq. (1.4)) described above was then generalized by Coffey *et al.* [3] to include a mean field potential (e.g., Eq. (1.5)). This paper, which considered the response to an ac field alone, gave analytic formulas for the nonlinear dielectric and Kerr effect relaxation based on an existing two mode approximation for linear response in the presence of a mean field potential $\sigma \sin^2 \vartheta$ (σ is the anisotropy parameter), whereby the linear response, consisting of a series of infinite relaxation modes, can be approximated

by two modes only [1]. These are the *slow* over-barrier relaxation (interwell) mode and a set of *fast* near-degenerate "intrawell" modes, represented as a single high frequency mode. In the combined field case, however, it is difficult to get closed form results due to the vector-valued coupling between each member of the hierarchy of differential-recurrence relations. Since the calculation of the dielectric response of polar molecules in a mean-field potential is analogous to the problem of magnetic relaxation of single domain ferromagnetic particles from a mathematical point of view, this approach will also be extended to the superimposed external dc bias and ac fields case for fine single domain magnetic nanoparticles with uniaxial anisotropy.

As mentioned above, the solution of the Fokker-Planck equation can be reduced to that of an infinite hierarchy of differential-recurrence equations for the statistical moments $\left\langle P_n\left(\cos\vartheta\right)\right\rangle(t)$ or $\left\langle Y_{n,m}\left(\vartheta,\varphi\right)\right\rangle(t)$. Generally, these differential-recurrence relations comprise three or more terms. The three-term differential-recurrence equation can be solved in terms of ordinary infinite continued fractions [5], while recurrence relations with more than three terms should be solved by the matrix continued fraction method by converting the equations to a three-term matrix recurrence relation [1]. Here, the scalar continued fraction method is just a special case of the matrix one. Efficient numerical algorithms for the calculation of the nonlinear ac stationary response of the magnetization of *uniaxial* magnetic nanoparticles have been proposed in Refs. [16-18] by assuming that the dc bias and ac driving fields *are directed along the easy axis* of the particle, so that the matrix continued fraction methods for *axially symmetric* potentials as discussed above may be applied. However, in this configuration many interesting nonlinear effects are suppressed because no dynamical coupling between the longitudinal and transverse precessional modes of motion exists. These mode coupling effects in the *nonlinear* ac stationary response can only be modelled for uniaxial particles driven by a strong ac field applied at *an angle* to the easy axis of the particle so that the axial symmetry is broken by the Zeeman energy [19-22]. Now, building on the axially symmetric solutions described in Refs. [16-18], an exact nonperturbative method for the determination of the nonlinear magnetization of magnetic nanoparticles with an *arbitrary* anisotropy potential and subjected to a strong ac driving field superimposed on a strong dc bias field has recently been given by Titov *et al*. [23]. The method is rooted in posing the solution of the averaged magnetic Langevin equation for the statistical moments (which are now the expectation values of the spherical harmonics) in terms of matrix continued fractions in

the frequency domain (see also Section 2.6). So far this method has been used to determine the dynamic susceptibilities (linear, cubic, etc.) and dynamic hysteresis loops in uniaxial magnetic nanoparticles in Refs. [21, 23].

Many disordered materials such as glass-forming liquids and polymers have very significant departures from the Debye behaviour resulting in anomalous relaxation [1, 24]. The relaxation processes in such complex systems are characterized by the temporally nonlocal behaviour arising from the energetic disorder, which produces obstacles or traps, simultaneously delaying the motion of the particle and producing memory effects [25]. Thus it is also useful to generalize the nonlinear normal relaxation results to anomalous relaxation via the fractional Fokker-Planck equation [1, 26].

1.1 Layout of the Thesis

This thesis is organized as follows:

In Chapter 2, the general theory of the dielectric and magnetic relaxation is presented. The derivations of the noninertial Fokker-Planck equation for the rotational Brownian motion of dipoles are reviewed first. Then, the differential-recurrence relations for the statistical moments, $\left\langle P_n\left(\cos\vartheta\right)\right\rangle(t)$ or $\left\langle Y_{n,m}\left(\cos\vartheta\right)\right\rangle(t)$, are derived for both the electric and magnetic cases. The general solutions in the frequency domain of these differential-recurrence relations are given via the matrix continued fraction method. These continued fraction solutions can be used for comparisons with our analytic approximate results for various models considered in the thesis. In addition, the two-mode approximation and methods of treating anomalous relaxation in dipolar systems are also discussed.

In Chapter 3, the perturbation method is used to calculate the nonlinear ac stationary response of noninteracting electric and magnetic dipoles for the particular case of a strong dc bias field superimposed on a strong ac field with a view towards encouraging the experimental detection of the frequency-dependent dc term, as well as the nonlinear effects due to the interaction of the two fields at the fundamental and second harmonic frequencies and the term with the fundamental frequency which also appears in the cubic response. In particular, we shall highlight the frequency dependence of the dc term and show the calculation of the dynamic Kerr-effect response as well. We shall also show how the calculation may be extended to anomalous relaxation governed by a fractional Fokker-Planck equation. This material has been published in Ref. [27].

In Chapter 4, the nonlinear dielectric and Kerr-effect relaxation of permanent electric dipoles, interacting via a mean field potential under the influence of ac and dc bias fields, are investigated by two complementary approaches. The first is based on perturbation theory, allowing one to calculate numerically the nonlinear ac stationary responses using powerful matrix methods, while the second semi-analytic approach, based on the two-mode approximation [1], effectively generalizes the existing analytic results for dipolar systems in superimposed ac and dc fields to a mean field potential. The results of this chapter has been published in Ref. [28].

In Chapter 5, Brown's continuous diffusion model [6, 29] is applied to investigate the dc magnetization of uniaxial magnetic nanoparticles in superimposed strong ac and dc fields. Both cases of an ensemble of fully aligned noninteracting particles and particles with randomly oriented easy axes are studied using a nonperturbative approach. Here, we focus for the first time on nonlinear frequency-dependent effects in the dc component of the magnetization, which were overlooked in previous studies. In the presence of a strong ac driving field, the dc component of the magnetization of uniaxial particles alters drastically leading to new nonlinear effects; in particular, it becomes frequency-dependent. This material was published in Ref. [30].

2 Diffusion Model of Orientational Relaxation in Dipolar Systems

In order to study the nonlinear response of dipolar systems in superimposed ac and dc bias fields, we start by describing how to setup the rotational diffusion model for the electric and magnetic dipoles where the derivations of the Fokker-Planck equations will be summarised. Then, the Fokker-Planck equation will be postulated in terms of infinite hierarchies of differential-recurrence equations for the statistical moments of different systems which will be solved numerically using the matrix continued fraction method. Moreover, the basic approximation approaches to yield the analytical formula of nonlinear responses will be introduced, as well as the equations for the generalization of the results to the anomalous relaxation.

2.1 Smoluchowski Equation for Electric Dipoles

The Debye theory [7] of dielectric relaxation commences with a special form of the Fokker-Planck equation for rotational Brownian motion in the space of a sphere when inertial effects are neglected, which is also called the rotational Smoluchowski equation. A detailed derivation of this equation is given by Debye [7]. However, we shall follow the derivation given in Section 1.15 of Ref. [1], which is based on the vector Euler-Langevin equation of Lewis *et al.* [31].

To study the rotational Brownian movement of a spherical body, one first assumes that the homogeneous sphere contains a rigid electric dipole $\boldsymbol{\mu}$ [1]. Then the rate of change of $\boldsymbol{\mu}(t)$ is given by the kinematic relation

$$\dot{\boldsymbol{\mu}}(t) = \boldsymbol{\omega}(t) \times \boldsymbol{\mu}(t), \tag{2.1}$$

where $\boldsymbol{\omega}(t)$ is the angular velocity of the body and obeys the Euler-Langevin equation

$$I\dot{\boldsymbol{\omega}}(t) + \varsigma\boldsymbol{\omega}(t) = \boldsymbol{\mu}(t) \times \mathbf{E}(t) + \boldsymbol{\lambda}(t). \tag{2.2}$$

Here I is the moment of inertia of the sphere, $\varsigma\boldsymbol{\omega}(t)$ is the damping torque due to the friction, $\boldsymbol{\mu}(t) \times \mathbf{E}(t)$ is the torque of the externally applied electic field, and $\boldsymbol{\lambda}(t)$ is the white noise driving torque which has the properties:

$$\overline{\lambda_n(t)} = 0, \quad \overline{\lambda_n(t)\lambda_m(t')} = 2kT\varsigma\delta_{n,m}\delta(t-t'), \tag{2.3}$$

where the indices $n,m = 1,\ 2,\ 3$ in Kronecker's delta, $\delta_{n,m}$, correspond to the Cartesian laboratory coordinate axes *X*, *Y*, *Z*. The angular velocity vector after omitting the inertial ($I \to 0$) term is

$$\boldsymbol{\omega}(t) = \varsigma^{-1}\left[\boldsymbol{\mu}(t)\times\mathbf{E}(t) + \boldsymbol{\lambda}(t)\right]. \tag{2.4}$$

Substituting Eq. (2.4) into the kinematic relation, Eq. (2.1), we obtain the Langevin equation for the motion of $\boldsymbol{\mu}$ in the noninertial limit

$$\dot{\boldsymbol{\mu}}(t) = \varsigma^{-1}\left[\boldsymbol{\mu}(t)\times\mathbf{E}(t) + \boldsymbol{\lambda}(t)\right]\times\boldsymbol{\mu}(t). \tag{2.5}$$

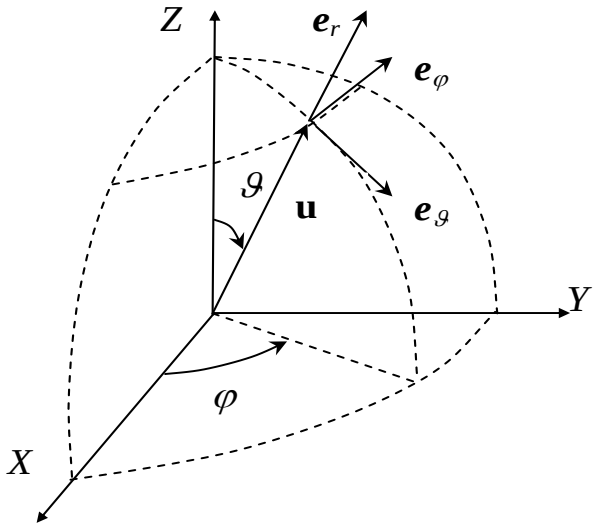

Fig. 2.1. Spherical polar coordinate system.

Now, the distribution of Brownian particles $W(\boldsymbol{\mu},t)$ of orientations $\boldsymbol{\mu}$ under the influence of an external field $\mathbf{E}(t)$ can be calculated via the continuity equation

$$\dot{W} + \mathrm{div}\mathbf{J} = 0, \tag{2.6}$$

where the current density (flux) $\mathbf{J} = \mathbf{J}_d + \mathbf{J}_{diff}$ contains a conservative part $\mathbf{J}_d$ called the drift current density which describes $\mathbf{J}$ in the absence of the thermal agitation (i.e. leaving out the term $\boldsymbol{\lambda}(t)$ in Eq. (2.5))

$$\mathbf{J}_d = W\dot{\mathbf{u}}, \tag{2.7}$$

where $\mathbf{u}$ is a unit vector along the dipole moment $\boldsymbol{\mu}$ described by the polar and azimuthal angles ϑ and φ of the spherical polar coordinate system (Fig. 2.1) so that the direction

cosines of $\mathbf{u}$ are given by $u_X = \sin\vartheta\cos\varphi,\ u_Y = \sin\vartheta\sin\varphi,\ u_Z = \cos\vartheta$. Now, the external field $\mathbf{E}(t) = -\text{grad}V(\boldsymbol{\mu}, t)$ can be written in the form of

$$\mathbf{E}(t) = -\frac{1}{\mu}\left(\frac{\partial V}{\partial u}\mathbf{e}_r + \frac{\partial V}{\partial \vartheta}\mathbf{e}_\vartheta + \frac{1}{\sin\vartheta}\frac{\partial V}{\partial \varphi}\mathbf{e}_\varphi\right), \tag{2.8}$$

where $\mathbf{e}_r$, $\mathbf{e}_\vartheta$ and $\mathbf{e}_\varphi$ are unit vectors in the direction of increasing r, ϑ and φ respectively. The vector products in Eq. (2.5) are then in spherical coordinates,

$$\boldsymbol{\mu}\times\mathbf{E} = \begin{vmatrix} \mathbf{e}_r & \mathbf{e}_\vartheta & \mathbf{e}_\varphi \\ 1 & 0 & 0 \\ -\dfrac{\partial V}{\partial u} & -\dfrac{\partial V}{\partial \vartheta} & -\dfrac{1}{\sin\vartheta}\dfrac{\partial V}{\partial \varphi} \end{vmatrix} = \frac{1}{\sin\vartheta}\frac{\partial V}{\partial \varphi}\mathbf{e}_\vartheta - \frac{\partial V}{\partial \vartheta}\mathbf{e}_\varphi \tag{2.9}$$

and

$$(\boldsymbol{\mu}\times\mathbf{E})\times\boldsymbol{\mu} = \begin{vmatrix} \mathbf{e}_r & \mathbf{e}_\vartheta & \mathbf{e}_\varphi \\ 0 & \dfrac{1}{\sin\vartheta}\dfrac{\partial V}{\partial \varphi} & -\dfrac{\partial V}{\partial \vartheta} \\ \mu & 0 & 0 \end{vmatrix} = -\mu\left(\frac{\partial V}{\partial \vartheta}\mathbf{e}_\vartheta + \frac{1}{\sin\vartheta}\frac{\partial V}{\partial \varphi}\mathbf{e}_\varphi\right), \tag{2.10}$$

so that the drift current density $\mathbf{J}_d$, Eq. (2.7), is

$$\mathbf{J}_d = -\varsigma^{-1}\left(\frac{\partial V}{\partial \vartheta}\mathbf{e}_\vartheta + \frac{1}{\sin\vartheta}\frac{\partial V}{\partial \varphi}\mathbf{e}_\varphi\right)W\,. \tag{2.11}$$

Then the diffusion part $\mathbf{J}_{diff}$ of the the current density, which accounts for the thermal agitation, is given by

$$\mathbf{J}_{diff} = -D_R\frac{\partial W}{\partial \mathbf{u}} = -D_R\left(\frac{\partial}{\partial \vartheta}\mathbf{e}_\vartheta + \frac{1}{\sin\vartheta}\frac{\partial}{\partial \varphi}\mathbf{e}_\varphi\right)W\,, \tag{2.12}$$

where the diffusion parameter D_R can be obtained from the stationary solution of Eq. (2.6) with the Boltzmann distribution $W_0(\vartheta,\varphi) = Z^{-1}e^{-V(\vartheta,\varphi)/(kT)}$, where Z is defined by Eq. (2.101). Hence, by substituting Eqs. (2.11) and (2.12) into the divergence of the total current density $\mathbf{J}$

$$\text{div}\mathbf{J} = \nabla\cdot\mathbf{J} = \frac{1}{\sin\vartheta}\frac{\partial}{\partial \vartheta}(\sin\vartheta J_\vartheta) + \frac{1}{\sin\vartheta}\frac{\partial J_\varphi}{\partial \varphi}\,, \tag{2.13}$$

where

$$J_\vartheta = -\varsigma^{-1}\frac{\partial V}{\partial \vartheta}W - D_R\frac{\partial}{\partial \vartheta},$$
$$J_\varphi = -\varsigma^{-1}\frac{1}{\sin\vartheta}\frac{\partial V}{\partial \varphi}W - D_R\frac{1}{\sin\vartheta}\frac{\partial}{\partial \varphi}W, \tag{2.14}$$

Eq. (2.6) yields the rotational Smoluchowski equation for the orientations of $\boldsymbol{\mu}$ on a unit sphere

$$2\tau_D\frac{\partial W}{\partial t} = \frac{1}{\sin\vartheta}\left\{\left[\frac{\partial}{\partial\vartheta}\left(\sin\vartheta\frac{\partial}{\partial\vartheta}\right)+\frac{1}{\sin\vartheta}\frac{\partial^2}{\partial\varphi^2}\right]W + \frac{1}{kT}\left[\frac{\partial}{\partial\vartheta}\left(\sin\vartheta\frac{\partial V}{\partial\vartheta}\right)W+\frac{\partial}{\partial\varphi}\left(\frac{1}{\sin\vartheta}\frac{\partial V}{\partial\varphi}\right)W\right]\right\}. \tag{2.15}$$

which can be written in a vector form as

$$\frac{\partial W}{\partial t} = (2\tau_D)^{-1}\left[\Delta W + \beta\nabla\cdot\left(W\nabla V\right)\right]. \tag{2.16}$$

Here $\tau_D = \varsigma/(2kT)$ is the Debye relaxation time, $\beta = (kT)^{-1}$ is the inverse thermal energy, k is Boltzmann's constant, T is the absolute temperature, and ∇ and Δ are the gradient and Laplacian on the surface of the unit sphere, respectively,

$$\nabla = \frac{\partial}{\partial\vartheta}\mathbf{e}_\vartheta + \frac{1}{\sin\vartheta}\frac{\partial}{\partial\varphi}\mathbf{e}_\varphi, \tag{2.17}$$

$$\Delta = \nabla^2 = \frac{1}{\sin\vartheta}\frac{\partial}{\partial\vartheta}\left(\sin\vartheta\frac{\partial}{\partial\vartheta}\right)+\frac{1}{\sin^2\vartheta}\frac{\partial^2}{\partial\varphi^2}. \tag{2.18}$$

Debye [7] specialized this equation to the case where an external field $\mathbf{E}$ is applied along the polar axis. Here, due to the axial symmetry, the azimuthal angle dependence may be ignored, so that Eq. (2.15) becomes

$$2\tau_D\frac{\partial W}{\partial t} = \frac{1}{\sin\vartheta}\frac{\partial}{\partial\vartheta}\left[\sin\vartheta\left(\frac{\partial W}{\partial\vartheta}+\beta W\frac{\partial V}{\partial\vartheta}\right)\right]. \tag{2.19}$$

2.2 Five-Term Differential-Recurrence Relations

The rotational diffusion Smoluchowski equation (2.19) for an axially symmetric problem can be rewritten as

$$2\tau_D\frac{\partial W}{\partial t} = \frac{\partial}{\partial x}\left[\left(1-x^2\right)\frac{\partial W}{\partial x}\right]+\beta\frac{\partial}{\partial x}\left[\left(1-x^2\right)W\frac{\partial V}{\partial x}\right], \tag{2.20}$$

where $x = \cos\vartheta$. The potential V, consisting of the Maier-Saupe uniaxial anisotropy potential and the external field potential of $\mathbf{E}(t)$ applied along the easy axis, can be written as [1]

$$\beta V = -\sigma \cos^2 \vartheta - \xi(t) \cos\vartheta = -\sigma x^2 - \xi(t) x, \tag{2.21}$$

where $\sigma = \beta K$ is a dimensionless inverse temperature parameter, K is the anisotropy constant and $\xi(t) = \beta\mu E(t)$ is a dimensionless external field parameter.

By substituting Eq. (2.21) into Eq. (2.20), we have the Fokker-Planck equation for our specific system,

$$2\tau_D \frac{\partial W}{\partial t} = \frac{\partial}{\partial x}\left[\left(1-x^2\right)\frac{\partial W}{\partial x}\right] - \frac{\partial}{\partial x}\left[\left(1-x^2\right)\left(2\sigma x + \xi(t)\right)W\right]. \tag{2.22}$$

The general solution of Eq. (2.22) has the form

$$W(\vartheta, t) = \sum_{n=0}^{\infty} a_n(t) P_n(x), \tag{2.23}$$

where $P_n(z)$ are the Legendre polynomials [32]. Since the Legendre polynomials form a complete orthogonal set over $[-1,1]$, an arbitrary function defined in the interval $[-1,1]$ can be expanded in a series of Legendre polynomials, just like the Fourier series.

Firstly, we consider the term of Eq. (2.22) due to the external field,

$$\frac{\partial}{\partial x}\left[-\xi(t) W\left(1-x^2\right)\right]. \tag{2.24}$$

Substituting Eq. (2.23) into this term gives us

$$\frac{\partial}{\partial x}\left[-\xi(t) W\left(1-x^2\right)\right] = \sum_{n=0}^{\infty} a_n \left\{-\xi(t)\left[\left(1-x^2\right)P_n' - 2xP_n\right]\right\}. \tag{2.25}$$

Making the use of the recurrence relations of the Legendre polynomials [32],

$$\left(1-x^2\right)P_n' = n\left(P_{n-1} - xP_n\right) \tag{2.26}$$

and

$$xP_n = \frac{1}{(2n+1)}\left[\,(n+1)P_{n+1} + nP_{n-1}\right], \tag{2.27}$$

Eq. (2.25) becomes

$$\frac{\partial}{\partial x}\left[-\xi(t)W\left(1-x^2\right)\right]=\sum_{n=0}^{\infty}a_n\left\{-\xi(t)\left[\frac{n(n-1)}{(2n+1)}P_{n-1}-\frac{(n+1)(n+2)}{2n+1}P_{n+1}\right]\right\}. \quad (2.28)$$

The remaining term in Eq. (2.22),

$$\frac{\partial}{\partial x}\left[\left(1-x^2\right)\frac{\partial W}{\partial x}\right]+\frac{\partial}{\partial x}\left[(-2\sigma x)W\left(1-x^2\right)\right], \quad (2.29)$$

may be written using Eqs. (2.23) and (2.27) and by making use of the Legendre's differential equation [32],

$$\frac{\partial}{\partial x}\left[\left(1-x^2\right)\frac{\partial P_n}{\partial x}\right]=-n(n+1)P_n, \quad (2.30)$$

so that

$$\begin{aligned}&\frac{\partial}{\partial x}\left[\left(1-x^2\right)\frac{\partial W}{\partial x}\right]+\frac{\partial}{\partial x}\left[(-2\sigma x)W\left(1-x^2\right)\right]\\&=\sum_{n=0}^{\infty}a_n\left\{-n(n+1)P_n-2\sigma\frac{\partial}{\partial x}\left[\frac{\left(1-x^2\right)}{(2n+1)}\left[\,(n+1)P_{n+1}+nP_{n-1}\right]\right]\right\}.\end{aligned} \quad (2.31)$$

Substituting Eqs. (2.31) and (2.28) into Eq. (2.22) gives us

$$\begin{aligned}2\tau_D\sum_{n=0}^{\infty}\dot{a}_nP_n=&\sum_{n=0}^{\infty}a_n\left\{-\xi(t)\left[\frac{n(n-1)}{(2n+1)}P_{n-1}-\frac{(n+1)(n+2)}{2n+1}P_{n+1}\right]\right\}\\&+\sum_{n=0}^{\infty}a_n\left\{-n(n+1)P_n-2\sigma\frac{\partial}{\partial x}\left[\frac{\left(1-x^2\right)}{(2n+1)}\left[\,(n+1)P_{n+1}+nP_{n-1}\right]\right]\right\}.\end{aligned} \quad (2.32)$$

Thus, by orthogonality, we have

$$\begin{aligned}\frac{2\tau_D}{n(n+1)}\dot{a}_n=&-\left[1-\frac{2\sigma}{(2n+3)(2n-1)}\right]a_n-\frac{2\sigma(n+2)}{(2n+5)(2n+3)}a_{n+2}\\&+\frac{2\sigma(n-1)}{(2n-3)(2n-1)}a_{n-2}-\xi(t)\left[\frac{1}{(2n+3)}a_{n+1}-\frac{1}{2n-1}a_{n-1}\right].\end{aligned} \quad (2.33)$$

We now rewrite the differential-recurrence relation, Eq. (2.33), in terms of the expectation values of the Legendre polynomials of order *n* (statistical moments), viz.,

$$f_n(t)=\left\langle P_n(x)\right\rangle(t)=\int_{-1}^{1}W(x,t)P_n(x)\,dx, \quad (2.34)$$

which, using Eq. (2.23) and the orthogonality relation for the Legendre polynomials $P_n(x)$,

$$\int_{-1}^{1} P_n(x) P_m(x)\, dx = \frac{2}{2n+1}\delta_{n,m}, \tag{2.35}$$

can be written as

$$\begin{aligned} f_n(t) &= \sum_{m=0}^{\infty} a_m(t) \int_{-1}^{1} P_m(x) P_n(x)\, dx \\ &= \sum_{m=0}^{\infty} a_m(t) \frac{2}{2m+1}\delta_{n,m} = \frac{2}{2n+1} a_n(t). \end{aligned} \tag{2.36}$$

Thus Eq. (2.33) becomes

$$\tau_D \dot{f}_n(t) + d_n f_n(t) + g_n f_{n+2}(t) + c_n f_{n-2}(t) = \xi(t) a_n \left[f_{n-1}(t) - f_{n+1}(t) \right], \tag{2.37}$$

where

$$\begin{aligned} a_n &= \frac{n(n+1)}{2(2n+1)}, \\ c_n &= -\frac{\sigma n(n+1)(n-1)}{(2n-1)(2n+1)}, \\ d_n &= \frac{n(n+1)}{2}\left[1 - \frac{2\sigma}{(2n-1)(2n+3)} \right], \\ g_n &= \frac{\sigma n(n+1)(n+2)}{(2n+3)(2n+1)}. \end{aligned} \tag{2.38}$$

This five-term differential-recurrence relation (2.37) is used to study the nonlinear dielectric relaxation and dynamic Kerr effect of permanent dipoles in an axially symmetric uniaxial mean field potential as shown in Chapter 4. Equation (2.37) can also be used to consider the nonlinear response of noninteracting electric and magnetic dipoles by setting $\sigma = 0$, so that Eq. (2.37) reduces to a three-term differential-recurrence relation

$$\tau_D \dot{f}_n(t) + \frac{n(n+1)}{2} f_n(t) = \xi(t) \frac{n(n+1)}{2(2n+1)} \left[f_{n-1}(t) - f_{n+1}(t) \right], \tag{2.39}$$

which we will use in Chapter 3.

2.3 Calculation of the Stationary Response of Electric Dipoles via the Matrix Continued Fraction Method

In the current situation the external fields are applied along the easy axis of the particle so that the problem becomes axially symmetric and the relaxation functions depend only on the colatitude angle ϑ. Thus, the solution of the Smoluchowski equation (2.19) reduces

to the solution of an infinite hierarchy of differential-recurrence equations (2.37) for the expectation values of the Legendre polynomials $P_n(\cos\vartheta)$. We remark that the Fokker-Planck equation (2.58) for the uniaxial magnetic nanoparticles under the influence of the combined fields applied along the easy axis has an identical mathematical form to the rotational Smoluchowski equation (2.19) used here so that it can be solved using the same method. The ac stationary solution of the five-term differential-recurrence equation (2.37) subjected to the combined ac and dc fields has been developed in Refs. [18, 33] which we will summarize in this section.

The ac stationary solution of Eq. (2.37) may be written as the Fourier series

$$f_n(t) = \sum_{k=-\infty}^{\infty} F_k^n(\omega) e^{ik\omega t} \tag{2.40}$$

where the Fourier amplitudes satisfy $F_{-k}^n = \left(F_k^n\right)^*$ (the asterisk denotes the complex conjugate). On substituting Eq. (2.40) and the applied field $\xi(t) = \xi_0 + \xi\cos\omega t$ into Eq. (2.37), we have the set of recurrence relations for the Fourier amplitudes F_k^n, viz.,

$$\begin{aligned} &-\left(d_n + ik\omega\tau_D\right)F_k^n - c_n F_k^{n-2} - g_n F_k^{n+2} \\ &+\xi_0 a_n\left(F_k^{n-1} - F_k^{n+1}\right) + \left(\xi/2\right)a_n\left(F_{k-1}^{n-1} + F_{k+1}^{n-1} - F_{k-1}^{n+1} - F_{k+1}^{n+1}\right) = 0, \end{aligned} \tag{2.41}$$

where the coefficients a_n, d_n, etc. are given by Eq. (2.38). Now, we introduce a column vector

$$\mathbf{C}_n = \begin{pmatrix} \mathbf{c}_{2n} \\ \mathbf{c}_{2n-1} \end{pmatrix}, \tag{2.42}$$

where the subvector $\mathbf{c}_n$ is

$$\mathbf{c}_0 = \begin{pmatrix} \vdots \\ 0 \\ 0 \\ 1 \\ 0 \\ 0 \\ \vdots \end{pmatrix}, \quad \mathbf{c}_n = \begin{pmatrix} \vdots \\ 0 \\ 0 \\ 0 \\ 0 \\ 0 \\ \vdots \end{pmatrix} (n<0), \quad \mathbf{c}_n = \begin{pmatrix} \vdots \\ F_{-2}^n \\ F_{-1}^n \\ F_0^n \\ F_1^n \\ F_2^n \\ \vdots \end{pmatrix} (n>0). \tag{2.43}$$

Now the nine-term scalar recurrence relation (2.41) can be transformed into a three-term matrix recurrence relation

$$\mathbf{Q}_n^- \mathbf{C}_{n-1} + \mathbf{Q}_n \mathbf{C}_n + \mathbf{Q}_n^+ \mathbf{C}_{n+1} = 0\,, \tag{2.44}$$

where the matrices $\mathbf{Q}_n^{\pm}$ and $\mathbf{Q}_n$ are defined as

$$\begin{aligned}
\mathbf{Q}_n^- &= \begin{pmatrix} -c_{2n}\mathbf{I} & \mathbf{O} \\ a_{2n-1}\mathbf{Y} & -c_{2n-1}\mathbf{I} \end{pmatrix}, \\
\mathbf{Q}_n &= \begin{pmatrix} \mathbf{Z}_{2n} & a_{2n}\mathbf{Y} \\ -a_{2n-1}\mathbf{Y} & \mathbf{Z}_{2n-1} \end{pmatrix}, \\
\mathbf{Q}_n^+ &= \begin{pmatrix} -g_{2n}\mathbf{I} & -a_{2n}\mathbf{Y} \\ \mathbf{O} & -g_{2n-1}\mathbf{I} \end{pmatrix}.
\end{aligned} \tag{2.45}$$

Here $\mathbf{I}$ and $\mathbf{O}$ are the identity and zero matrices of infinite dimension, respectively, and $\mathbf{Y}$ and $\mathbf{Z}_n$ are defined as

$$\begin{aligned}
\left(\mathbf{Y}\right)_{r,s} &= \delta_{r,s-1}\xi/2 + \delta_{r,s}\xi_0 + \delta_{r,s+1}\xi/2, \\
\left(\mathbf{Z}_n\right)_{r,s} &= \delta_{r,s} z_{n,s},
\end{aligned} \tag{2.46}$$

where $z_{n,s} = -d_n - i\omega\tau_D s$ and $-\infty < r, s < \infty.$

Since Eq. (2.44) is a frequency-dependent matrix three-term recurrence relation, it can be solved using the matrix continued fraction method where we introduce a new function $\mathbf{S}_n(\omega)$ and assume that

$$\mathbf{C}_n(\omega) = \mathbf{S}_n(\omega)\mathbf{Q}_n^- \mathbf{C}_{n-1}(\omega)\,. \tag{2.47}$$

We now have via successive iterations of Eq. (2.47),

$$\mathbf{C}_n = \mathbf{S}_n(\omega)\mathbf{Q}_n^- \cdots \mathbf{S}_1(\omega)\mathbf{Q}_1^- \mathbf{C}_0 = \left(\prod_{k=0}^{n-1} \mathbf{S}_{n-k}(\omega)\mathbf{Q}_{n-k}^-\right)\mathbf{C}_0\,. \tag{2.48}$$

Now our task is to determine $\mathbf{S}_n(\omega)$. By applying Eq. (2.47) to Eq. (2.44) we have

$$\mathbf{Q}_n^- \mathbf{C}_{n-1} + \mathbf{Q}_n \mathbf{S}_n(\omega)\mathbf{Q}_n^- \mathbf{C}_{n-1} + \mathbf{Q}_n^+ \mathbf{S}_{n+1}(\omega)\mathbf{Q}_{n+1}^- \mathbf{S}_n(\omega)\mathbf{Q}_n^- \mathbf{C}_{n-1} = 0\,, \tag{2.49}$$

where $\mathbf{S}_n(\omega)$ can be obtained directly as

$$\mathbf{S}_n(\omega) = -\left[\mathbf{Q}_n + \mathbf{Q}_n^+ \mathbf{S}_{n+1}(\omega)\mathbf{Q}_{n+1}^-\right]^{-1}. \tag{2.50}$$

Therefore, by solving this matrix three-term recurrence relation (2.44), we can calculate the Fourier amplitudes F_k^n which can be used later to evaluate the nonlinear stationary response of permanent electric dipoles (see Chapters 3 and 4) and uniaxial magnetic nanoparticles with an axially symmetric potential.

2.4 Fokker-Planck Equation for Magnetic Dipoles

When the size of a ferromagnetic nanoparticle is below a certain critical size (typically 15nm in radius), the particle is said to stay in a single domain state where the magnetization is uniform for all applied magnetic fields [4]. In this situation, the magnetization of the nanoparticles can be written as a single giant magnetic moment $\mathbf{M}$ (~10^4–10^5 μ_B) which is the sum of all the aligned individual magnetic moments carried by the atoms of the nanoparticles. Fine single-domain magnetic nanoparticles exhibit thermal instability of the magnetization, resulting in the magnetic after-effect or Néel relaxation, because of thermal agitation originating in a heat bath. To develop this dynamical behaviour of the magnetization $\mathbf{M}(t)$ for an individual particle, Brown [1, 6] started with Gilbert's equation [1, 4] (see Fig. 2.2)

$$\dot{\mathbf{M}}(t) = \gamma\left[\mathbf{M}(t)\times\left[\mathbf{H} - \eta\dot{\mathbf{M}}(t)\right]\right], \tag{2.51}$$

and added a white noise term to accounting for thermal agitation to create a *magnetic Langevin equation*,

$$\dot{\mathbf{M}}(t) = \gamma\left[\mathbf{M}(t)\times\left[\mathbf{H} - \eta\dot{\mathbf{M}}(t) + \mathbf{h}(t)\right]\right]. \tag{2.52}$$

Here, γ is the gyromagnetic ratio, η is the damping parameter, $\mathbf{H} = -\partial V / \left(\mu_0 \partial \mathbf{M}\right)$ is the effective magnetic field, $\mu_0 = 4\pi\cdot 10^{-7}\,\mathrm{JA^{-2}m^{-1}}$ is the permeability of free space in SI units, V is the Gibbs free energy density (the total free energy is vV), and $\mathbf{h}(t)$ is a random magnetic field with Gaussian white noise properties:

$$\overline{h_n(t)} = 0, \quad \overline{h_n(t)h_m(t')} = \left(2kT\eta / v\right)\delta_{n,m}\delta\left(t - t'\right), \tag{2.53}$$

where the indices $n, m = 1, 2, 3$ in Kronecker's delta $\delta_{n,m}$ correspond to the Cartesian laboratory coordinate axes X, Y, Z and v is the volume of the particle.

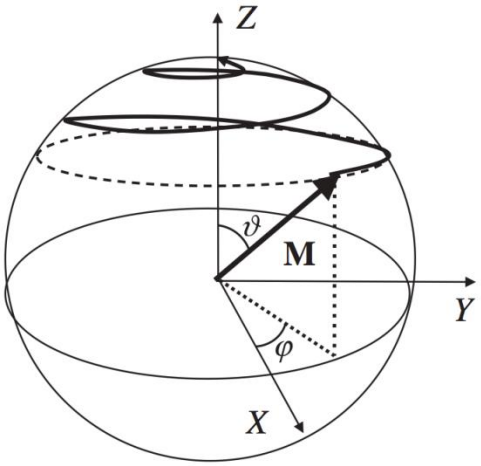

Fig. 2.2. Magnetization **M** with spherical polar coordinates ϑ and φ. In the absence of damping **M** will precess along orbits of constant energy called Stoner-Wohlfarth orbits [34] (dashed line). According to Eq. (2.51) if damping is involved the precession will slowly collapse by spiraling towards an energy minimum (solid line).

Assuming that the single-domain particle is at its saturation magnetization M_S so that only the direction of **M** can change, we may then write $\mathbf{M} = M_S\mathbf{u}$, where **u** is a unit vector along **M**, and Eq. (2.52) without the thermal agitation becomes

$$\dot{\mathbf{u}} = -\frac{h'}{\alpha}\left(\mathbf{u}\times\frac{\partial V}{\partial \mathbf{u}}\right) + h'\mathbf{u}\times\left(\mathbf{u}\times\frac{\partial V}{\partial \mathbf{u}}\right), \tag{2.54}$$

where the dimensionless damping constant $\alpha = \eta\gamma M_S$ and $h' = \alpha\gamma / \left[\left(1+\alpha^2\right)\mu_0 M_S\right]$. The orientation of **u** is specified by the polar and azimuthal angles ϑ and φ of the spherical polar coordinate system (Fig. 2.1) so that the direction cosines of **u** are given by $u_X = \sin\vartheta\cos\varphi$, $u_Y = \sin\vartheta\sin\varphi$, and $u_Z = \cos\vartheta$. Now, let us consider a statistical ensemble of identical particles and let $W(\vartheta,\varphi,t)d\Omega$ be the probability that **M** has orientation (ϑ,φ) within the solid angle $d\Omega = \sin\vartheta\, d\vartheta d\varphi$ on the unit sphere. Since the Fokker-Planck equation describes the evolution of a probability density function $W(\vartheta,\varphi,t)$ of magnetization orientations on the surface of a sphere of constant radius M_S (see Fig. 2.2), it can be related to the probability current **J** along the sphere by a continuity equation, just like we treated the Smoluchowski equation in Section 2.1,

$$\dot{W} + \mathrm{div}\mathbf{J} = 0 \tag{1.55}$$

where the probability current **J** consists of a deterministic part, which describes the probability current in the absence of thermal agitation, and a diffusive part, which represents the effect of thermal agitation,

$$\mathbf{J} = W\dot{\mathbf{u}} - k'\partial_{\mathbf{u}} W\,, \tag{2.56}$$

where k' is a constant to be determined later and the deterministic part of the probability current, $W\dot{\mathbf{u}}$, uses the deterministic equation (2.54). By substituting the divergence of Eq. (2.56) in spherical polar coordinates into the continuity equation (1.55) and evaluating k' by requiring that the Boltzmann distribution $W_0(\vartheta,\varphi) = Z^{-1}e^{-\nu V(\vartheta,\varphi)/(kT)}$ (Z is the partition function) should be its stationary (equilibrium) solution (in a similar way to the electric dipoles case in Section 2.1), Eq. (1.55) yields Brown's Fokker-Planck equation

$$\begin{aligned} 2\tau_N \frac{\partial W}{\partial t} = L_{FP}W = \frac{1}{\sin\vartheta}\Bigg\{ &\left[\frac{\partial}{\partial\vartheta}\left(\sin\vartheta\frac{\partial}{\partial\vartheta}\right) + \frac{1}{\sin\vartheta}\frac{\partial^2}{\partial\varphi^2}\right]W \\ &+ \frac{\nu}{kT}\left[\frac{\partial}{\partial\vartheta}\left(\sin\vartheta\frac{\partial V}{\partial\vartheta} - \alpha^{-1}\frac{\partial V}{\partial\varphi}\right)W + \frac{\partial}{\partial\varphi}\left(\alpha^{-1}\frac{\partial V}{\partial\vartheta} + \frac{1}{\sin\vartheta}\frac{\partial V}{\partial\varphi}\right)W\right]\Bigg\}, \end{aligned} \tag{2.57}$$

which may be written in a compact vector form for $W(\mathbf{u},t)$ as

$$2\tau_N \frac{\partial W}{\partial t} = \Delta W + \frac{\beta}{\alpha}\left(\mathbf{u}\cdot\left[\nabla V\times\nabla W\right]\right) + \beta\left(\nabla\cdot W\nabla V\right). \tag{2.58}$$

Here ∇ and Δ are, respectively, the gradient and the Laplacian operator on the surface of the unit sphere, $\tau_N = \tau_0(\alpha+\alpha^{-1})$ is the characteristic free diffusion time of $\mathbf{M}(t)$ (τ_N is of the order of $10^{-10}-10^{-8}$ s) with $\tau_0 = \beta\mu_0 M_S/(2\gamma)$, $\beta = \nu/(kT)$, k is Boltzmann's constant, and T is the absolute temperature. The term in $\beta\alpha^{-1}$ is the precessional (gyromagnetic) term which gives rise to ferromagnetic resonance (usually in the GHz range) and the term in β is the alignment term. It is worth noting that, by omitting the second (precessional) term on the right hand side (when $\alpha\to\infty$), Eq. (2.58) is essentially similar to the rotational Smoluchowski equation (2.16) describing dielectric and Kerr-effect relaxation in polar liquids [15], as derived in Section 2.1. However, the precessional term has a profound effect on the magnetization dynamics, especially in the nonlinear case, because it may couple, depending on the *direction* of the applied field, the longitudinal and transverse modes in Eq. (2.58). This coupling is discussed further in Section 5.3.

2.5 11-Term Differential-Recurrence Relations

Just as in Section 2.2 where the Smoluchowski equation for electric dipoles was converted to a differential-recurrence relation for the expectation values of the Legendre polynomials $\left\langle P_n\left(\cos\vartheta\right)\right\rangle(t)$, Eq. (2.37), the magnetic Fokker-Planck equation (2.57) can be converted into a differential-recurrence relation for the expectation values of the spherical harmonics $\left\langle Y_{n,m}\left(\vartheta,\varphi\right)\right\rangle(t)$. This equation is given in a general form, Eq. (2.73), which can be then applied to a specific free energy density. The derivation can be based on either the Langevin equation [1, 29] or the Fokker-Planck equation [1, 5]. Here we shall follow the derivation in Section 9.2.2 of Ref. [1] and then apply it to the case of a uniaxial anisotropy in the presence of an external field, Eq. (2.75), to produce the 11-term differential-recurrence relation, Eq. (2.80).

Since $W\left(\vartheta,\varphi,t\right)$ in the Fokker-Planck equation (2.57) should be physically meaningful (positive and real), the solution of Eq. (2.57) is sought in the form of [1]

$$W\left(\vartheta,\varphi,t\right)=\Psi\left(\vartheta,\varphi,t\right)\Psi^{*}\left(\vartheta,\varphi,t\right), \tag{2.59}$$

where the asterisk denotes the complex conjugate and $\Psi\left(\vartheta,\varphi,t\right)$ is expanded in spherical harmonics $Y_{l,m}\left(\vartheta,\varphi\right)$ as

$$\Psi\left(\vartheta,\varphi,t\right)=\sum_{l,m}f_{l,m}\left(t\right)Y_{l,m}\left(\vartheta,\varphi\right). \tag{2.60}$$

Due to the orthogonality of the spherical harmonics

$$\int_{0}^{2\pi}\int_{0}^{\pi}Y_{l,m}Y_{l',m'}^{*}d\Omega=\delta_{l,l'}\delta_{m,m'}, \tag{2.61}$$

where $d\Omega=\sin\vartheta d\vartheta d\varphi$, the normalisation condition for $W\left(\vartheta,\varphi,t\right)$ is

$$\int_{0}^{2\pi}\int_{0}^{\pi}W\left(\vartheta,\varphi,t\right)d\Omega=\left|f_{l,m}\left(t\right)\right|^{2}=1. \tag{2.62}$$

It is worth noting that W is similar to the probability density $\left|\Psi\right|^{2}$, which obeys the continuity equation $\partial_{t}\left|\Psi\right|^{2}+\operatorname{div}\mathbf{j}=0$ (Ψ is the wave function and $\mathbf{j}$ is the probability current density), so this problem is analogous to the quantum mechanics case [35].

By using Eqs. (2.57), (2.59), (2.60), and

$$\int_0^{2\pi}\int_0^{\pi} Y_{l,m}Y_{l',m'}Y^*_{l'',m''}d\Omega = \sqrt{\frac{(2l+1)(2l'+1)}{4\pi(2l''+1)}}C^{l'',0}_{l,0,l',0}C^{l'',m''}_{l,m,l',m'}, \tag{2.63}$$

and reducing the products of $Y_{l,m}(\vartheta,\varphi)$ to a sum of $Y_{l,m}(\vartheta,\varphi)$ [36]

$$Y_{l,m}Y_{l_1,m_1} = \sqrt{\frac{(2l+1)(2l_1+1)}{4\pi}}\sum_{l_2=|l-l_1|}^{l+l_1}\frac{C^{l_2,0}_{l,0,l_1,0}C^{l_2,m+m_1}_{l,m,l_1,m_1}}{\sqrt{2l_2+1}}Y_{l_2,m+m_1}, \tag{2.64}$$

where $C^{c,r}_{a,\alpha,b,\beta}$ are the Clebsch-Gordan coefficients [36], the moment system for the averaged spherical harmonics can be obtained by means of the transformation

$$\begin{aligned}
&\frac{d}{dt}\langle Y_{l,m}\rangle(t)\\
&=\int_0^{2\pi}\int_0^{\pi} Y_{l,m}\dot{W}(\vartheta,\varphi,t)\,d\Omega\\
&=\sum_{l',l'',m',m''} f_{l',m'}(t)\,f^*_{l'',m''}(t)\int_0^{2\pi}\int_0^{\pi} Y_{l,m}L_{FP}\left(Y_{l',m'}Y^*_{l'',m''}\right)d\Omega\\
&=\sum_{l',l'',l''',m',m'',m'''}\sqrt{\frac{(2l'+1)(2l''+1)}{4\pi(2l'''+1)}}C^{l''',0}_{l',0,l'',0}C^{l''',m'''}_{l',m',l'',m''}\,f_{l',m'}(t)\,f^*_{l'',m''}(t)\int_0^{2\pi}\int_0^{\pi} Y_{l,m}L_{FP}Y^*_{l''',m'''}d\Omega\\
&=\sum_{l',m'} d_{l',m',l,m}(t)\langle Y_{l',m'}\rangle(t),
\end{aligned} \tag{2.65}$$

where

$$d_{l',m',l,m} = \int_0^{2\pi}\int_0^{\pi} Y_{l,m}L_{FP}Y^*_{l',m'}d\Omega, \tag{2.66}$$

and

$$\begin{aligned}
\langle Y_{l,m}\rangle(t) &= \int_0^{2\pi}\int_0^{\pi} Y_{l,m}W(\vartheta,\varphi,t)\,d\Omega\\
&=\sum_{l',l'',m',m''} f_{l',m'}(t)\,f^*_{l'',m''}(t)\int_0^{2\pi}\int_0^{\pi} Y_{l,m}Y_{l',m'}Y^*_{l'',m''}d\Omega\\
&=\sum_{l',l'',m',m''}\sqrt{\frac{(2l+1)(2l'+1)}{4\pi(2l''+1)}}C^{l'',0}_{l,0,l',0}C^{l'',m''}_{l,m,l',m'}\,f_{l',m'}(t)\,f^*_{l'',m''}(t).
\end{aligned} \tag{2.67}$$

In order to evaluate $L_{FP}Y^*_{l',m'}$ in Eq. (2.66) we write the Fokker-Planck operator, Eq. (2.57), entirely in terms of the angular momentum operators $\hat{L}_Z$, $\hat{L}_\pm$ and $\hat{L}^2$, which are defined as [36]

$$\hat{L}_Z = -i\frac{\partial}{\partial\varphi}, \quad \hat{L}_{\pm} = e^{\pm i\varphi}\left(\pm\frac{\partial}{\partial\vartheta} + i\cot\vartheta\frac{\partial}{\partial\varphi}\right), \quad \hat{L}^2 = -\Delta\,. \tag{2.68}$$

Thus

$$\begin{aligned} L_{FP}Y^*_{l',m'} = {} & \frac{\beta}{4\tau_N}\left[\hat{L}^2VY^*_{l',m'} - \hat{L}^2VY^*_{l',m'} - \hat{L}^2VY^*_{l',m'}\right] - \frac{1}{2\tau_N}\hat{L}^2Y^*_{l',m'} \\ & + \frac{i}{4\tau_N\alpha}\sqrt{\frac{3}{2\pi}}\left[(Y_{1,1})^{-1}\left(\hat{L}_+V_+\hat{L}_zY^*_{l',m'} - \hat{L}_zV_+\hat{L}_+Y^*_{l',m'}\right)\right. \\ & \left. + (Y_{1,-1})^{-1}\left(\hat{L}_-V_-\hat{L}_zY^*_{l',m'} - \hat{L}_zV_-\hat{L}_-Y^*_{l',m'}\right)\right], \end{aligned} \tag{2.69}$$

where

$$\beta V = V_+ + V_-\,. \tag{2.70}$$

Furthermore, by writing the half sided sums of the potential as linear combinations of spherical harmonics

$$V_- = \sum_{r=1}^{\infty}\sum_{s=-r}^{-1}v_{r,s}Y_{r,s}, \quad V_+ = \sum_{r=1}^{\infty}\sum_{s=0}^{r}v_{r,s}Y_{r,s}\,, \tag{2.71}$$

and using the action of the angular momentum operators,

$$\begin{aligned} \hat{L}_ZY_{l,m} &= mY_{l,m}, \\ \hat{L}_{\pm}Y_{l,m} &= \sqrt{l(l+1)-m(m\pm1)}Y_{l,m\pm1}, \\ \hat{L}^2Y_{l,m} &= l(l+1)Y_{l,m}, \end{aligned} \tag{2.72}$$

Eqs. (2.64) and (2.63), Eq. (2.65) finally yields the differential-recurrence relation for the averaged spherical harmonics $\langle Y_{l,m}\rangle(t)$ after tedious manipulation,

$$\tau_N\frac{d}{dt}\langle Y_{l,m}\rangle(t) = \sum_{l',m'}e_{l,m,l',m'}\langle Y_{l',m'}\rangle(t)\,, \tag{2.73}$$

where the coefficients are

$$
\begin{aligned}
e_{l,m,l',m\pm s}(t) = &-\frac{l(l+1)}{2}\delta_{l,l'}\delta_{s,0} + (-1)^m \frac{\beta}{4}\sqrt{\frac{(2l'+1)(2l+1)}{\pi}} \\
&\sum_{r=s}^{\infty} v_{r,\pm s}\left\{\frac{\left[-l(l+1)-r(r+1)+l'(l'+1)\right]}{2\sqrt{2r+1}} C_{l,0,l',0}^{r,0} C_{l,m,l',-m\mp s}^{r,\mp s}\right. \\
&+\frac{i}{\alpha}\sqrt{\frac{(2r+1)(r-s)!}{(r+s)!}} \sum_{\substack{L=s-\varepsilon_{r,s} \\ \Delta L=2}}^{r-1} \sqrt{\frac{(L+s-1)!}{(L-s+1)!}} C_{l,0,l',0}^{L,0} \\
&\left.\left[m\sqrt{(L-s+1)(L+s)}\, C_{l,m,l',\mp s-m}^{L,\mp s} \pm s\sqrt{(l\mp m)(l\pm m+1)}\, C_{l,m\pm 1,l',\mp s-m}^{L,\mp(s-1)}\right]\right\}.
\end{aligned}
\tag{2.74}
$$

Equation (2.73) is a general differential-recurrence relation which can be used for any potentials. In order to consider the case of a particular potential, the coefficients $e_{l,m,l',m'}$ should be evaluated via Eqs. (2.70) and (2.71).

Now, for example, we shall consider the free-energy density V of a uniaxial particle in superimposed homogeneous external dc bias and ac magnetic fields $\mathbf{H}_0 + \mathbf{H}\cos\omega t$ of arbitrary strengths and orientations relative to the easy axis of the particle as used in Chapter 5,

$$
\beta V = -\sigma\cos^2\vartheta - \xi_0(\mathbf{u}\cdot\mathbf{H}_0)/H_0 - \xi\cos\omega t(\mathbf{u}\cdot\mathbf{H})/H\,, \tag{2.75}
$$

where $\sigma = \beta K$, $\xi_0 = \mu_0\beta H_0 M_S$, $\xi = \mu_0\beta H M_S$ are the dimensionless anisotropy and external field parameters, and K is the anisotropy constant. If $\mathbf{H}_0$ and $\mathbf{H}$ are parallel, Eq. (2.75) can be written as

$$
\begin{aligned}
\beta V &= -\sigma\cos^2\vartheta - (\xi_0 + \xi\cos\omega t)(\mathbf{u}\cdot\mathbf{h}) \\
&= -\sigma\cos^2\vartheta - (\xi_0 + \xi\cos\omega t)(\gamma_1\sin\vartheta\cos\varphi + \gamma_2\sin\vartheta\sin\varphi + \gamma_3\cos\vartheta),
\end{aligned}
\tag{2.76}
$$

where $\mathbf{h} = \mathbf{H}/H$ and $\gamma_1, \gamma_2, \gamma_3$ are the direction cosines of $\mathbf{h}$.

Using the spherical harmonics of degree 1 and 2 [36],

$$
Y_{1,0} = \sqrt{\frac{3}{4\pi}}\cos\vartheta, \quad Y_{1,\pm 1} = \mp\sqrt{\frac{3}{8\pi}}\sin\vartheta e^{\pm i\varphi}, \quad Y_2^0 = \frac{1}{4}\sqrt{\frac{5}{\pi}}\cdot(3\cos^2\vartheta - 1)\,, \tag{2.77}
$$

and letting $\xi(t) = \xi_0 + \xi\cos\omega t$, the free energy density Eq. (2.76) can be expanded in terms of spherical harmonics as

$$
\beta V = -\frac{4\sigma}{3}\sqrt{\frac{\pi}{5}}Y_{2,0} - \xi(t)\sqrt{\frac{2\pi}{3}}\left\{\sqrt{2}\gamma_3 Y_{1,0} + (\gamma_1 + i\gamma_2)Y_{1,-1} - (\gamma_1 - i\gamma_2)Y_{1,1}\right\}. \tag{2.78}
$$

Thus, we have equations for the coefficients $v_{r,\pm s}$ in Eq. (2.74):

$$
\begin{aligned}
v_{2,0} &= -\frac{4\sigma}{3}\sqrt{\frac{\pi}{5}}, \\
v_{1,0} &= -2\xi(t)\gamma_3\sqrt{\frac{\pi}{3}}, \\
v_{1,\pm 1} &= \pm\xi(t)\left(\gamma_1 \mp i\gamma_2\right)\sqrt{\frac{2\pi}{3}}.
\end{aligned}
\tag{2.79}
$$

On using Eq. (2.79) in the evolution equation of the statistical moments $\langle Y_{l,m}\rangle(t)$, Eq. (2.73), we obtain the 11-term differential-recurrence relation for the specific free energy density, Eq. (2.76), via Mathematica®, viz.,

$$
\begin{aligned}
&\tau_N \frac{d}{dt}\langle Y_{l,m}\rangle(t) \\
&= v_{l,m}\langle Y_{l-2,m}\rangle(t) + w_{l,m}\langle Y_{l-1,m}\rangle(t) + x_{l,m}\langle Y_{l,m}\rangle(t) + y_{l,m}\langle Y_{l+1,m}\rangle(t) + z_{l,m}\langle Y_{l+2,m}\rangle(t) \\
&+ w^{-}_{l,m}\langle Y_{l-1,m-1}\rangle(t) + x^{-}_{l,m}\langle Y_{l,m-1}\rangle(t) + y^{-}_{l,m}\langle Y_{l+1,m-1}\rangle(t) \\
&+ w^{+}_{l,m}\langle Y_{l-1,m+1}\rangle(t) + x^{+}_{l,m}\langle Y_{l,m+1}\rangle(t) + y^{+}_{l,m}\langle Y_{l+1,m+1}\rangle(t) \\
&+ \left(e^{i\omega t} + e^{-i\omega t}\right)\Big[w^{t}_{l,m}\langle Y_{l-1,m}\rangle(t) + x^{t}_{l,m}\langle Y_{l,m}\rangle(t) + y^{t}_{l,m}\langle Y_{l+1,m}\rangle(t) \\
&+ w^{-t}_{l,m}\langle Y_{l-1,m-1}\rangle(t) + x^{-t}_{l,m}\langle Y_{l,m-1}\rangle(t) + y^{-t}_{l,m}\langle Y_{l+1,m-1}\rangle(t) \\
&+ w^{+t}_{l,m}\langle Y_{l-1,m+1}\rangle(t) + x^{+t}_{l,m}\langle Y_{l,m+1}\rangle(t) + y^{+t}_{l,m}\langle Y_{l+1,m+1}\rangle(t)\Big],
\end{aligned}
\tag{2.80}
$$

where the coefficients $x_{l,m}$, $y^{t}_{l,m}$, etc. are given in Appendix 2A.

2.6 Calculation of the Stationary Response via the Matrix Continued Fraction Method for Magnetic Dipoles

Efficient numerical algorithms for the calculation of the nonlinear ac stationary response of the magnetization of *uniaxial* magnetic nanoparticles have been proposed [16-18] by assuming that the dc bias and ac driving fields *are directed along the easy axis* of the particle. In this case, the Fokker-Planck equation which arises from the axial symmetry is mathematically identical to the Smoluchowski equation, occurring in the nonlinear dielectric relaxation and Kerr effect of permanent electric dipoles, whose stationary solution has been demonstrated in Section 2.3. However, in the *nonaxially symmetric* configuration where a strong ac field is applied at *an angle* to the easy axis of the particle, the axial symmetry is broken by the Zeeman energy [19-22] so that the coupling of the

longitudinal and transverse precessional modes causes many interesting nonlinear effects in the ac stationary response. Now, building on the axially symmetric solutions described in Refs. [16-18] and Section 2.3, an exact nonperturbative method for the determination of the Fourier amplitudes, and so the nonlinear magnetization of magnetic nanoparticles with an *arbitrary* anisotropy potential and subjected to a strong ac driving field superimposed on a strong dc bias field, has recently been given by Titov *et al*. [23]. Thus, we are going to use their method to investigate the ac stationary response governed by the 11-term differential-recurrence relation (2.80) for the spherical harmonics $Y_{l,m}(\vartheta,\varphi)$.

In order to solve Eq. (2.80), we introduce the column vectors $\mathbf{c}_n(t)\,(n=1,2,3,...)$ with $\mathbf{c}_0=\langle Y_{0,0}\rangle=1/\sqrt{4\pi}$ so that Eq. (2.80) becomes

$$\begin{aligned}\tau_N\partial_t\mathbf{c}_n(t)&=\mathbf{q}_n^-\mathbf{c}_{n-1}(t)+\mathbf{q}_n\mathbf{c}_n(t)+\mathbf{q}_n^+\mathbf{c}_{n+1}(t)\\&\quad+\left[\mathbf{p}_n^-\mathbf{c}_{n-1}(t)+\mathbf{p}_n\mathbf{c}_n(t)+\mathbf{p}_n^+\mathbf{c}_{n+1}(t)\right]\left(e^{i\omega t}+e^{-i\omega t}\right),\end{aligned}\tag{2.81}$$

where $\mathbf{c}_n(t)$ is the statistical moment vector

$$\mathbf{c}_n(t)=\begin{pmatrix}\langle Y_{2n,-2n}\rangle(t)\\ \vdots\\ \langle Y_{2n,2n}\rangle(t)\\ \langle Y_{2n-1,-2n+1}\rangle(t)\\ \vdots\\ \langle Y_{2n-1,2n-1}\rangle(t)\end{pmatrix},\tag{2.82}$$

and the supermatrix coefficients $\mathbf{q}_n$, $\mathbf{q}_n^{\pm}$, $\mathbf{p}_n$ and $\mathbf{p}_n^{\pm}$ are

$$\begin{aligned}\mathbf{q}_n&=\begin{pmatrix}\mathbf{X}_{2n}&\mathbf{W}_{2n}\\ \mathbf{Y}_{2n-1}&\mathbf{X}_{2n-1}\end{pmatrix},\quad \mathbf{q}_n^+=\begin{pmatrix}\mathbf{Z}_{2n}&\mathbf{Y}_{2n}\\ \mathbf{0}&\mathbf{Z}_{2n-1}\end{pmatrix},\quad \mathbf{q}_n^-=\begin{pmatrix}\mathbf{V}_{2n}&\mathbf{0}\\ \mathbf{W}_{2n-1}&\mathbf{V}_{2n-1}\end{pmatrix},\\ \mathbf{p}_n&=\begin{pmatrix}\mathbf{X}_{2n}^t&\mathbf{W}_{2n}^t\\ \mathbf{Y}_{2n-1}^t&\mathbf{X}_{2n-1}^1\end{pmatrix},\quad \mathbf{p}_n^+=\begin{pmatrix}\mathbf{0}&\mathbf{Y}_{2n}^t\\ \mathbf{0}&\mathbf{0}\end{pmatrix},\quad \mathbf{p}_n^-=\begin{pmatrix}\mathbf{0}&\mathbf{0}\\ \mathbf{W}_{2n-1}^t&\mathbf{0}\end{pmatrix}.\end{aligned}\tag{2.83}$$

Here the matrix elements of the diagonal submatrices $\mathbf{X}_{2n}$, $\mathbf{X}_{2n}^t$ etc. are given by

$$
\begin{aligned}
\left(\mathbf{V}_l\right)_{n,m} &= \delta_{n-2,m} v_{l,-l+m+1}, \\
\left(\mathbf{W}_l\right)_{n,m} &= \delta_{n-2,m} w^{-}_{l,-l+m+1} + \delta_{n-1,m} w_{l,-l+m} + \delta_{n,m} w^{+}_{l,-l+m-1}, \\
\left(\mathbf{X}_l\right)_{n,m} &= \delta_{n-1,m} x^{-}_{l,-l+m} + \delta_{n,m} x_{l,-l+m-1} + \delta_{n+1,m} x^{+}_{l,-l+m-2}, \\
\left(\mathbf{Y}_l\right)_{n,m} &= \delta_{n,m} y^{-}_{l,-l+m-1} + \delta_{n+1,m} y_{l,-l+m-2} + \delta_{n+2,m} y^{+}_{l,-l+m-3}, \\
\left(\mathbf{Z}_l\right)_{n,m} &= \delta_{n+2,m} z_{l,-l+m-3}, \\
(\mathbf{W}^t_l)_{n,m} &= \delta_{n-2,m} w^{-t}_{l,-l+m+1} + \delta_{n-1,m} w^{t}_{l,-l+m} + \delta_{n,m} w^{+t}_{l,-l+m-1}, \\
(\mathbf{X}^t_l)_{n,m} &= \delta_{n-1,m} x^{-t}_{l,-l+m} + \delta_{n,m} x^{t}_{l,-l+m-1} + \delta_{n+1,m} x^{+t}_{l,-l+m-2}, \\
(\mathbf{Y}^t_l)_{n,m} &= \delta_{n,m} y^{-t}_{l,-l+m-1} + \delta_{n+1,m} y^{t}_{l,-l+m-2} + \delta_{n+2,m} y^{+t}_{l,-l+m-3},
\end{aligned}
\tag{2.84}
$$

where the coefficients are given in Appendix 2A.

Thus the 11-term differential-recurrence relations, Eq. (2.80), have been transformed into a matrix six-term differential-recurrence relation, Eq. (2.81), where three matrix terms contains the static coefficients ($\mathbf{q}_n$ and $\mathbf{q}^{\pm}_n$) and three matrix terms with the sinusoidal coefficients ($\mathbf{p}_n$ and $\mathbf{p}^{\pm}_n$), Eq. (2.81). Since we only seek the stationary ac response, which is independent of the initial conditions, we can write $Y_{n,m}(t)$ in the form of the time Fourier series,

$$
Y_{n,m}(t) = \sum_{k=-\infty}^{\infty} c^k_{n,m}(\omega) e^{ik\omega t}. \tag{2.85}
$$

Thus, the various time-dependent vectors in Eq. (2.81) can be represented in terms of frequency-dependent vectors according to

$$
\mathbf{c}_n(t) = \begin{pmatrix} \langle Y_{2n,-2n} \rangle(t) \\ \vdots \\ \langle Y_{2n,2n} \rangle(t) \\ \langle Y_{2n-1,-2n+1} \rangle(t) \\ \vdots \\ \langle Y_{2n-1,2n-1} \rangle(t) \end{pmatrix} = \sum_{k=-\infty}^{\infty} \begin{pmatrix} c^k_{2n,-2n}(\omega) \\ \vdots \\ c^k_{2n,2n}(\omega) \\ c^k_{2n-1,-2n+1}(\omega) \\ \vdots \\ c^k_{2n-1,2n-1}(\omega) \end{pmatrix} e^{ik\omega t} = \sum_{k=-\infty}^{\infty} \mathbf{c}^k_n(\omega) e^{ik\omega t}. \tag{2.86}
$$

Thereby Eq. (2.81) becomes

$$
\begin{aligned}
&\sum_{k=-\infty}^{\infty} \Big\{ e^{ik\omega t} \Big[\mathbf{q}^{-}_n \mathbf{c}^k_{n-1}(\omega) + \left(\mathbf{q}_n - \tau_N ik\omega \mathbf{I}\right) \mathbf{c}^k_n(\omega) + \mathbf{q}^{+}_n \mathbf{c}^k_{n+1}(\omega) \Big] \\
&+ (e^{i(k+1)\omega t} + e^{i(k-1)\omega t}) \Big[\mathbf{p}^{-}_n \mathbf{c}^k_{n-1}(\omega) + \mathbf{p}_n \mathbf{c}^k_n(\omega) + \mathbf{p}^{+}_n \mathbf{c}^k_{n+1}(\omega) \Big] \Big\} = 0.
\end{aligned}
\tag{2.87}
$$

Thus, by orthogonality, we must have

$$\begin{aligned}&\mathbf{q}_n^-\mathbf{c}_{n-1}^k(\omega)+\left(\mathbf{q}_n-\tau_N ik\omega\mathbf{I}\right)\mathbf{c}_n^k(\omega)+\mathbf{q}_n^+\mathbf{c}_{n+1}^k(\omega)\\&+\mathbf{p}_n^-\mathbf{c}_{n-1}^{k-1}(\omega)+\mathbf{p}_n\mathbf{c}_n^{k-1}(\omega)+\mathbf{p}_n^+\mathbf{c}_{n+1}^{k-1}(\omega)\\&+\mathbf{p}_n^-\mathbf{c}_{n-1}^{k+1}(\omega)+\mathbf{p}_n\mathbf{c}_n^{k+1}(\omega)+\mathbf{p}_n^+\mathbf{c}_{n+1}^{k+1}(\omega)=0\end{aligned}\tag{2.88}$$

or, on simplification,

$$\begin{aligned}&\mathbf{q}_n^-\mathbf{c}_{n-1}^k(\omega)+\left(\mathbf{q}_n-\tau_N ik\omega\mathbf{I}\right)\mathbf{c}_n^k(\omega)+\mathbf{q}_n^+\mathbf{c}_{n+1}^k(\omega)\\&+\mathbf{p}_n^-\left(\mathbf{c}_{n-1}^{k-1}(\omega)+\mathbf{c}_{n-1}^{k+1}(\omega)\right)+\mathbf{p}_n\left(\mathbf{c}_n^{k-1}(\omega)+\mathbf{c}_n^{k+1}(\omega)\right)\\&+\mathbf{p}_n^+\left(\mathbf{c}_{n+1}^{k-1}(\omega)+\mathbf{c}_{n+1}^{k+1}(\omega)\right)=0,\end{aligned}\tag{2.89}$$

which can be arranged as the supermatrix three-term algebraic recurrence relation,

$$\mathbf{Q}_n^-\mathbf{C}_{n-1}(\omega)+\mathbf{Q}_n(\omega)\mathbf{C}_n(\omega)+\mathbf{Q}_n^+\mathbf{C}_{n+1}(\omega)=0\,,\tag{2.90}$$

where

$$\mathbf{C}_0=\begin{pmatrix}\vdots\\\mathbf{0}\\\mathbf{0}\\\mathbf{c}_0^0\\\mathbf{0}\\\mathbf{0}\\\vdots\end{pmatrix}=\sqrt{\frac{1}{4\pi}}\begin{pmatrix}\vdots\\0\\0\\1\\0\\0\\\vdots\end{pmatrix},\quad \mathbf{C}_n(\omega)=\begin{pmatrix}\vdots\\\mathbf{c}_n^{-2}(\omega)\\\mathbf{c}_n^{-1}(\omega)\\\mathbf{c}_n^0(\omega)\\\mathbf{c}_n^1(\omega)\\\mathbf{c}_n^2(\omega)\\\vdots\end{pmatrix},n=1,2,3,\ldots,\tag{2.91}$$

and the supermatrix coefficients are given by

$$\left(\mathbf{Q}_n\right)_{r,s}=\delta_{r,s-1}\mathbf{p}_n+\delta_{r,s}\left(\mathbf{q}_n-ri\tau_N\omega\mathbf{I}\right)+\delta_{r,s+1}\mathbf{p}_n\,,\tag{2.92}$$

$$\left(\mathbf{Q}_n^{\pm}\right)_{r,s}=\delta_{r,s-1}\mathbf{p}_n^{\pm}+\delta_{r,s}\mathbf{q}_n^{\pm}+\delta_{r,s+1}\mathbf{p}_n^{\pm}\,,\tag{2.93}$$

where $-\infty<r,s<\infty$.

Since Eq. (2.90) is a frequency-dependent matrix three-term recurrence relation, similarly it can be solved using the matrix continued fraction method where we introduce a new function $\mathbf{S}_n(\omega)$ and assume that

$$\mathbf{C}_n(\omega)=\mathbf{S}_n(\omega)\mathbf{Q}_n^-(\omega)\mathbf{C}_{n-1}(\omega)\,.\tag{2.94}$$

By successive iterations of Eq. (2.94) we then have

$$\mathbf{C}_n=\mathbf{S}_n(\omega)\mathbf{Q}_n^-\cdots\mathbf{S}_1(\omega)\mathbf{Q}_1^-\mathbf{C}_0=\left(\prod_{k=0}^{n-1}\mathbf{S}_{n-k}(\omega)\mathbf{Q}_{n-k}^-\right)\mathbf{C}_0\,.\tag{2.95}$$

Now our task is to determine $\mathbf{S}_n(\omega)$. By applying Eq. (2.94) to Eq. (2.90) we have

$$\mathbf{Q}_n^- \mathbf{C}_{n-1} + \mathbf{Q}_n \mathbf{S}_n(\omega) \mathbf{Q}_n^- \mathbf{C}_{n-1} + \mathbf{Q}_n^+ \mathbf{S}_{n+1}(\omega) \mathbf{Q}_{n+1}^- \mathbf{S}_n(\omega) \mathbf{Q}_n^- \mathbf{C}_{n-1} = 0, \tag{2.96}$$

where $\mathbf{S}_n(\omega)$ can be obtained directly as

$$\mathbf{S}_n(\omega) = -\left[\mathbf{Q}_n + \mathbf{Q}_n^+ \mathbf{S}_{n+1}(\omega) \mathbf{Q}_{n+1}^-\right]^{-1}. \tag{2.97}$$

Therefore, by solving this matrix three-term recurrence relation (2.90), we can calculate the coefficients $c_{n,m}^k(\omega)$ which can be used later to calculate the ac stationary response of uniaxial magnetic nanoparticles subjected to strong ac and dc fields.

2.7 Static Susceptibilities

So far the nonlinear response of the permanent electric dipoles with a mean field potential subjected to ac and dc bias fields, the 5-term differential-recurrence relation (2.37) for the averages of the Legendre polynomials $f_n(t)$ has been derived in Section 2.2. Now, we are interested in the equilibrium ensemble averages $f_n(0)$ evaluated by letting the frequency of the ac field tend to zero. The expansions of $f_n(0)$ in terms of ac field strength ξ^k are defined as the static susceptibilities χ_{nk}, which are the initial values of the dynamic susceptibilities $\chi_{nk}(\omega)$ in the frequency domain and will be used to normalize $\chi_{nk}(\omega)$ in the two-mode approximation in Section 2.8. Moreover this method can be applied to the approximation of initial values of the magnetization of the uniaxial superparamagnetic particles in Chapter 5.

As we defined in Section 2.2, $f_n(t)$ is the expectation values of the Legendre polynomials of order n (statistical moments), viz.,

$$f_n(t) = \left\langle P_n(x) \right\rangle(t) = \int_{-1}^{1} W(x,t) P_n(x)\, dx, \tag{2.98}$$

and the equilibrium averages $\langle P_n \rangle_0$ are defined as

$$\langle P_n \rangle_0 = \int_{-1}^{1} W_0(x) P_n(x)\, dx, \tag{2.99}$$

where $W_0(x)$ is the Boltzmann distribution, viz.,

$$W_0(x) = Z^{-1} e^{\sigma x^2 + \xi_0 x}, \tag{2.100}$$

and Z is the partition function, viz.,

$$Z = \int_{-1}^{1} e^{\sigma x^2 + \xi_0 x} dx . \tag{2.101}$$

In the case of superimposed ac and dc fields $\xi_0 + \xi \cos \omega t$ in the static limit, $\omega \to 0$, the initial values $f_n(0)$ to cubic order in ξ are

$$\begin{aligned} f_n(0) &= \frac{\int_{-1}^{1} P_n(x) e^{\sigma x^2 + (\xi+\xi_0)x} dx}{\int_{-1}^{1} e^{\sigma x^2 + (\xi+\xi_0)x} dx} = \frac{\langle P_n \rangle_0 + \xi \langle x P_n \rangle_0 + \frac{1}{2}\xi^2 \langle x^2 P_n \rangle_0 + \frac{1}{6}\xi^3 \langle x^3 P_n \rangle_0 + o(\xi^3)}{1 + \xi \langle x \rangle_0 + \frac{1}{2}\xi^2 \langle x^2 \rangle_0 + \frac{1}{6}\xi^3 \langle x^3 \rangle_0 + o(\xi^3)} \\ &= \langle P_n \rangle_0 + \xi \left(\langle x P_n \rangle_0 - \langle x \rangle_0 \langle P_n \rangle_0 \right) \\ &+ \xi^2 \left[\frac{1}{2} \left(\langle x^2 P_n \rangle_0 - \langle x^2 \rangle_0 \langle P_n \rangle_0 \right) - \langle x \rangle_0 \left(\langle x P_n \rangle_0 - \langle x \rangle_0 \langle P_n \rangle_0 \right) \right] \\ &+ \xi^3 \left[\frac{1}{6} \left(\langle x^3 P_n \rangle_0 - \langle x^3 \rangle_0 \langle P_n \rangle_0 \right) + \langle x \rangle_0 \langle P_n \rangle_0 \left(\langle x^2 \rangle_0 - \langle x \rangle_0^2 \right) \right. \\ &\left. - \frac{1}{2} \langle x \rangle_0 \left(\langle x^2 P_n \rangle_0 - \langle x \rangle_0 \langle x P_n \rangle_0 \right) - \frac{1}{2} \langle x P_n \rangle_0 \left(\langle x^2 \rangle_0 - \langle x \rangle_0^2 \right) \right] + o(\xi^3). \end{aligned} \tag{2.102}$$

Because $P_1(x) = x$ and $P_2(x) = (3x^2 - 1)/2$, we have the first-, second-, and third-order contributions to $f_n(0)$, respectively,

$$f_n^{(1)}(0) = \xi \chi_{n1} = \xi \left(\langle P_1 P_n \rangle_0 - \langle P_1 \rangle_0 \langle P_n \rangle_0 \right), \tag{2.103}$$

$$f_n^{(2)}(0) = \xi^2 \chi_{n2} = \xi^2 \left[\frac{1}{3} \left(\langle P_2 P_n \rangle_0 - \langle P_2 \rangle_0 \langle P_n \rangle_0 \right) - \langle P_1 \rangle_0 \left(\langle P_1 P_n \rangle_0 - \langle P_1 \rangle_0 \langle P_n \rangle_0 \right) \right], \tag{2.104}$$

$$\begin{aligned} f_n^{(3)}(0) = \xi^3 \chi_{n3} = \xi^3 \left[\frac{1}{6} \left(\langle P_1^3 P_n \rangle_0 - \langle P_1^3 \rangle_0 \langle P_n \rangle_0 \right) + \langle P_1 \rangle_0 \langle P_n \rangle_0 \left(\langle P_1^2 \rangle_0 - \langle P_1 \rangle_0^2 \right) \right. \\ \left. - \frac{1}{2} \langle P_1 \rangle_0 \left(\langle P_1^2 P_n \rangle_0 - \langle P_1 \rangle_0 \langle P_1 P_n \rangle_0 \right) - \frac{1}{2} \langle P_1 P_n \rangle_0 \left(\langle P_1^2 \rangle_0 - \langle P_1 \rangle_0^2 \right) \right], \end{aligned} \tag{2.105}$$

where $\chi_{nk}\,(k = 1, 2, 3)$ are the static susceptibilities and the index k in $f_n^{(k)}$ and in χ_{nk} is the order of ξ.

For the zero dc field case, $\xi_0 = 0$, the above results are dramatically simplified. Here, the odd term $f_{2n-1}(0)$ are expressed via the stationary averages up to cubic order in ξ as

$$
\begin{aligned}
f_{2n-1}(0) &= \xi \left\langle x P_{2n-1} \right\rangle_0 + \frac{\xi^3}{6}\left(\left\langle x^3 P_{2n-1} \right\rangle_0 - 3\left\langle x^2 \right\rangle_0 \left\langle x P_{2n-1} \right\rangle_0 \right) + o(\xi^3) \\
&= \xi \left\langle P_1 P_{2n-1} \right\rangle_0 + \frac{\xi^3}{30}\left[2\left\langle P_3 P_{2n-1} \right\rangle_0 - 3\left(5\left\langle P_1^2 \right\rangle_0 + 1 \right) \left\langle P_1 P_{2n-1} \right\rangle_0 \right] + o(\xi^3).
\end{aligned}
\tag{2.106}
$$

Similarly, the even term $f_{2n}(0)$ up to second order in ξ are given by

$$
\begin{aligned}
f_{2n}(0) &= \left\langle P_{2n} \right\rangle_0 + \frac{\xi^2}{2}\left(\left\langle x^2 P_{2n} \right\rangle_0 - \left\langle x^2 \right\rangle_0 \left\langle P_{2n} \right\rangle_0 \right) + o(\xi^2) \\
&= \left\langle P_{2n} \right\rangle_0 + \frac{\xi^2}{3}\left(\left\langle P_2 P_{2n} \right\rangle_0 - \left\langle P_2 \right\rangle_0 \left\langle P_{2n} \right\rangle_0 \right) + o(\xi^2).
\end{aligned}
\tag{2.107}
$$

2.8 Two-Mode Approximation

In a system with several thermal equilibrium states, the linear approximation of the expected value of the relevant dynamical variable in the stationary state is sufficient in the case where the external stimulus is much lower than the thermal energy. As far as the electric dipolar system (cf. Section 2.2) is concerned, the *linear* response of dipoles in a mean field potential comprising an infinity of relaxation modes may be accurately represented by two modes only as demonstrated by Kalmykov *et al.* [3, 37], namely, a slowest interwell barrier crossing mode and a fast mode representing the infinity of high-frequency near-degenerate "intrawell" modes approximated as a single mode. This two-mode approximation combined with Morita's treatment [38, 39] (where the distribution function induced by an ac stimulus may be calculated by the nonperturbative Green function) can then be used to derive the analytical formula for the nonlinear response of permanent electric dipoles as shown in Chapter 4, as well as the dc magnetization of uniaxial magnetic nanoparticles as shown in Chapter 5.

In linear response theory [1], in order to get the linear ac stationary response $f_n^{(1)}(t)$ (the index '(1)' means the response is linear in the ac field ξ), we suppose that a small probing field $\xi_1 \ll 1$ applied along the easy axis at $t = -\infty$ is removed at $t = 0$. The step-off solution $f_{n,off}^{(1)}(t)$ is then given by [3, 38]

$$
f_{n,off}^{(1)}(t) = \xi_1 \chi_{n1} \Phi_{n1}(t), \tag{2.108}
$$

where the normalized equilibrium correlation functions $\Phi_{km}(t)$ are defined as

$$\Phi_{km}(t)=\frac{\langle P_k(t)P_m(0)\rangle_0-\langle P_k(0)\rangle_0\langle P_m(0)\rangle_0}{\langle P_k(0)P_m(0)\rangle_0-\langle P_k(0)\rangle_0\langle P_m(0)\rangle_0}, \tag{2.109}$$

and χ_{n1} is the static susceptibility (see Eq. (2.103))

$$\chi_{n1}=\chi_{n1}(0)=\langle P_nP_1\rangle_0-\langle P_n\rangle_0\langle P_1\rangle_0. \tag{2.110}$$

The Green function (the unit impulse response) of this unperturbed system is the time derivative of the step-on response, viz.,

$$G(t)=-\dot{\Phi}_{n1}(t), \tag{2.111}$$

where the negative sign in front of $\dot{\Phi}_{n1}(t)$ means the field is switched off at $t=0$. Thus the linear ac stationary response to an ac field $\xi(t)$ can be written as

$$f_n^{(1)}(t)=-\chi_{n1}\int_{-\infty}^{t}\dot{\Phi}_{n1}(t-t')\xi(t')dt'. \tag{2.112}$$

If we consider a system in the absence of a dc bias field and write $\xi(t)=\xi e^{i\omega t}$, Eq. (2.112) yields

$$\begin{aligned} f_n^{(1)}(t)&=-\chi_{n1}\xi\int_{-\infty}^{t}\dot{\Phi}_{n1}(t-t')e^{i\omega t'}dt' \\ &=-\chi_{n1}\xi\int_{-\infty}^{t}\dot{\Phi}_{n1}(t')e^{i\omega(t-t')}d(t-t') \\ &=\xi e^{i\omega t}\left(-\chi_{n1}\int_0^{\infty}\dot{\Phi}_{n1}(t')e^{-i\omega t'}dt'\right) \\ &=\xi e^{i\omega t}\chi_{n1}(\omega). \end{aligned} \tag{2.113}$$

Similarly, if we consider a sinusoidal ac field $\xi(t)=\xi\cos\omega t$, we get

$$f_n^{(1)}(t)=\xi\,\mathrm{Re}\left[e^{i\omega t}\chi_{n1}(\omega)\right] \tag{2.114}$$

We introduce the normalized complex susceptibilities $X_{n1}(\omega)=\chi_{n1}(\omega)/\chi_{n1}$ (cf. Eq. (2.113)) via the normalized equilibrium correlation function $\Phi_{n1}(t)$ as

$$X_{n1}(\omega)=\frac{\chi_{n1}(\omega)}{\chi_{n1}}=-\int_0^{\infty}\dot{\Phi}_{n1}(t)e^{-i\omega t}dt=1-i\omega\int_0^{\infty}\Phi_{n1}(t)e^{-i\omega t}dt. \tag{2.115}$$

The time behaviour of $\Phi_{n1}(t)$ is characterized by three time constants, namely the integral relaxation time τ_n defined as the area under the decaying $\Phi_{n1}(t)$,

$$\tau_n = \int_0^\infty \Phi_{n1}(t)\,dt\,, \tag{2.116}$$

the effective relaxation time τ_n^{eff} describing the initial decay of $\Phi_{n1}(t)$ defined by

$$\tau_n^{\text{eff}} = -\frac{1}{\dot{\Phi}_{n1}(0)}\,, \tag{2.117}$$

and the longest relaxation time defined by the inverse of the smallest nonvanishing eigenvalue λ_1 of the Fokker-Planck operator L_{FP} which describes the slowest relaxation mode [1]. When one has, say, a double-well potential, the smallest nonvanishing eigenvalue λ_1 of the system is the sum of long-time rates of escape of particles over the potential barriers. If the potential is symmetric, λ_1 may be approximated by the inverse of the integral relaxation time. This is also true if the imposed field causing the asymmetry in a skewed or biased double-well potential is not too large. Otherwise, the smallest nonvanishing eigenvalue λ_1 will diverge exponentially from the inverse of the integral relaxation time due to the depletion of the population of the shallower of the two wells by the action of the applied field. The critical value of the applied field at which this occurs depends on the shape of the double-well potential and is far less than that needed to entirely destroy the double well structure (i.e, the nucleation field). Now, the low-frequency behaviour of the normalized susceptibility $X_{n1}(\omega)$ is evaluated by taking the low-frequency limit $\omega \to 0$ in Eq. (2.115),

$$X_{n1}(\omega) = 1 - i\omega \int_0^\infty \Phi_{n1}(t)\,dt + \cdots = 1 - i\omega\tau_n + \ldots\,, \tag{2.118}$$

while the high-frequency limit is obtained by taking the limit $\omega \to \infty$,

$$\begin{aligned} X_{n1}(\omega) &= 1 - i\omega \int_0^\infty \Phi_{n1}(t) e^{i\omega t}\,dt \\ &= 1 - i\omega \left[\frac{-\Phi_{n1}(t) e^{-i\omega t}}{i\omega} \bigg|_0^\infty + \int_0^\infty \frac{\dot{\Phi}_{n1}(t) e^{-i\omega t}}{i\omega} dt \right] \\ &= -\frac{\dot{\Phi}_{n1}(0)}{i\omega} + \cdots = -\frac{i}{\omega \tau_n^{\text{eff}}} + \cdots . \end{aligned} \tag{2.119}$$

Thus, the low- and high-frequency behaviour of $X_{n1}(\omega)$ is completely determined by the integral and effective relaxation times, respectively. Hence the equivalent definitions of τ_n and τ_n^{eff} can be given via Eqs. (2.118) and (2.119) as

$$\tau_n = \lim_{\omega\to 0}\frac{X_{n1}(0)-X_{n1}(\omega)}{i\omega},\quad \tau_n^{\text{eff}} = -i\lim_{\omega\to\infty}\frac{1}{\omega X_{n1}(\omega)}. \tag{2.120}$$

Here, the integral and effective relaxation times, τ_n and τ_n^{eff}, are given by the exact analytic equations [1]

$$\tau_n = \frac{2\tau_D}{Z\left(\langle P_nP_1\rangle_0 - \langle P_n\rangle_0\langle P_1\rangle_0\right)}\int_{-1}^{1}\frac{\psi_1(z)\psi_n(z)e^{\sigma z^2+\xi_0 z}}{1-z^2}dz, \tag{2.121}$$

and

$$\tau_n^{\text{eff}} = -\frac{1}{\dot{\Phi}_{n1}(0)} = \frac{\tau_D}{\chi_{n1}}\left[d_n\chi_{n1} + g_n\chi_{n+21} + c_n\chi_{n-21} + \xi_0 a_n\left(\chi_{n+11}-\chi_{n-11}\right)\right], \tag{2.122}$$

where

$$\psi_n(z) = \int_{-1}^{z}\left[P_n(x) - \langle P_n\rangle_0\right]e^{\sigma x^2+\xi_0 x}dx. \tag{2.123}$$

The correlation function $\Phi_{n1}(t)$ generally comprises an infinity of relaxation modes (decaying exponentials), i.e., $\Phi_{n1}(t) = \sum_k c_k^n e^{-\lambda_k t}$. However, we can suppose $\Phi_{n1}(t)$ may be approximated by two modes only [27, 40],

$$\Phi_{n1}(t) = \Delta_{n1}e^{-\lambda_1 t} + (1-\Delta_{n1})e^{-t/\tau_W^{(n1)}}, \tag{2.124}$$

where the parameters Δ_{n1} and $\tau_W^{(n1)}$ are given by

$$\Delta_{n1} = \frac{\tau_n/\tau_n^{\text{eff}} - 1}{\lambda_1\tau_n - 2 + \left(\lambda_1\tau_n^{\text{eff}}\right)^{-1}}, \tag{2.125}$$

$$\tau_W^{(n1)} = \frac{\lambda_1\tau_n - 1}{\lambda_1 - 1/\tau_n^{\text{eff}}}. \tag{2.126}$$

Equations (2.125) and (2.126) are the solutions of algebraic equations obtained by substituting Eq. (2.128) into Eqs. (2.118) and (2.119), viz.

$$\begin{aligned}\Delta_{n1}/\lambda_1 + \left(1-\Delta_n\right)\tau_W^{(n1)} &= \tau_n,\\ \Delta_{n1}\lambda_1 + \left(1-\Delta_{n1}\right)/\tau_W^{(n1)} &= 1/\tau_n^{\text{eff}}.\end{aligned} \tag{2.127}$$

By inserting Eq. (2.124) into Eq. (2.115), $\chi_{n1}(\omega)$ is obtained as the sum of two Lorentzians

$$\frac{\chi_{n1}(\omega)}{\chi_{n1}} = \frac{\Delta_{n1}}{1+i\omega/\lambda_1} + \frac{1-\Delta_{n1}}{1+i\omega\tau_W^{(n1)}}. \tag{2.128}$$

2.9 Anomalous Relaxation

One of the most noteworthy features of the dielectric relaxation of disordered materials and complex liquids such as glass forming liquids, liquid crystals, amorphous polymers, etc. is the failure of the Debye theory [7] of normal dielectric relaxation to adequately describe the low-frequency spectra of their linear dielectric susceptibilities. Our results in Chapters 3 and 4 based on the random walk of rotational Brownian motion where the mean-square displacement of each jump is fixed at fixed time intervals, may be extended to the case of a continuous time random walk where no mean waiting time exists (see Sections 3.5 and 4.7). The relaxation processes in such complex systems are characterized by the temporally nonlocal behaviour arising from the energetic disorder, which produces obstacles or traps, simultaneously delaying the motion of the particle and producing memory effects.

A significant amount of experimental data on anomalous relaxation of complex liquids supports the empirical equation of Havriliak-Negami [41]:

$$\chi_{HN}(\omega) = \frac{\chi_S}{[1+(i\omega\tau_D)^{\alpha}]^{\nu}}, \tag{2.129}$$

where χ_S is the static susceptibility and α $(0 < \alpha \leq 1)$ and ν $(0 < \nu \leq 1)$ are parameters with values which are usually obtained by fitting to experimental data. For the particular cases $\nu = 1$ and $\alpha = 1$, Eq. (2.129) reduces, respectively, to the other well-known phenomenological equations of Cole and Cole [42] and Cole and Davidson [43],

$$\chi_{CC}(\omega) = \frac{\chi_S}{1+(i\omega\tau_D)^{\alpha}}, \tag{2.130}$$

$$\chi_{CD}(\omega) = \frac{\chi_S}{(1+i\omega\tau_D)^{\nu}}. \tag{2.131}$$

In the context of the linear susceptibility, the Cole-Cole parameter α is a *broadening* parameter because the dielectric loss spectrum broadens as α is reduced, while the Cole-Davidson parameter ν in Eqs. (2.129) and (2.131) is a *skewing* parameter. The interested reader can find detailed discussions of anomalous relaxation behaviour in complex disordered systems and various underlying microscopic models in Refs. [1, 24-26, 44-47].

Equations (2.129) - (2.131), which are generalizations of the Debye equation for the complex susceptibility, viz.,

$$\chi_D(\omega) = \frac{\chi_S}{1 + i\omega\tau_D}, \tag{2.132}$$

may be derived using a variety of microscopic models of the relaxation process. For example, Debye [7] extended Einstein's treatment of the translational Brownian motion to the rotational Brownian motion of noninteracting permanent dipoles subjected to an external time-varying field. It might also happen that the motion which prevails is different for different kinds of dipoles. Moreover, both large and small jump transitions may exist simultaneously. The above observations lead us to the second microscopic (relaxator) model considered by Debye [7] (and much extended by Fröhlich [48]), which is a Poisson-like process, where relaxation occurs due to rare members of an assembly of dipoles crossing over a potential barrier by large jumps due to the shuttling action of thermal agitation. This model also produces a relaxation spectrum of the form of Eq. (2.132). However, the overbarrier relaxation time has Arrhenius-like behaviour as it depends exponentially on the height of the potential barrier.

The Cole-Cole, Cole-Davidson, and Havriliak-Negami relaxation processes can be modelled via fractional diffusion equations by using the method of Nigmatullin and Ryabov [49]. According to this approach, the conventional kinetic equation describing the ac stationary response to a forcing function $F(t) = Fe^{i\omega t}$, namely,

$$\left(\tau_D \frac{d}{dt} + 1\right) f(t) = F(t), \tag{2.133}$$

for a system characterized by the single exponential relaxation function $f(t) = e^{-t/\tau_D}$ and, hence, the Debye equation for the complex susceptibility, Eq. (2.132), may be generalized to a fractional kinetic equation of fractional order α, so describing a system with Cole-Cole anomalous relaxation behaviour as [25]

$$\left((\tau_D)^\alpha \, {}_{-\infty}D_t^\alpha + 1\right) f(t) = F(t), \tag{2.134}$$

where the fractional derivative ${}_{-\infty}D_t^\alpha$ is given by the Riemann-Liouville definition [44],

$${}_{-\infty}D_t^\alpha \left[f(t) \right] = \frac{1}{\Gamma(1-\alpha)} \frac{d}{dt} \int_{-\infty}^{t} \frac{f(t')dt'}{(t-t')^\alpha}, \tag{2.135}$$

$\Gamma(z)$ is the gamma function, and $0<\alpha<1$. The physical meaning of the parameter α is the *fractal dimension* of the set of waiting times, which is the scaling of the waiting time segments in the random walk with magnification. The fractional exponent α measures the statistical self-similarity (or how the whole looks similar to its parts) of the waiting time segments [45]. Assuming that the ac field can be written as $F(t)=Fe^{i\omega t}$, the solution of Eq. (2.134) yields the Cole-Cole equation (2.130). In the time domain, the exponential relaxation function $f(t)=e^{-t/\tau_D}$ for the normal diffusion becomes $f(t)=E_\alpha\left[-(t/\tau_D)^\alpha\right]$ for anomalous relaxation, where $E_\alpha(z)$ is the Mittag-Leffler function defined as [44]

$$E_\alpha(z)=\sum_{n=0}^{\infty}\frac{z^n}{\Gamma(1+n\alpha)}. \tag{2.136}$$

The Mittag–Leffler function interpolates between the initial stretched exponential form $E_\alpha[-(t/\tau_{\rm D})^\alpha]\sim e^{-(t/\tau_{\rm D})^\alpha/\Gamma(1+\alpha)}$ and the long-time inverse power-law behaviour $E_\alpha[-(t/\tau_{\rm D})^\alpha]\sim(t/\tau_{\rm D})^{-\alpha}/\Gamma(1-\alpha)$ [1]. In like manner, one may also introduce the fractional kinetic equation [25, 45, 47]

$$\left((\tau_D)^\alpha\,{}_{-\infty}D_t^\alpha+1\right)^\nu f(t)=F(t), \tag{2.137}$$

to incorporate the Havriliak-Negami anomalous relaxation. The fractional derivatives in Eqs. (2.134) and (2.137) are memory functions with a slowly decaying power law kernel in the time. Such behaviour arises from random torques with an anomalous waiting time distribution. We shall demonstrate that the characteristic times of the normal diffusion process, namely τ_n, $\tau_n^{\rm eff}$ and $1/\lambda_1$ allow one to evaluate the nonlinear dielectric and Kerr-effect responses for anomalous diffusion (see Sections 3.5 and 4.7). Moreover, these characteristic times yield simple analytical equations describing the anomalous relaxation of the system. Just as for normal diffusion, the exact solution of the problem reduces to the solution of the infinite hierarchies of differential-recurrence equations for the relevant relaxation functions.

Appendix 2A: Coefficients in the 11-Term Differential-Recurrence Relations

We now write explicitly the coefficients in the 11-term recurrence relation for the response (2.80). Here the superscript *t* denotes the sinusoidal components, σ is the dimensionless

anisotropy parameter, ξ_0 and ξ are external field parameters, α is the damping parameter, and γ_1, γ_2, and γ_3 are the direction cosines of the external fields.

$$x_{n,m} = \frac{\sigma\left[n(n+1)-3m^2\right]}{(2n-1)(2n+3)} - \frac{n(n+1)}{2} - i\frac{m\xi_0\gamma_3}{2\alpha},$$

$$x^t_{n,m} = -i\frac{m\xi\gamma_3}{4\alpha},$$

$$x^{\pm}_{n,m} = \mp i\frac{\xi_0(\gamma_1 \mp i\gamma_2)}{4\alpha}\sqrt{(1+n\pm m)(n\mp m)},$$

$$x^{\pm t}_{n,m} = \mp i\frac{\xi(\gamma_1 \mp i\gamma_2)}{8\alpha}\sqrt{(1+n\pm m)(n\mp m)},$$

$$y_{n,m} = -\left(\frac{\xi_0\gamma_3 n}{2} + \frac{im\sigma}{\alpha}\right)\sqrt{\frac{(n+1)^2-m^2}{(2n+1)(2n+3)}},$$

$$y^t_{n,m} = -\left(\frac{\xi\gamma_3 n}{4}\right)\sqrt{\frac{(n+1)^2-m^2}{(2n+1)(2n+3)}},$$

$$y^{\pm}_{n,m} = \pm\frac{n\xi_0}{4}(\gamma_1 \mp i\gamma_2)\sqrt{\frac{(1+n\pm m)(2+n\pm m)}{(1+2n)(3+2n)}},$$

$$y^{\pm t}_{n,m} = \pm\frac{n\xi}{8}(\gamma_1 \mp i\gamma_2)\sqrt{\frac{(1+n\pm m)(2+n\pm m)}{(1+2n)(3+2n)}},$$

$$w_{n,m} = \left(\frac{(n+1)}{2}\xi_0\gamma_3 - \frac{im\sigma}{\alpha}\right)\sqrt{\frac{n^2-m^2}{4n^2-1}},$$

$$w^t_{n,m} = \frac{\xi\gamma_3(n+1)}{4}\sqrt{\frac{n^2-m^2}{4n^2-1}},$$

$$w^{\pm}_{n,m} = \pm\frac{\xi_0(\gamma_1 \mp i\gamma_2)(n+1)}{4}\sqrt{\frac{(n\mp m)(n\mp m-1)}{4n^2-1}},$$

$$w^{\pm t}_{n,m} = \pm\frac{\xi(\gamma_1 \mp i\gamma_2)(n+1)}{8}\sqrt{\frac{(n\mp m)(n\mp m-1)}{4n^2-1}},$$

$$z_{n,m} = -\frac{\sigma n}{2n+3}\sqrt{\frac{\left[(n+1)^2 - m^2\right]\left[(n+2)^2 - m^2\right]}{(2n+1)(2n+5)}},$$

$$v_{n,m} = \frac{\sigma(n+1)}{2n-1}\sqrt{\frac{\left[(n-1)^2 - m^2\right](n^2 - m^2)}{(2n+1)(2n-3)}}.$$

3 Nonlinear AC Stationary Response of Noninteracting Electric and Magnetic Dipoles

In Chapter 2, the approach to solving the orientation relaxation problem of the electric dipoles is introduced. The response of electric dipoles under the influence of the heat bath and applied fields can be described by the rotational diffusion equation (2.16) or (2.19) (or Smoluchowski equation) which can be reduced to an infinite hierarchy of differential-recurrence equations for the averaged Legendre polynomials, Eq. (2.37), that can be solved numerically with the matrix continued fraction method. Now, in this charpter we will apply Eq. (2.19) to the simplest case of noninteracting dipoles under the influence of strong ac and dc bias fields using the perturbation theory approach.

The theory of electric polarization of dielectric fluids is essential for understanding dielectric and electro-optical relaxation phenomena. This problem was originally treated by Debye [7], who calculated the linear dielectric susceptibility of noninteracting polar molecules subjected to a weak ac electric field $\mathbf{E}(t) = \mathbf{E}\cos\omega t$ using the rotational diffusion model when inertial effects are negligible and the rotation of the molecule can be described by a random walk over small angular orientations. Now, in the linear response, the complex dielectric susceptibility is independent of the electric field strength **E** so that the orientational electric polarization of noninteracting permanent dipoles in an ac field $\mathbf{E}(t)$ depends solely on the first order Legendre polynomial averaged over dipole orientations $\langle P_1(\cos\vartheta)\rangle(t)$, ϑ being the polar angle of the electric dipole moment vector $\boldsymbol{\mu}$ of the molecule. Later, the original Debye calculation was generalized using perturbation theory to nonlinear phenomena in polar dielectrics subjected to strong external fields [50, 51]. In particular, we cite the dynamic Kerr-effect response, governed by the averaged second order Legendre polynomial $\langle P_2(\cos\vartheta)\rangle(t)$, and the nonlinear dielectric effect [2, 51]. The conclusions for the Kerr-effect relaxation in a pure sinusoid electric field are that the square law nonlinearity rectifies $\mathbf{E}(t)$, yielding a frequency-dependent dc response, superimposed on a dephased second harmonic one [2]. In the nonlinear dielectric relaxation, additional terms in the fundamental, third, etc. harmonic appear in $\langle P_1\rangle(t)$ [2, 51]. For example, Coffey and Paranjape [2] have extended the Debye theory to include terms cubic in the applied field using perturbation theory. The small

perturbation parameter is, as usual, the ratio of the interaction energy of a dipole with the applied field to the thermal energy kT (k is the Boltzmann constant and T is the absolute temperature). In particular, they considered the response to a strong alternating (ac) field alone and a weak field superimposed on a strong dc one. In the second of these cases, the ac field was supposed so weak that terms in its square and higher are negligible. The response exhibits typical nonlinear behaviour in so far as it always depends on the *precise form* of the driving fields unlike the linear response. These nonlinear effects have been confirmed by experimental data (e.g., Ref. [10, 11, 52-57]). Additionally, the Debye theory has also been extended to nonlinear effects in dipolar systems in arbitrarily large external fields (see, for example, Refs. [12, 13, 58-60]).

Subsequently, the perturbation calculation was verified numerically for the strong ac field situation by Déjardin and Kalmykov [12] who also considered the *strong* ac and dc field case [13]. They achieved this by solving the differential-recurrence relation generated by the rotational Smoluchowski equation [1] using matrix continued fraction methods in the frequency domain. All the results are summarized in section 7.6 of Ref. [1]. Following the work of Coffey and Paranjape [2], Déjardin *et al.* [8, 14] extended the perturbation calculation to include the *nonlinear* ac terms in the constant plus ac field case, showing that the *combined* effect of the two strong fields is to give rise to additional dispersion and absorption phenomena which do not appear at all when only the linear term in the ac field is considered. These comprise a *time-independent* but *frequency-dependent* dc term in the response, as well as a second harmonic contribution and one at the fundamental frequency which is cubic in the ac field. These terms do not appear if the nonlinear response due to a strong ac field alone is calculated. Despite these novel features in the combined field nonlinear response, experimental investigations of the nonlinear dielectric response seem to have been largely confined to that due to the strong ac field alone. For example, the results of Coffey and Paranjape [2] for the strong ac field have been favourably compared with nonlinear response measurements by De Smet *et al.* [10] and Jadżyn *et al* [11, 56].

Now, for *electric* dipoles, which typically have a small dipole moment, it is often difficult to realize experimentally the strong nonlinear response conditions because of the consequent small value of the interaction energy between a dipole and the electric field. However, in a ferrofluid consisting of blocked single-domain ferromagnetic particles in a colloidal suspension, it is much easier to create the strong nonlinear regime because of the

large magnetic moment, $10^4 \sim 10^5 \ \mu_B$, of such particles. This feature of a typical ferrofluid particle was recognized by Fannin *et al*. [61, 62] who were able to detect nonlinear relaxation effects due to strong ac fields in the magnetic susceptibility of a ferrofluid. The terminology 'blocked' refers to the fact that the solid state-like or Néel [4] magnetization relaxation mechanism over the internal anisotropy-Zeeman energy barriers inside the single domain particle due to the shuttling action of the Brownian motion [4, 6, 63] is assumed to be frozen. Finally, we should recall that the Debye theory is based on the extension of Einstein's theory [1] of the translational Brownian motion to orientational relaxation. Now, that theory pertains to a very large particle of size visible in a microscope (e.g., a pollen grain) immersed in a 'sea' of very small particles. Therefore, one would expect that the ferrofluid situation, where the relaxation effects begin to appear at low MHz frequencies because of the great size of the particles, provides a much more suitable vehicle for the verification of the Debye theory than minute electric dipoles.

Thus, the perturbation calculation of the combined field situation will be revisited with a view towards encouraging the experimental detection of the frequency-dependent dc term, as well as the nonlinear effects due to the interaction of the two fields at the fundamental and second harmonic frequencies, and the term with the fundamental frequency which also appears in the cubic response (see Eq. (3.28)). In particular, we shall highlight the frequency dependence of the dc term and show the calculation of the dynamic Kerr-effect response as well. Additionally, we shall also show how the calculation may be extended to anomalous relaxation governed by a fractional Fokker-Planck equation [1].

3.1 AC Stationary Solution for the Statistical Moments

The basis of the Debye theory [7] of orientational relaxation of polar fluids is the rotational diffusion Smoluchowski equation for the evolution of the probability distribution function $W(\vartheta, t)$ in the configuration space of polar angles of an ensemble of rigid noninteracting electric dipoles of moment $\boldsymbol{\mu}$, undergoing rotational Brownian motion at absolute temperature T under the influence of an external time-varying electric field $\mathbf{E}(t)$ which has been derived in the preview chapter (Section 2.1, Eq. (2.19)), viz.,

$$\frac{\partial W}{\partial t} = \frac{1}{2\tau_D \sin\vartheta} \frac{\partial}{\partial \vartheta} \left[\sin\vartheta \left(\frac{\partial W}{\partial \vartheta} + \frac{1}{kT} W \frac{\partial V}{\partial \vartheta} \right) \right]. \tag{3.1}$$

In Eq. (3.1), $W(\vartheta,t)\sin\vartheta\, d\vartheta$ is the probability that at time t a dipole has an orientation lying between colatitudes ϑ and $\vartheta+d\vartheta$ relative to the direction of $\mathbf{E}(t)$, $V(\vartheta,t)$ is the potential of the dipole due to $\mathbf{E}(t)$, $\tau_D=\varsigma/(2kT)$ is the Debye relaxation time where $\varsigma=8\pi\eta a^3$ is the viscous drag coefficient of a dipole which is treated as a rigid sphere of radius a rotating in a fluid of viscosity η representing all the microscopic degrees of freedom of the surroundings, and $W(\vartheta,t)$ is the surface density of orientations of dipoles on the unit sphere. Here we consider a strong unidirectional field $\mathbf{E}_0$ superimposed on a *strong* alternating field $\mathbf{E}\cos\omega_0 t$, so that

$$V(\vartheta,t)=-\mu E(t)\cos\vartheta=-\mu\left(E_0+E\cos\omega_0 t\right)\cos\vartheta=-\mu E_0\left(1+\lambda\cos\omega_0 t\right)\cos\vartheta, \quad (3.2)$$

where $\lambda=E/E_0$ and ω_0 is the driving frequency. Furthermore, the potential is axially symmetric so that $W(\vartheta,t)$ is independent of the azimuthal angle φ.

The general solution of Eq. (3.1) is of the form of the Fourier series (i.e. substituting Eq. (2.36) into Eq. (2.23)),

$$W(\vartheta,t)=\sum_{n=0}^{\infty}(n+1/2)\,f_n(t)P_n(\cos\vartheta), \quad (3.3)$$

where $f_n(t)=\langle P_n(\cos\vartheta)\rangle(t)$ are the expectation values of the Legendre polynomials of order n (statistical moments) given by Eq. (2.34). Proceeding as in Section 2.2, Eqs. (3.1) - (3.3) reduce to a three-term differential-recurrence relation (i.e. Eq. (2.39)) [1],

$$\frac{d}{dt}f_n(t)=-\frac{n(n+1)}{2\tau_D}\left\{f_n(t)-\frac{\mu E(t)}{kT(2n+1)}\left[f_{n-1}(t)-f_{n+1}(t)\right]\right\}. \quad (3.4)$$

In general, the solution $y(t)$ of the first-order ordinary differential equation,

$$\frac{dy(t)}{dt}+\alpha y(t)=f(t), \quad (3.5)$$

where α is a constant, in $t_0<u<t$ is [64]

$$y(t)=y(t_0)e^{-\alpha(t-t_0)}+\int_{t_0}^{t}e^{-\alpha(t-u)}f(u)\,du. \quad (3.6)$$

Since we confine our attention to the stationary response, the field is assumed to be switched on at the instant $t_0 = -\infty$ so that all the initial effects can be ignored, viz.,

$$\lim_{t_0 \to -\infty} y(t_0) e^{-\alpha(t-t_0)} = 0, \tag{3.7}$$

so that Eq. (3.6) reduces to

$$y(t) = \int_{-\infty}^{t} e^{-\alpha(t-u)} f(u)\, du. \tag{3.8}$$

Similarly Eq. (3.4) has the stationary solution (i.e., pertaining to the forced response) for an arbitrary $\mathbf{E}(t)$ in the form of

$$f_n(t) = \frac{n(n+1)\xi_0}{2\tau_D(2n+1)} \int_{-\infty}^{t} e^{-\frac{n(n+1)}{2\tau}(t-u)} e(u)\left[f_{n-1}(u) - f_{n+1}(u) \right] du. \tag{3.9}$$

While Eq. (3.9) is entirely general, if we consider $V(\vartheta, t)$ given by Eq. (3.2) we would have $e(t) = 1 + \lambda \cos\omega_0 t$ and $\xi_0 = \mu E_0 / (kT)$. Equation (3.9) indicates that, if we can calculate the Fourier coefficients $f_n(t)$ for a given $\mathbf{E}(t)$, we will then have the time evolution of the observables $W(\vartheta, t)$ via Eq. (3.3). Here, our goal is to evaluate the ac stationary response of the electric polarization $P(t)$ and dynamic Kerr effect $K(t)$ ac stationary responses [1, 7], which are defined as

$$P(t) = b_1 \langle P_1(\cos\vartheta) \rangle(t) = b_1 f_1(t), \tag{3.10}$$

$$K(t) = b_2 \langle P_2(\cos\vartheta) \rangle(t) = b_2 f_2(t), \tag{3.11}$$

where the coefficients b_1 and b_2 depend on the concentration of polar particles, particle depolarization factors, the relative permittivity, and other parameters. Here, for simplicity, we assume that $b_1 = 1$ and $b_2 = 1$, i.e., we consider normalized responses only. Furthermore, we suppose that the internal field effects and the long-range torques due to the connection between the dipole moments and the Maxwell fields may be ignored [1]. In the dynamic nonlinear response, these effects present a very difficult problem [65]. However, in the first approximation they may be ignored for dilute systems.

3.2 Successive Approximation Solution for $f_1(t)$ and $f_2(t)$

The rotational diffusion equation (3.1) and its alternative representation as a differential-recurrence relation, Eq. (3.4), (which may also be derived from the appropriate Langevin

equation [1]), although in itself a linear equation, implicitly contains all the nonlinear behaviour. The linear response, which is in the first order of the external field strength, can be enough to describe the dielectric response when the external stimulus is very small compared to the thermal energy. The perturbation procedure to determine corrections to the linear response may be implemented as follows. First we write out the integral equation (3.9) explicitly for the first few $f_n(t)$, viz.

$$f_0 = 1, \tag{3.12}$$

$$f_1(t) = \frac{\xi_0}{3\tau_D}\int_{-\infty}^{t} e^{-\frac{(t-u)}{\tau_D}} e(u)\left[\, f_0 - f_2(u)\right] du\,, \tag{3.13}$$

$$f_2(t) = \frac{3\xi_0}{5\tau_D}\int_{-\infty}^{t} e^{-\frac{3(t-u)}{\tau_D}} e(u)\left[\, f_1(u) - f_3(u)\right] du\,. \tag{3.14}$$

Assuming that $\xi_0 < 1$ in order to maintain convergence, the first approximation of the dielectric response, using Eq. (3.12) and leaving out $f_2(u)$, is

$$f_1(t) = \frac{\xi_0}{3\tau_D}\int_{-\infty}^{t} e^{-\frac{t-u}{\tau_D}} e(u)\, du\,, \tag{3.15}$$

which is the linear solution. Similarly, the first approximation of $f_2(t)$ can be obtained by omitting the term $f_3(t)$ in Eq. (3.14) and replacing the term $f_1(t)$ by Eq. (3.15). Then by substituting this approximation of $f_2(t)$ and Eq. (3.15) into Eq. (3.13), the second approximation of $f_1(t)$ yields

$$f_1(t) = -\frac{\xi_0^3}{15{\tau_D}^3}\int_{-\infty<u_2\le u_1\le u\le t} e^{-\frac{t-u}{\tau_D}} e^{-\frac{3(u-u_1)}{\tau_D}} e^{-\frac{u_1-u_2}{\tau_D}} e(u_2)e(u_1)e(u)\, du_2 du_1 du\,, \tag{3.16}$$

and these successive approximation steps are repeated to get higher order approximations. The formal solutions for $f_1(t)$ and $f_2(t)$ will then be rendered by the perturbation method. We have in general for the dielectric response

$$\begin{aligned} f_1(t) = \frac{\xi_0}{3\tau_D}\Bigg\{ & \int_{-\infty}^{t} e^{-\frac{t-u}{\tau_D}} e(u)\, du \\ & -\frac{\xi_0^2}{5{\tau_D}^2}\int_{-\infty<u_2\le u_1\le u\le t} e^{-\frac{t-u}{\tau_D}} e^{-\frac{3(u-u_1)}{\tau_D}} e^{-\frac{u_1-u_2}{\tau_D}} e(u_2)e(u_1)e(u)\, du_2 du_1 du + \cdots \Bigg\}, \end{aligned} \tag{3.17}$$

and in general for the dynamic Kerr-effect response

$$f_2(t)=\frac{1}{5}\left\{\frac{{\xi_0}^2}{{\tau_D}^2}\int_{-\infty}^{t}\int_{-\infty}^{u} e^{-\frac{3(t-u)}{\tau_D}} e^{-\frac{(u-u_1)}{\tau_D}} e(u_1)e(u)\,du_1 du \right.$$
$$\left. -\frac{18}{35}\frac{{\xi_0}^4}{{\tau_D}^4}\int_{-\infty<u_3\le\cdots\le t} e^{-\frac{3(t-u)}{\tau_D}} e^{-\frac{6(u-u_1)}{\tau_D}} e^{-\frac{3(u_1-u_2)}{\tau_D}} e^{-\frac{(u_2-u_3)}{\tau_D}} e(u_3)e(u_2)e(u)\,du_3\cdots du\ +\ldots\right\}. \tag{3.18}$$

Notice that the leading term in Eq. (3.17) is simply the linear dielectric response, while the Kerr-effect response (3.18) is intrinsically nonlinear due to the product of the stimulus, $\xi_0 e(u)$, with $f_1(u)$ in the leading term of Eq. (3.14). So far the procedure is entirely general. Next we consider the particular time variation given in Eq. (3.2), so that the solutions are best obtained using two sided Fourier transforms.

3.3 Analytical Form of Responses via Fourier Transforms

Before we solve Eqs. (3.17) and (3.18) using the two-sided Fourier transform, we first consider the first order differential equation given by Eqs. (3.5) - (3.8). First, by taking the two-sided Fourier transform of Eq. (3.5), we get

$$Y(\omega)=\frac{F(\omega)}{\mathrm{i}\omega+\alpha}, \tag{3.19}$$

where $Y(\omega)$ and $F(\omega)$ are the Fourier transforms of $y(t)$ and $f(t)$ respectively. If we ignore initial conditions (i.e. the stimulus is applied in the infinite past, see Eq. (3.7)), we can then use Eq. (3.8) to write

$$\mathrm{F}\left\{\int_{-\infty}^{t} e^{-\alpha(t-u)} f(u)\,du\right\}=\frac{F(\omega)}{\mathrm{i}\omega+\alpha}. \tag{3.20}$$

The solution $y(t)$ in the time domain can then be obtained by taking the inverse Fourier Transform of Eq. (3.19), viz.,

$$y(t)=\mathrm{F}^{-1}\{Y(\omega)\}=\frac{1}{2\pi}\int_{-\infty}^{\infty}\frac{F(\omega)}{\mathrm{i}\omega+\alpha}\mathrm{e}^{i\omega t}d\omega. \tag{3.21}$$

Now, in order to solve Eq. (3.17), we start by taking the two-sided Fourier transform of its first term using Eq. (3.20),

$$\mathrm{F}\left\{\left[f_1(t)\right]_1\right\} \equiv \mathrm{F}\left\{\frac{\xi_0}{3\tau_D}\int_{-\infty}^{t} e^{-\frac{(t-u)}{\tau_D}} e(u)\,du\right\} = \frac{\xi_0}{3\tau_D}\frac{E(\omega)}{\mathrm{i}\omega+\tau_D^{-1}}, \tag{3.22}$$

where, for $e(t)=1+\lambda\cos\omega_0 t$,

$$E(\omega)=\mathrm{F}\left\{e(t)\right\}=2\pi\delta(\omega)+\lambda\pi\left[\delta(\omega+\omega_0)+\delta(\omega-\omega_0)\right]. \tag{3.23}$$

Thus, substituting Eq. (3.23) in Eq. (3.22), we get

$$\mathrm{F}\left\{\left[f_1(t)\right]_1\right\} \equiv \frac{\xi_0}{3\tau_D}\frac{2\pi\delta(\omega)+\lambda\pi\left[\delta(\omega+\omega_0)+\delta(\omega-\omega_0)\right]}{\mathrm{i}\omega+\tau_D^{-1}}. \tag{3.24}$$

The first term of the dielectric response in the time domain can then be calculated by taking the inverse Fourier transform of Eq. (3.24),

$$\left[f_1(t)\right]_1 \equiv \frac{1}{2\pi}\int_{-\infty}^{\infty}\frac{\xi_0}{3}\frac{2\pi\delta(\omega)+\lambda\pi\left[\delta(\omega+\omega_0)+\delta(\omega-\omega_0)\right]}{\mathrm{i}\omega\tau_D+1}\mathrm{e}^{i\omega t}d\omega. \tag{3.25}$$

Since

$$\int_{-\infty}^{\infty} f(x)\delta(x-\alpha)\,dx = f(\alpha), \tag{3.26}$$

Eq. (3.25) may be written as

$$\left[f_1(t)\right]_1 \equiv \frac{\xi_0}{3}+\lambda\frac{\xi_0}{3}\left(\frac{\cos\omega_0 t+\omega_0\tau_D\sin\omega_0 t}{1+\omega_0^2\tau_D{}^2}\right). \tag{3.27}$$

The other terms of $f_1(t)$ and terms of $f_2(t)$ can also be obtained in a similar way (see Appendix 3A) and consequently we find, after elementary but tedious manipulations and changing the notation $\omega_0 \to \omega$ for simplification, the nonlinear dielectric response as

$$
\begin{aligned}
f_1(t) = \frac{\xi_0}{3}\Bigg\{ & 1-\frac{\xi_0^2}{15}-\frac{\lambda^2\xi_0^2}{5\left(1+\omega^2{\tau_D}^2\right)}\left(\frac{1}{6}+\frac{3+\omega^2{\tau_D}^2}{9+\omega^2{\tau_D}^2}\right) \\
& +\frac{\lambda}{1+\omega^2{\tau_D}^2}\left[1-\frac{\xi_0^2}{15}\frac{27+\omega^2{\tau_D}^2-2\omega^4{\tau_D}^4}{\left(1+\omega^2{\tau_D}^2\right)\left(9+\omega^2{\tau_D}^2\right)}\right]\cos\omega t \\
& +\frac{\lambda\omega\tau_D}{1+\omega^2{\tau_D}^2}\left[1-\frac{\xi_0^2}{15}\frac{42+19\omega^2{\tau_D}^2+\omega^4{\tau_D}^4}{\left(1+\omega^2{\tau_D}^2\right)\left(9+\omega^2{\tau_D}^2\right)}\right]\sin\omega t \\
& -\frac{\lambda^2\xi_0^2}{90\left(1+\omega^2{\tau_D}^2\right)}\Bigg[\frac{\left(81-153\omega^2{\tau_D}^2-62\omega^4{\tau_D}^4-8\omega^6{\tau_D}^6\right)\cos2\omega t}{\left(1+4\omega^2{\tau_D}^2\right)\left(9+\omega^2{\tau_D}^2\right)\left(1+(4/9)\omega^2{\tau_D}^2\right)} \\
& +\frac{\omega\tau_D\left(252+88\omega^2{\tau_D}^2+16\omega^4{\tau_D}^4\right)\sin2\omega t}{\left(1+4\omega^2{\tau_D}^2\right)\left(9+\omega^2{\tau_D}^2\right)\left(1+(4/9)\omega^2{\tau_D}^2\right)}\Bigg] \\
& -\frac{\lambda^3\xi_0^2}{30\left(1+\omega^2{\tau_D}^2\right)}\Bigg[\frac{\left(27-13\omega^2{\tau_D}^2\right)\cos\omega t}{18\left(1+\omega^2{\tau_D}^2\right)\left(1+(4/9)\omega^2{\tau_D}^2\right)}+\frac{\omega\tau_D\left(21+\omega^2{\tau_D}^2\right)\sin\omega t}{9\left(1+\omega^2{\tau_D}^2\right)\left(1+(4/9)\omega^2{\tau_D}^2\right)} \\
& +\frac{\left(3-17\omega^2{\tau_D}^2\right)\cos3\omega t}{6\left(1+9\omega^2{\tau_D}^2\right)\left(1+(4/9)\omega^2{\tau_D}^2\right)}+\frac{\omega\tau\left(7-3\omega^2{\tau_D}^2\right)\sin3\omega t}{3\left(1+9\omega^2{\tau_D}^2\right)\left(1+(4/9)\omega^2{\tau_D}^2\right)}\Bigg]\Bigg\}+O\left(\xi_0^5\right).
\end{aligned}
\tag{3.28}
$$

and the Kerr-effect response as

$$
\begin{aligned}
f_2(t) = \frac{{\xi_0}^2}{5}\Bigg\{ & \frac{1}{3}+\lambda\frac{2\left(3+\omega^2{\tau_D}^2\right)\cos\omega t+\omega\tau_D\left(5+\omega^2{\tau_D}^2\right)\sin\omega t}{\left(1+\omega^2{\tau_D}^2\right)\left(9+\omega^2{\tau_D}^2\right)} \\
& +\frac{\lambda^2}{6\left(1+\omega^2{\tau_D}^2\right)}\left[1+\frac{\left(1-2\omega^2{\tau_D}^2/3\right)\cos2\omega t+\left(5\omega\tau_D/3\right)\sin2\omega t}{1+4\omega^2{\tau_D}^2/9}\right]\Bigg\}+O\left(\xi_0^4\right).
\end{aligned}
\tag{3.29}
$$

In particular, we are interested in the frequency-dependent dc components of $f_1(t)$ and $f_2(t)$ given by

$$
f_1^{dc}(\omega) = -\frac{\xi^2\xi_0}{15\left(1+\omega^2{\tau_D}^2\right)}\left(\frac{1}{6}+\frac{3+\omega^2{\tau_D}^2}{9+\omega^2{\tau_D}^2}\right), \tag{3.30}
$$

and

$$
f_2^{dc}(\omega) \equiv \frac{\xi^2}{30\left(1+\omega^2{\tau_D}^2\right)}, \tag{3.31}
$$

respectively.

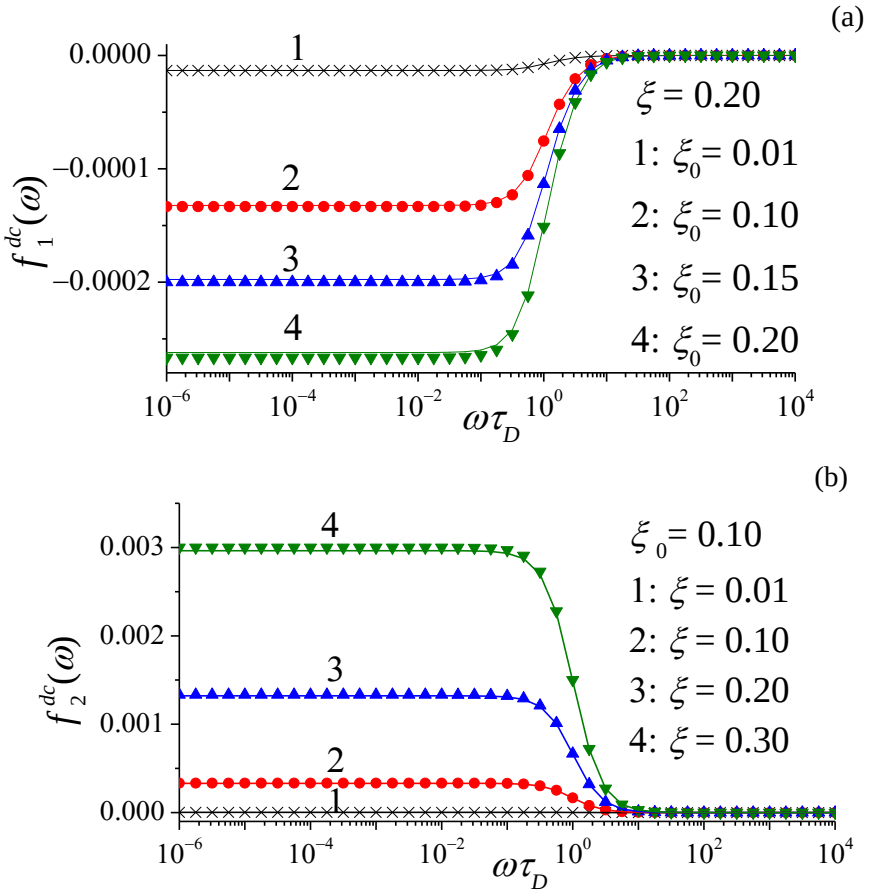

Fig. 3.1. Freqency-dependent dc components of dielectric response $f_1^{dc}(\omega)$ (a) and Kerr-effect response $f_2^{dc}(\omega)$ (b) vs. $\omega\tau_D$ for various values of the ac field amplitude ξ and the dc field amplitude ξ_0 showing pronounced frequency-dependence caused by the strong entanglement of the dc and ac responses. Solid lines: the matrix continued fraction solution in Section 2.3. Symbols: the dc response approximate equations (3.30) and (3.31), respectively.

The observable given by Eq. (3.28) pertains to the normal nonlinear dielectric relaxation of noninteracting rigid dipoles under the combined influence of strong dc bias and ac fields and, with appropriate changes of notation, also pertains to the magnetic relaxation of a blocked ferrofluid. The most striking features of Eq. (3.28), when compared with the single ac field case, are the appearance of a frequency-dependent dc term $O(\lambda^2)$ (see Fig. 3.1), terms in the second harmonic of the applied field $O(\lambda^2)$, and a correction $O(\lambda^3)$ at the fundamental ac frequency to the third harmonic term. In the weak ac and strong dc field case, all that appears is the correction $\lambda\xi_0^2$ at the fundamental frequency to the linear response as well as the frequency independent $\xi_0^2/15$ term due to the action of the strong dc field alone. The frequency-dependent but time-independent term (the first

line of Eq. (3.28)) is also the result previously obtained by Déjardin *et al.* [14] confirming the present perturbation calculation. The appearance of the frequency-dependent dc and the other harmonic terms in Eq. (3.28) alluded to above suggests that experiments like those described in Refs. [61, 62, 66] should be made on ferrofluid systems with the objective of detecting these terms. The methods we have described may be extended to a mean field potential whereupon the integral equation (3.9) above becomes vector-valued (details are available in [3, 23, 67] and Chapter 4 of this thesis).

3.4 Application to Noninteracting Magnetic Dipoles

It is worth noting that, by applying Eq. (3.28) to the magnetization of an assembly of noninteracting magnetic dipoles in superimposed ac and dc fields as in a ferrofluid, it is customary [23] to write the applied field as $\mathbf{H}_0 + \mathbf{H}\cos\omega t$ and the resulting magnetization as

$$M_H(t) = \chi_0(\xi, \xi_0, \omega) + \sum_{k=1}^{\infty} \xi^k \,\mathrm{Re}[\chi_k(\xi, \xi_0, \omega) e^{ik\omega t}], \tag{3.32}$$

where $\xi_0 = \mu_0 \mu H_0 / (kT)$, $\xi = \mu_0 \mu H / (kT)$, the dc term is given by

$$\chi_0(\xi, \xi_0, \omega) = \chi_S H_0 \left[1 - \frac{1}{15}\xi_0^2 - \frac{1}{60}\left(\frac{5}{1+\omega^2\tau_{ND}^2} + \frac{1}{1+\omega^2\tau_{ND}^2/9} \right)\xi^2 + \ldots \right], \tag{3.33}$$

where $\chi_S = N_0 \mu_0 \mu^2 / (3kT)$ is the static susceptibility, μ is the magnitude of the magnetic dipole moment of a ferrofluid particle, and N_0 is the number of particles per unit volume. Here, the Debye relaxation time is now denoted by τ_{ND} in order to distinguish it from the exponentially long overbarrier or Néel relaxation time. By inspection of the first line of Eq. (3.28) with suitable replacements, Eq. (3.33) is entirely equivalent to the dc term of the nonlinear dielectric response.

3.5 Generalization to Anomalous Relaxation

The nonlinear dielectric relaxation treated in previous sections via the rotational diffusion model may be extended to anomalous relaxation by using the fractional kinetic equation approach (see Section 2.9 for detials). Here we only consider as a definite example the Cole-Cole relaxation mechanism given by Eqs. (2.130) and (2.134), and characterized by the anomalous exponent α. Other relaxation mechanisms can be treated in like manner

[26]. The generalization of the theory based on a fractional version of the Smoluchowski equation (3.1), namely,

$$ {}_{-\infty}D_t^{\alpha} W = \frac{1}{2(\tau_D)^{\alpha} \sin\vartheta} \frac{\partial}{\partial \vartheta} \left[\sin\vartheta \left(\frac{\partial W}{\partial \vartheta} + \frac{1}{kT} W \frac{\partial V}{\partial \vartheta} \right) \right], \tag{3.34} $$

has been fully explained in Section 2.9 and Refs. [1, 25, 46]. Here the general solution of Eq. (3.34) is also of the form of the Fourier series, Eq. (3.3). Now, just as for the normal diffusion, we can obtain from Eq. (3.34) the fractional analogue of the recurrence equation (3.4) for the response functions $f_n(t) = \langle P_n(\cos\vartheta) \rangle (t)$ [26],

$$ \left(\tau_{D,n}^{\alpha} \, {}_{-\infty}D_t^{\alpha} + 1 \right) f_n(t) = \frac{\xi_0 + \xi \cos\omega t}{2n+1} \left[f_{n-1}(t) - f_{n+1}(t) \right], \tag{3.35} $$

where $\tau_{D,n}^{\alpha} = 2(\tau_D)^{\alpha} / \left[n(n+1) \right]$ and ${}_{-\infty}D_t^{\alpha}$ is defined by Eq. (2.135). Under linear response conditions, $\xi << 1$, and $\xi_0 = 0$, Eq. (3.35) yields the linear susceptibility from Eq. (2.130). Moreover, just as for the normal diffusion, Eq. (3.35) also allows one to evaluate the nonlinear ac stationary responses (see for details [26]). In particular, we have the generalization of Eq. (3.33), viz.,

$$ \chi_0(\xi, \xi_0, \omega) = \chi_s H_0 \left[1 - \frac{1}{15} \xi_0^2 - \frac{1}{60} \mathrm{Re} \left(\frac{5}{1 + (i\omega\tau_{ND})^{\alpha}} + \frac{1}{1 + (i\omega\tau_{ND})^{\alpha} / 3} \right) \xi^2 + \ldots \right]. \tag{3.36} $$

Such a generalization is likely to be important as the Cole-Cole relaxation behaviour has proved useful in the analysis of magnetic and dielectric relaxation data.

3.6 Conclusion

In this chapter, we have emphasised the rectifying effect of a strong dc bias field superimposed on a strong ac field on the electric polarization (or magnetization) and the Kerr-effect response of an assembly of noninteracting dipolar particles. Furthermore, we have suggested that experiments should be designed to detect the frequency-dependent but time-independent dc component of the nonlinear ac stationary response induced by the bias field (see Eq. (3.28)). In this context, the appearance of individual nonlinear fundamental and third harmonic frequency components in Eq. (3.28) is also important because the latter frequency components may on occasion be easier to detect than the frequency-dependent dc one. Moreover, because they constitute part of the relaxation

process, they will also serve as experimental evidence of a frequency-dependent dc response.

We have also demonstrated how the anomalous nonlinear dielectric and magnetic relaxation can be treated by using fractional kinetic equations. The results obtained can explain the anomalous nonlinear relaxation of complex dipolar systems, where the relaxation process is characterized by a broad distribution of relaxation times (see Eq. (3.36)). The advantage of having kinetic equations incorporating the anomalous relaxation then becomes apparent, as it is now possible to study the effect of the nonlinear anomalous behaviour on fundamental parameters associated with the fractional diffusion. We finally remark that the perturbation method of the calculation of nonlinear ac responses is quite general. The method can also be applied to nonlinear dielectric and Kerr-effect relaxation of molecules under the influence of a mean-field potential. This will be discussed in Chapter 4.

Appendix 3A: Analytical Forms of Responses $f_1(t)$ and $f_2(t)$

In Section 3.3, we only show the calculation of the first term of the dielectric response (3.17). Here we present the details of the calculation of the second term of $f_1(t)$ (cf. Eq. (3.17)) and terms of $f_2(t)$ (cf. Eq. (3.18)) via the Fourier transform method. First we consider the second term of $f_1(t)$ (cf. Eq. (3.17)),

$$\left[f_1(t) \right]_2 = -\frac{\gamma^3}{5\tau_D{}^3} \int\limits_{-\infty<u_2\le u_1\le u\le t} e^{-\frac{(t-u)}{\tau_D}} e^{-\frac{3(u-u_1)}{\tau_D}} e^{-\frac{(u_1-u_2)}{\tau_D}} e(u_2) e(u_1) e(u) du_2 du_1 du \,. \quad \text{(3A.1)}$$

Proceeding as in Section 3.3, Eqs. (3.19) - (3.27), the innermost integral of Eq. (3A.1) becomes

$$\int\limits_{-\infty}^{u_1} e^{-\frac{(u_1-u_2)}{\tau_D}} e(u_2)\, du_2 = \tau_D + \lambda\tau_D \left(\frac{\cos\omega_0 u_1 + \omega_0\tau_D \sin\omega_0 u_1}{1+\omega_0^2\tau_D{}^2} \right). \quad \text{(3A.2)}$$

Substituting the result (3A.2) into Eq. (3A.1), the middle integral of Eq. (3A.1), again proceeding in the way of Fourier transform, becomes

$$
\begin{aligned}
&\int_{-\infty}^{u} e^{-\frac{3(u-u_1)}{\tau_D}} \int_{-\infty}^{u_1} e^{-\frac{(u_1-u_2)}{\tau_D}} e(u_2)\,du_2 e(u_1)\,du_1 \\
&= \int_{-\infty}^{u} e^{-\frac{3(u-u_1)}{\tau_D}} \left(\tau_D + \lambda \tau_D \frac{\cos\omega_0 u_1 + \omega_0 \tau_D \sin\omega_0 u_1}{1+\omega_0^2 {\tau_D}^2} \right) \left(1+\lambda\cos\omega_0 u_1\right) du_1 \\
&= \frac{{\tau_D}^2}{3} + \lambda {\tau_D}^2 \frac{2\left(3+\omega_0^2{\tau_D}^2\right)\cos\omega_0 u + \omega_0\tau_D\left(5+\omega_0^2{\tau_D}^2\right)\cos\omega_0 u}{\left(1+\omega_0^2{\tau_D}^2\right)\left(9+\omega_0^2{\tau_D}^2\right)} \\
&+\lambda^2 \frac{{\tau_D}^2}{6\left(1+\omega_0^2{\tau_D}^2\right)} \left[1 + \frac{\left(1-(2/3)\omega_0^2{\tau_D}^2\right)\cos 2\omega_0 u + (5/3)\omega_0\tau_D \sin 2\omega_0 u}{1+(4/9)\omega_0^2{\tau_D}^2} \right].
\end{aligned}
\tag{3A.3}
$$

Similarly, substituting the result (3A.3) into Eq. (3A.1), the outer integral of Eq. (3A.1) yields

$$
\begin{aligned}
&\int_{-\infty<u_2\le u_1\le u\le t} e^{-\frac{(t-u)}{\tau_D}} e^{-\frac{3(u-u_1)}{\tau_D}} e^{-\frac{(u_1-u_2)}{\tau_D}} e(u_2)e(u_1)e(u)\,du_2 du_1 du \\
&= \frac{{\tau_D}^2}{3}\int_{-\infty}^{t} e^{-\frac{(t-u)}{\tau_D}}\,du + \lambda\frac{{\tau_D}^2}{3}\int_{-\infty}^{t} e^{-\frac{(t-u)}{\tau_D}}\cos\omega_0 u\,du \\
&+\frac{\lambda{\tau_D}^2}{\left(1+\omega_0^2{\tau_D}^2\right)\left(9+\omega_0^2{\tau_D}^2\right)}\int_{-\infty}^{t} e^{-\frac{(t-u)}{\tau_D}}\left[2\left(3+\omega_0^2{\tau_D}^2\right)\cos\omega_0 u + \omega_0\tau_D\left(5+\omega_0^2{\tau_D}^2\right)\sin\omega_0 u\right] du \\
&+\lambda^2\int_{-\infty}^{t} e^{-\frac{(t-u)}{\tau_D}}\left\{\frac{{\tau_D}^2}{6\left(1+\omega_0^2{\tau_D}^2\right)}\left[1+\frac{\left(1-2\omega_0^2{\tau_D}^2/3\right)\cos 2\omega_0 u + 5\omega_0\tau_D\left(\sin 2\omega_0 u\right)/3}{1+4\omega_0^2{\tau_D}^2/9}\right]\right\} du \\
&+\frac{\lambda^2{\tau_D}^2}{\left(1+\omega_0^2{\tau_D}^2\right)\left(9+\omega_0^2{\tau_D}^2\right)}\int_{-\infty}^{t} e^{-\frac{(t-u)}{\tau_D}}\left[2\left(3+\omega_0^2{\tau_D}^2\right)\cos^2\omega_0 u\right. \\
&\left.+\omega_0\tau_D\left(5+\omega_0^2{\tau_D}^2\right)\sin\omega_0 u\cos\omega_0 u\right] du \\
&+\lambda^3\int_{-\infty}^{t} e^{-\frac{(t-u)}{\tau_D}}\left\{\frac{{\tau_D}^2}{6\left(1+\omega_0^2{\tau_D}^2\right)}\left[1+\frac{\left(1-2\omega_0^2{\tau_D}^2/3\right)\cos 2\omega_0 u + 5\omega_0\tau_D\left(\sin 2\omega_0 u\right)/3}{1+4\omega_0^2{\tau_D}^2/9}\right]\right\}\cos\omega_0 u\,du.
\end{aligned}
\tag{3A.4}
$$

Now, proceeding as in Section 3.3, Eqs. (3.19) - (3.27), we can calculate each term of Eq. (3A.4) separately. The first term is

$$
\frac{{\tau_D}^2}{3}\int_{-\infty}^{t} e^{-\frac{(t-u)}{\tau_D}}\,du = \frac{{\tau_D}^2}{3}. \tag{3A.5}
$$

The second term of Eq. (3A.4) is

$$
\lambda\frac{{\tau_D}^2}{3}\int_{-\infty}^{t} e^{-\frac{(t-u)}{\tau_D}}\cos\omega_0 u\,du = \lambda\frac{{\tau_D}^2}{3}\frac{\cos\omega_0 t + \omega_0\tau_D\sin\omega_0 t}{1+\omega_0^2{\tau_D}^2} \tag{3A.6}
$$

The third term of Eq. (3A.4) is calculated as

$$\frac{\lambda {\tau_D}^2}{\left(1+{\omega_0}^2{\tau_D}^2\right)\left(9+\omega_0^2{\tau_D}^2\right)}\int_{-\infty}^{t} e^{-\frac{(t-u)}{\tau_D}}\left[2\left(3+{\omega_0}^2{\tau_D}^2\right)\cos\omega_0 u+\omega_0\tau_D\left(5+{\omega_0}^2{\tau_D}^2\right)\sin\omega_0 u\right]du$$
$$=\lambda\frac{{\tau_D}^3}{\left(1+{\omega_0}^2{\tau_D}^2\right)\left(9+\omega_0^2{\tau_D}^2\right)}\frac{\left[\cos\omega_0 t\left(6-3\omega_0^2{\tau_D}^2-\omega_0^4{\tau_D}^4\right)+\omega_0\tau_D\sin\omega_0 t\left(11+3\omega_0^2{\tau_D}^2\right)\right]}{\left(1+{\omega_0}^2{\tau_D}^2\right)}. \quad (3A.7)$$

The fourth term of Eq. (3A.4) becomes

$$\lambda^2\int_{-\infty}^{t} e^{-\frac{(t-u)}{\tau_D}}\left\{\frac{{\tau_D}^2}{6\left(1+{\omega_0}^2{\tau_D}^2\right)}\left[1+\frac{\left(1-2\omega_0^2{\tau_D}^2/3\right)\cos 2\omega_0 u+5\omega_0\tau_D\left(\sin 2\omega_0 u\right)/3}{1+4\omega_0^2{\tau_D}^2/9}\right]\right\}du$$
$$=\lambda^2\frac{{\tau_D}^2}{6\left(1+{\omega_0}^2{\tau_D}^2\right)}\left\{\int_{-\infty}^{t} e^{-\frac{(t-u)}{\tau_D}}du+\frac{1-2\omega_0^2{\tau_D}^2/3}{1+4\omega_0^2{\tau_D}^2/9}\int_{-\infty}^{t} e^{-\frac{(t-u)}{\tau_D}}\cos 2\omega_0 u du\right.$$
$$\left.+\frac{5\omega_0\tau_D/3}{1+4\omega_0^2{\tau_D}^2/9}\int_{-\infty}^{t} e^{-\frac{(t-u)}{\tau_D}}\sin 2\omega_0 u du\right\} \quad (3A.8)$$
$$=\lambda^2\frac{{\tau_D}^3}{6\left(1+{\omega_0}^2{\tau_D}^2\right)}\left\{1+\frac{\cos 2\omega_0 t\left(1-4\omega_0^2{\tau_D}^2\right)+\omega_0\tau_D\sin 2\omega_0 t\left(11/3-4\omega_0^2{\tau_D}^2/3\right)}{\left(1+4\omega_0^2{\tau_D}^2/9\right)\left(1+4\omega_0^2{\tau_D}^2\right)}\right\}.$$

The fifth term of Eq. (3A.4) becomes

$$\frac{\lambda^2{\tau_D}^2}{\left(1+{\omega_0}^2{\tau_D}^2\right)\left(9+\omega_0^2{\tau_D}^2\right)}\int_{-\infty}^{t} e^{-\frac{(t-u)}{\tau_D}}\left[2\left(3+{\omega_0}^2{\tau_D}^2\right)\cos^2\omega_0 u\right.$$
$$\left.+\omega_0\tau_D\left(5+{\omega_0}^2{\tau_D}^2\right)\sin\omega_0 u\cos\omega_0 u\right]du$$
$$=\frac{\lambda^2{\tau_D}^2\left(3+{\omega_0}^2{\tau_D}^2\right)}{\left(1+{\omega_0}^2{\tau_D}^2\right)\left(9+\omega_0^2{\tau_D}^2\right)}\int_{-\infty}^{t} e^{-\frac{(t-u)}{\tau_D}}\left(\cos 2\omega_0 u+1\right)du$$
$$+\frac{\lambda^2{\tau_D}^2\omega_0\tau_D\left(5+{\omega_0}^2{\tau_D}^2\right)}{2\left(1+{\omega_0}^2{\tau_D}^2\right)\left(9+\omega_0^2{\tau_D}^2\right)}\int_{-\infty}^{t} e^{-\frac{(t-u)}{\tau_D}}\sin 2\omega_0 u du \quad (3A.9)$$
$$=\frac{\lambda^2{\tau_D}^3}{\left(1+{\omega_0}^2{\tau_D}^2\right)\left(9+\omega_0^2{\tau_D}^2\right)}\left[\left(3+{\omega_0}^2{\tau_D}^2\right)+\frac{\cos 2\omega_0 t\left(3-4\omega_0^2{\tau_D}^2-\omega_0^4{\tau_D}^4\right)}{1+4\omega_0^2{\tau_D}^2}\right.$$
$$\left.+\frac{\omega_0\tau_D\sin 2\omega_0 t\left(17/2+5\omega_0^2{\tau_D}^2/2\right)}{1+4\omega_0^2{\tau_D}^2}\right].$$

Finally the sixth term in Eq. (3A.4) becomes

$$\lambda^3 \int_{-\infty}^{t} e^{-\frac{(t-u)}{\tau_D}} \left\{ \frac{{\tau_D}^2}{6\left(1+{\omega_0}^2{\tau_D}^2\right)} \right.$$
$$\left. \times \left[1+\frac{\left(1-2\omega_0^2{\tau_D}^2/3\right)\cos 2\omega_0 u + 5\omega_0\tau_D\left(\sin 2\omega_0 u\right)/3}{1+4\omega_0^2{\tau_D}^2/9} \right] \right\} \cos\omega_0 u du$$
$$= \frac{\lambda^3 {\tau_D}^3}{6\left(1+{\omega_0}^2{\tau_D}^2\right)} \left\{ \frac{\cos\omega_0 t\left(27-13\omega_0^2{\tau_D}^2\right)+\omega_0\tau_D\sin\omega_0 t\left(42+2\omega_0^2{\tau_D}^2\right)}{18\left(1+\omega_0^2{\tau_D}^2\right)\left(1+4\omega_0^2{\tau_D}^2/9\right)} \right.$$
$$\left. + \frac{\cos 3\omega_0 t\left(3-17\omega_0^2{\tau_D}^2\right)/2+\omega_0\tau_D\left(7-3\omega_0^2{\tau_D}^2\right)\sin 3\omega_0 t}{3\left(1+4\omega_0^2{\tau_D}^2/9\right)\left(1+9\omega_0^2{\tau_D}^2\right)} \right\}. \tag{3A.10}$$

Thus, by substituting Eqs. (3A.5) - (3A.10) into Eq. (3A.4) we can get the second term of $f_1(t)$. Therefore the third order approximation of $f_1(t)$ is obtained as the sum of this second term and the first term given by Eq. (3.27), viz.

$$f_1(t) = \frac{\xi_0}{3}\left\{1-\frac{\xi_0^2}{15}-\frac{\lambda^2\xi_0^2}{5\left(1+{\omega_0}^2{\tau_D}^2\right)}\left(\frac{1}{6}+\frac{3+{\omega_0}^2{\tau_D}^2}{9+{\omega_0}^2{\tau_D}^2}\right)\right.$$
$$+\frac{\lambda}{1+{\omega_0}^2{\tau_D}^2}\left[1-\frac{\xi_0^2}{15}\frac{27+{\omega_0}^2{\tau_D}^2-2{\omega_0}^4{\tau_D}^4}{\left(1+{\omega_0}^2{\tau_D}^2\right)\left(9+{\omega_0}^2{\tau_D}^2\right)}\right]\cos\omega_0 t$$
$$+\frac{\lambda\omega_0\tau_D}{1+{\omega_0}^2{\tau_D}^2}\left[1-\frac{\xi_0^2}{15}\frac{42+19{\omega_0}^2{\tau_D}^2+{\omega_0}^4{\tau_D}^4}{\left(1+{\omega_0}^2{\tau_D}^2\right)\left(9+{\omega_0}^2{\tau_D}^2\right)}\right]\sin\omega_0 t$$
$$-\frac{\lambda^2\xi_0^2}{90\left(1+{\omega_0}^2{\tau_D}^2\right)}\left[\frac{\left(81-153{\omega_0}^2{\tau_D}^2-62{\omega_0}^4{\tau_D}^4-8{\omega_0}^6{\tau_D}^6\right)\cos 2\omega_0 t}{\left(1+4{\omega_0}^2{\tau_D}^2\right)\left(9+{\omega_0}^2{\tau_D}^2\right)\left(1+(4/9){\omega_0}^2{\tau_D}^2\right)}\right.$$
$$\left.+\frac{\omega_0\tau_D\left(252+88{\omega_0}^2{\tau_D}^2+16{\omega_0}^4{\tau_D}^4\right)\sin 2\omega_0 t}{\left(1+4{\omega_0}^2{\tau_D}^2\right)\left(9+{\omega_0}^2{\tau_D}^2\right)\left(1+(4/9){\omega_0}^2{\tau_D}^2\right)}\right]$$
$$-\frac{\lambda^3\xi_0^2}{30\left(1+{\omega_0}^2{\tau_D}^2\right)}\left[\frac{\left(27-13{\omega_0}^2{\tau_D}^2\right)\cos\omega_0 t}{18\left(1+{\omega_0}^2{\tau_D}^2\right)\left(1+(4/9){\omega_0}^2{\tau_D}^2\right)}+\frac{\omega_0\tau_D\left(21+{\omega_0}^2{\tau_D}^2\right)\sin\omega_0 t}{9\left(1+{\omega_0}^2{\tau_D}^2\right)\left(1+(4/9){\omega_0}^2{\tau_D}^2\right)}\right.$$
$$\left.\left.+\frac{\left(3-17{\omega_0}^2{\tau_D}^2\right)\cos 3\omega_0 t}{6\left(1+9{\omega_0}^2{\tau_D}^2\right)\left(1+(4/9){\omega_0}^2{\tau_D}^2\right)}+\frac{\omega_0\tau\left(7-3{\omega_0}^2{\tau_D}^2\right)\sin 3\omega_0 t}{3\left(1+9{\omega_0}^2{\tau_D}^2\right)\left(1+(4/9){\omega_0}^2{\tau_D}^2\right)}\right]\right\}+O\left(\xi_0^5\right). \tag{3A.11}$$

Now we consider the analytical form of the Kerr effect $f_2(t)$ by evaluating only the first term in Eq. (3.18), viz.

$$f_2(t) = \frac{1}{5}\frac{{\xi_0}^2}{{\tau_D}^2}\int_{-\infty<u_1\le u\le t} e^{-\frac{3(t-u)}{\tau_D}} e^{-\frac{(u-u_1)}{\tau_D}} e(u_1)e(u)du_1 du. \tag{3A.12}$$

Now, proceeding as in Section 3.3, Eqs. (3.19) - (3.27), the inner integral of Eq. (3A.12) becomes

$$\begin{aligned}\int_{-\infty}^{u} e^{-\frac{(u-u_1)}{\tau_D}} e(u_1)\,du_1 &= \int_{-\infty}^{u} e^{-\frac{(u-u_1)}{\tau_D}} \left(1+\lambda\cos\omega_0 u_1\right) du_1 \\ &= \tau_D + \lambda\tau_D\left(\frac{\cos\omega_0 u + \omega_0\tau_D \sin\omega_0 u}{1+\omega_0{}^2\tau_D{}^2}\right),\end{aligned} \tag{3A.13}$$

so that the outer integral of Eq. (3A.12) becomes

$$\begin{aligned}e(u)\left[\int_{-\infty}^{u} e^{-\frac{(u-u_1)}{\tau_D}} e(u_1)\,du_1\right] &= \left(1+\lambda\cos\omega_0 u\right)\left[\tau_D + \lambda\tau_D\left(\frac{\cos\omega_0 u + \omega_0\tau_D\sin\omega_0 u}{1+\omega_0{}^2\tau_D{}^2}\right)\right] \\ &= \tau_D + \lambda\tau_D\left(\frac{\cos\omega_0 u + \omega_0\tau_D\sin\omega_0 u}{1+\omega_0{}^2\tau_D{}^2}\right) + \lambda\tau_D\cos\omega_0 u \\ &\quad + \lambda^2\tau_D\left(\frac{\cos^2\omega_0 u + \omega_0\tau_D\sin\omega_0 u\cos\omega_0 u}{1+\omega_0{}^2\tau_D{}^2}\right).\end{aligned} \tag{3A.14}$$

Thus, by substituting Eq. (3A.14) into Eq. (3A.12), the first term approximation of $f_2(t)$ yields

$$\begin{aligned}f_2(t) = \frac{1}{5}\frac{\xi_0{}^2}{\tau_D{}^2}\Bigg\{&\int_{-\infty}^{t} e^{-\frac{3(t-u)}{\tau_D}}\tau_D du + \int_{-\infty}^{t} e^{-\frac{3(t-u)}{\tau_D}}\lambda\tau_D\cos\omega_0 u\,du \\ &+ \int_{-\infty}^{t} e^{-\frac{3(t-u)}{\tau_D}}\lambda\tau_D\left(\frac{\cos\omega_0 u + \omega_0\tau_D\sin\omega_0 u}{1+\omega_0{}^2\tau_D{}^2}\right)du \\ &+ \int_{-\infty}^{t} e^{-\frac{3(t-u)}{\tau_D}}\lambda^2\tau_D\left(\frac{\cos^2\omega_0 u + \omega_0\tau_D\sin\omega_0 u\cos\omega_0 u}{1+\omega_0{}^2\tau_D{}^2}\right)du\Bigg\}.\end{aligned} \tag{3A.15}$$

Again proceeding as in Section 3.3, Eqs. (3.19) - (3.27), the first term of Eq. (3A.15) becomes

$$\int_{-\infty}^{t} e^{-\frac{3(t-u)}{\tau_D}}\tau_D du = \frac{\tau_D{}^2}{3}. \tag{3A.16}$$

The second term of Eq. (3A.15) becomes

$$\int_{-\infty}^{t} e^{-\frac{3(t-u)}{\tau_D}}\lambda\tau_D\cos\omega_0 u\,du = \frac{\lambda\tau_D}{2(9/\tau_D{}^2+\omega_0^2)}\left(6\left(\cos\omega_0 t\right)/\tau_D + 2\omega_0\sin\omega_0 t\right), \tag{3A.17}$$

using

$$\mathrm{F}\left\{\cos\omega_0 u\right\} = \pi\left[\delta(\omega+\omega_0)+\delta(\omega-\omega_0)\right]. \tag{3A.18}$$

The third term of Eq. (3A.15) becomes

$$\begin{aligned}&\int_{-\infty}^{t} e^{-\frac{3(t-u)}{\tau_D}} \lambda\tau_D \left(\frac{\cos\omega_0 u + \omega_0\tau_D \sin\omega_0 u}{1+{\omega_0}^2{\tau_D}^2} \right) du \\ &= \frac{\lambda\tau_D}{1+{\omega_0}^2{\tau_D}^2} \left[\int_{-\infty}^{t} e^{-\frac{3(t-u)}{\tau_D}} \cos\omega_0 u du + \int_{-\infty}^{t} e^{-\frac{3(t-u)}{\tau_D}} \omega_0\tau_D \sin\omega_0 u du \right].\end{aligned} \tag{3A.19}$$

As the first term of Eq. (3A.19) has been given by Eq. (3A.17), we only need to consider the second term so that, by using

$$\mathrm{F}\left\{\sin\omega_0 u\right\} = \frac{\pi}{i}\left[\delta(\omega-\omega_0) - \delta(\omega+\omega_0)\right] \tag{3A.20}$$

and proceeding as in Section 3.3, Eqs. (3.19) - (3.21), we have the second term of Eq. (3A.19),

$$\int_{-\infty}^{t} e^{-\frac{3(t-u)}{\tau_D}} \omega_0\tau_D \sin\omega_0 u du = \frac{-2\omega_0^2\tau_D \cos\omega_0 t + 6\omega_0 \sin\omega_0 t}{2(9/{\tau_D}^2 + \omega_0^2)}. \tag{3A.21}$$

Thus the third term in Eq. (3A.15) is evaluated from Eqs. (3A.17) - (3A.21) as

$$\begin{aligned}&\frac{\lambda\tau_D}{1+{\omega_0}^2{\tau_D}^2} \left[\int_{-\infty}^{t} e^{-\frac{3(t-u)}{\tau_D}} \cos\omega_0 u du + \int_{-\infty}^{t} e^{-\frac{3(t-u)}{\tau_D}} \omega_0\tau_D \sin\omega_0 u du \right] \\ &= \frac{\lambda\tau_D \left[\cos\omega_0 t\left(6/\tau_D - 2\omega_0^2\tau_D\right) + \left(\sin\omega_0 t\right) 8\omega_0 \right]}{2\left(1+{\omega_0}^2{\tau_D}^2\right)\left(9/{\tau_D}^2 + \omega_0^2\right)}.\end{aligned} \tag{3A.22}$$

Proceeding as in Section 3.3, Eqs. (3.19) - (3.27), we get the fourth term of Eq. (3A.15)

$$\begin{aligned}&\int_{-\infty}^{t} e^{-\frac{3(t-u)}{\tau_D}} \lambda^2\tau_D \left(\frac{\cos^2\omega_0 u + \omega_0\tau_D \sin\omega_0 u \cos\omega_0 u}{1+{\omega_0}^2{\tau_D}^2} \right) du \\ &= \frac{\lambda^2\tau_D}{2\left(1+{\omega_0}^2{\tau_D}^2\right)} \int_{-\infty}^{t} e^{-\frac{3(t-u)}{\tau_D}} \left(1+\cos 2\omega_0 u + \omega_0\tau_D \sin 2\omega_0 u\right) du \\ &= \frac{\lambda^2\tau_D}{2\left(1+{\omega_0}^2{\tau_D}^2\right)} \left\{ \frac{\tau_D}{3} + \frac{\tau_D}{6} \left[\frac{\left(1-i\omega_0\tau_D\right)\mathrm{e}^{i2\omega_0 t}}{i2\omega_0\tau_D/3+1} + \frac{\left(1+i\omega_0\tau_D\right)\mathrm{e}^{-i2\omega_0 t}}{-i2\omega_0\tau_D/3+1} \right] \right\}.\end{aligned} \tag{3A.23}$$

Obviously the second and third terms in Eq. (3A.23) are complex conjugates so that Eq. (3A.23) is reduced to

$$\int_{-\infty}^{t} e^{-\frac{3(t-u)}{\tau_D}} \lambda^2 \tau_D \left(\frac{\cos^2 \omega_0 u + \omega_0 \tau_D \sin \omega_0 u \cos \omega_0 u}{1+\omega_0{}^2 \tau_D{}^2} \right) du$$
$$= \frac{\lambda^2 \tau_D{}^2}{6\left(1+\omega_0{}^2 \tau_D{}^2\right)} \left\{ 1 + \frac{\left(1-2\omega_0^2 \tau_D{}^2/3\right)\cos 2\omega_0 t + 5\omega_0 \tau_D \left(\sin 2\omega_0 t\right)/3}{1+4\omega_0^2 \tau_D{}^2/9} \right\}. \quad \text{(3A.24)}$$

Finally, we can substitute these four terms, i.e. Eqs. (3A.16), (3A.17), (3A.22), and (3A.24), into Eq. (3A.15) to get the second order approximation of $f_2(t)$ by evaluating the first term of Eq. (3.29) only, viz.

$$f_2(t) = \frac{\xi_0{}^2}{5} \left\{ \frac{1}{3} + \lambda \frac{2\left(3+\omega_0{}^2 \tau_D{}^2\right)\cos \omega_0 t + \omega_0 \tau_D \left(5+\omega_0{}^2 \tau_D{}^2\right)\sin \omega_0 t}{\left(1+\omega_0{}^2 \tau_D{}^2\right)\left(9+\omega_0^2 \tau_D{}^2\right)} \right.$$
$$\left. + \frac{\lambda^2}{6\left(1+\omega_0{}^2 \tau_D{}^2\right)} \left[1 + \frac{\left(1-2\omega_0^2 \tau_D{}^2/3\right)\cos 2\omega_0 t + 5\omega_0 \tau_D \left(\sin 2\omega_0 t\right)/3}{1+4\omega_0^2 \tau_D{}^2/9} \right] \right\} + O\left(\xi_0{}^4\right). \quad \text{(3A.25)}$$

4 AC Stationary Response of Permanent Electric Dipoles in the Mean Field Potential

In chapter 3, the Debye theory [7] of dielectric relaxation of noninteracting rigid electric dipoles under the *combined* influence of a time varying and a dc bias applied fields was extended to consider the nonlinear effects of a strong ac and dc bias field using perturbation theory, following the method of Coffey and Paranjape [2]. Nevertheless, these calculations still assume assemblies of noninteracting dipoles, implying that the Debye model and its extensions may not be used for dense dipolar systems, where intermolecular interactions occur. However, experimental data of such dipolar systems may be explained using a more sophisticated model of the noninertial rotational Brownian motion of dipoles in an external mean field potential V (e.g., [68-72]). In particular, this mean field approximation was used to treat nematic liquid crystals in Refs. [70-72], where the linear dielectric response was calculated via the rotational Brownian motion in the Maier-Saupe uniaxial anisotropy potential

$$V = -K\cos^2\vartheta. \tag{4.1}$$

Here K is the anisotropy constant and ϑ is the colatitude, i.e., the angle between $\boldsymbol{\mu}$ and the Z-axis of the laboratory coordinate system. The mean field approximation has a restricted applicability because it ignores local order effects. Nevertheless, it is easily visualized and permits quantitative evaluation of dielectric parameters, so demonstrating the effect of intermolecular interactions on dielectric parameters that must be accounted for to agree with experimental results [73, 74].

Now, the theory of dielectric relaxation of nematic liquid crystals bears a close resemblance to the theory of magnetic relaxation of single domain ferromagnetic particles as formulated by Brown [6], which we will use to investigate the dc magnetization in the next chapter. Brown's major contribution to this theory was the derivation of the Fokker-Planck equation (2.57) for the distribution function of the particle magnetic moment orientations on the unit sphere. For the longitudinal relaxation in uniaxial magnetic nanoparticles, this Fokker-Planck equation becomes mathematically identical to that used in the theory of dielectric relaxation of nematic liquid crystals [1], Eq. (2.19). Various numerical methods have also been developed [18, 21, 23, 75] for calculating the nonlinear

ac stationary response of dipolar molecules (electric dipoles) in the Maier-Saupe uniaxial potential, Eq. (4.1), and for that of uniaxial magnetic nanoparticles (magnetic dipoles), which, in most respects, is just a replica of dielectric relaxation of nematics. Such numerical approaches cannot yield, however, simple formulas for comparison with experiments and the qualitative behaviour of the nonlinear response is not obvious. Preliminary steps towards an accurate analytical treatment of the nonlinear response of dipoles in the uniaxial potential, Eq. (4.1), were made in Refs. [3, 67] (see also Chapter 3), showing that the nonlinear response to an ac driving field $\mathbf{E}(t)$ can be evaluated by utilizing the so-called two-mode approximation [1, 37, 40] (see Eqs. (4.33) and (4.34)) combined with Morita's treatment [38, 39] of the nonlinear response of dipolar systems, whereby the distribution function induced by an external perturbing field may be calculated from the appropriate Green function in the absence of the perturbation, with the linear response theory as a special case, which we showed in Section 2.8. Thus the *linear* response of dipoles in a mean field potential comprising an infinity of relaxation modes may be accurately represented by two modes only [1, 37, 40], namely, a slowest interwell barrier crossing mode and a fast mode representing the infinity of high-frequency near-degenerate "intrawell" modes approximated as a single mode. Here we generalize this approach [3, 37, 40, 67] to include the effects of an external dc bias field on the *nonlinear* ac stationary response of a system of permanent dipoles in the uniaxial mean field potential, Eq. (4.1). Both matrix perturbation and analytical solutions are given for the ac stationary response of the first- and second-rank response functions, $\langle P_1(\cos\vartheta)\rangle(t)$ and $\langle P_2(\cos\vartheta)\rangle(t)$, determining, respectively, the nonlinear dielectric and Kerr-effect responses. Our calculations are, in particular, motivated by recent measurements of the nonlinear frequency-dependent polarization response in strong dc electric fields [76], where the influence of the dc field on the glass temperature T_g of glycerol was demonstrated, showing that T_g increases in proportion with the square of the dc field amplitude. Hence an accurate representation of the nonlinear components of the ac stationary dielectric response spectrum is required in order to compare with experimental data [76, 77].

4.1 Noninertial Rotational Diffusion Model in the Mean Field Potential

We shall consider the nonlinear ac stationary response of a rigid dipolar particle undergoing rotational Brownian motion in a mean field potential, Eq. (4.1), acted on by strong external superimposed dc $\mathbf{E}_0$ and ac $\mathbf{E}(t) = \mathbf{E}\cos\omega t$ fields. Each particle contains a rigid dipole $\boldsymbol{\mu}$. For simplicity we suppose that both $\mathbf{E}_0$ and $\mathbf{E}$ are directed along the *Z*-axis of the laboratory coordinate system so that the potential will be polar angle dependent only. Effects due to the anisotropy of the polarizability of the particles can also be neglected when only permanent dipoles are considered (no induced dipoles). The calculation of the nonlinear ac stationary response of permanent dipoles to an ac driving field usually starts with the rotational diffusion or Smoluchowski equation for the distribution function $W(\boldsymbol{\mu}, t)$ of orientations of dipole moments $\boldsymbol{\mu}$ on the surface of the unit sphere under the influence of external electric fields [1] (see Section 2.1), which in this case we write as,

$$\frac{\partial W}{\partial t} = L_{FP}W + L_t W\,, \tag{4.2}$$

where

$$L_{FP}W = (2\tau_D)^{-1}\left[\Delta W + \beta\nabla\cdot\left(W\nabla V\right)\right], \tag{4.3}$$

is the unperturbed Fokker-Planck operator, which contains the effect of the potential *V* due to the mean field and the time-independent dc bias field, while

$$L_t W = (2\tau_D)^{-1}\beta\nabla\cdot\left(W\nabla V_t\right), \tag{4.4}$$

contains the effect of the time-dependent potential V_t due to the ac field $\mathbf{E}(t)$. Here ∇ and Δ are the gradient and Laplacian on the surface of the unit sphere, defined by Eqs. (2.17) and (2.18) respectively, τ_D is the Debye relaxation time, and $\beta = (kT)^{-1}$ is the inverse thermal energy. When the superimposed effective field (due to the uniaxial anisotropy) and external dc bias field $\mathbf{E}_0$ are directed along the *Z*-axis of the laboratory coordinate system, the axially symmetric potential $V(\vartheta)$ is given by

$$\beta V(\vartheta) = -\sigma\cos^2\vartheta - \xi_0\cos\vartheta\,, \tag{4.5}$$

where $\sigma = \beta K$ is the dimensionless anisotropy or inverse temperature parameter (K is the anisotropy constant, see Eq. (4.1)) and $\xi_0 = \beta\mu E_0$ is the dimensionless dc bias field parameter. The time-dependent ac field is assumed to be parallel to the dc bias field so that

$$\beta V_t(\vartheta, t) = -\xi \cos\vartheta \cos\omega t\,, \tag{4.6}$$

where $\xi = \beta\mu E$ is the dimensionless ac field parameter.

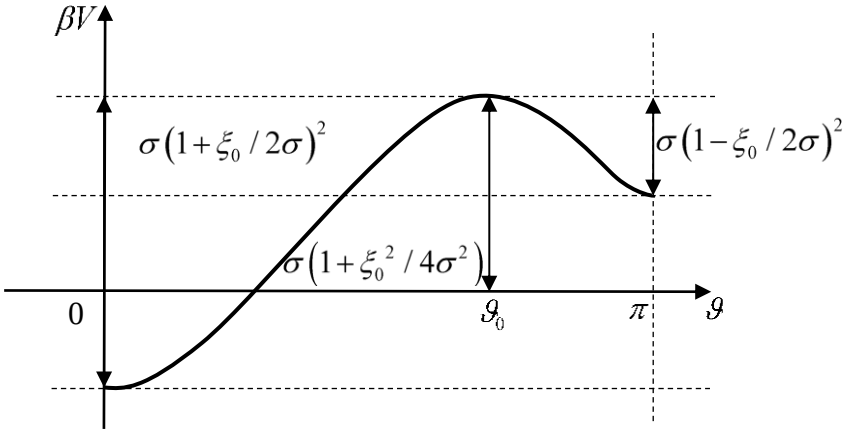

Fig. 4.1. The profile of the uniaxial potential, Eq. (4.5), which has two non-equivalent wells with minima at $\vartheta = 0$ and π separated by a barrier at $\vartheta_0 = \arccos(-\xi_0/2\sigma)$. For a positive, finite dc field, $\xi_0 > 0$, the dipoles in the shallower well at $\vartheta = \pi$ are inhibited from crossing into the deeper well by the potential barrier of height $\sigma(1-\xi_0/2\sigma)^2$. However, the dipoles populating the deeper well at $\vartheta = 0$ have smaller probability to escape from the well, owing to the elevated potential barrier height $\sigma(1+\xi_0/2\sigma)^2$. Thus the escape rate strongly depends on the dc field strength which affects the orientational relaxation and, hence, the dielectric and Kerr-effect responses.

As discussed in Section 2.2, the Smoluchowski equation (4.2) can be written in the form of a differential-recurrence relation for the expectation values of the Legendre polynomials $f_n(t) = \langle P_n(\cos\vartheta)\rangle(t)$, viz.,

$$\tau_D \frac{d}{dt} f_n(t) + d_n f_n(t) + c_n f_{n-2}(t) + g_n f_{n+2}(t) = a_n\left(\xi_0 + \xi\cos\omega t\right)\left[f_{n-1}(t) - f_{n+1}(t)\right], \tag{4.7}$$

where $n = 1, 2, \cdots$ and the coefficients a_n, c_n, d_n, and g_n are given by Eq. (2.38).

In particular, we shall be interested in averages of the Legendre polynomial of order 1, $f_1(t) = \langle P_1(\cos\theta)\rangle(t)$, and 2, $f_2(t) = \langle P_2(\cos\theta)\rangle(t)$, pertaining to the dielectric response and dynamic Kerr-effect responses, respectively.

4.2 Matrix Perturbation Solution

Now, although the applied ac electric field in experiments [10, 11, 52-57] can be high enough (≥ 10^6 V/m) to observe nonlinear effects, the energy of the dipole in the field $|V_t|$ remains sufficiently weak compared to the thermal energy to allow one to use perturbation theory in the calculation of the ac stationary response for a weak ac field $\xi(t) = \xi \cos \omega t$ ($\xi << 1$) since the electric dipole moment is quite small. Thus, we may seek perturbation solutions of Eq. (4.7) in the form

$$f_n(t) = f_n^{(0)} + f_n^{(1)}(t) + f_n^{(2)}(t) + f_n^{(3)}(t) + \cdots, \tag{4.8}$$

where $f_n^{(m)} \propto \xi^m$, yielding the coupled differential-recurrence relations

$$\begin{aligned} &\tau_D \frac{d}{dt} f_n^{(m)}(t) + d_n f_n^{(m)}(t) + c_n f_{n-2}^{(m)}(t) + g_n f_{n+2}^{(m)}(t) \\ &= \xi_0 a_n \left[f_{n-1}^{(m)}(t) - f_{n+1}^{(m)}(t) \right] + \xi a_n \left[f_{n-1}^{(m-1)}(t) - f_{n+1}^{(m-1)}(t) \right] \cos \omega t, \end{aligned} \tag{4.9}$$

$m = 1, 2, \ldots$, with the initial conditions at $t = -\infty$ given by

$$f_n^{(0)}(-\infty) = f_n^{(0)}, \quad f_n^{(m)}(-\infty) = 0 \ \ (m = 1, 2, \ldots). \tag{4.10}$$

For $\xi = 0$, the system of dipoles is in equilibrium with Boltzmann distribution

$$W_0(\vartheta) = Z^{-1} e^{\sigma \cos^2 \vartheta + \xi_0 \cos \vartheta}, \tag{4.11}$$

where Z is the partition function (see Eq. (2.101)), so that $f_n^{(0)} = \langle P_n \rangle_0$ can be calculated as

$$f_n^{(0)} = \int_0^{\pi} P_n(\cos \vartheta) W_0(\vartheta) \sin \vartheta d\vartheta. \tag{4.12}$$

Clearly, the equilibrium averages $f_n^{(0)}$ also satisfy the following five-term recurrence equation:

$$c_n f_{n-2}^{(0)} + d_n f_n^{(0)} + g_n f_{n+2}^{(0)} - \xi_0 a_n \left(f_{n-1}^{(0)} - f_{n+1}^{(0)} \right) = 0. \tag{4.13}$$

Equations (4.9) and (4.13) are seven- and five-term differential-recurrence relations, respectively, which can be solved for weak ac fields ($\xi << 1$) using matrix perturbation

methods [64, 67]. To proceed, we rearrange Eqs. (4.9) and (4.13) for $f_n^{(0)}$ and $f_n^{(m)}(t)$ (m = 1, 2, 3, …) into matrix form as the set of coupled linear matrix differential equations:

$$\frac{d}{dt}\mathbf{c}^{(1)}(t) + \mathbf{A}\mathbf{c}^{(1)}(t) = \xi(t)\mathbf{c}_1, \tag{4.14}$$

$$\frac{d}{dt}\mathbf{c}^{(m)}(t) + \mathbf{A}\mathbf{c}^{(m)}(t) = \xi(t)\mathbf{B}\mathbf{c}^{(m-1)}(t), \tag{4.15}$$

with the initial conditions $\mathbf{c}^{(0)}(-\infty) = \mathbf{c}^{(0)}$ and $\mathbf{c}^{(m)}(-\infty) = \mathbf{0}$ (m = 1, 2, 3, …) yielded by Eq. (4.10). Here, $\xi(t) = \xi\cos\omega t$ and the infinite column vectors $\mathbf{c}^{(m)}(t)$ and $\mathbf{c}_1$ are given by

$$\mathbf{c}^{(m)}(t) = \begin{pmatrix} f_1^{(m)}(t) \\ f_2^{(m)}(t) \\ \vdots \\ f_n^{(m)}(t) \\ \vdots \end{pmatrix}, \quad \mathbf{c}_1 = \begin{pmatrix} \tau_D^{-1}a_1 \\ 0 \\ 0 \\ 0 \\ \vdots \end{pmatrix} + \mathbf{B}\mathbf{c}^{(0)}, \quad \mathbf{c}^{(0)} = \begin{pmatrix} \langle P_1 \rangle_0 \\ \langle P_2 \rangle_0 \\ \vdots \\ \langle P_n \rangle_0 \\ \vdots \end{pmatrix}, \tag{4.16}$$

while the matrix elements of the time-independent five-diagonal matrix $\mathbf{A}$ and two-diagonal matrix $\mathbf{B}$ are

$$\begin{aligned} (\mathbf{A})_{p,q} &= \frac{1}{\tau_D}\left(\delta_{p,q+2}c_p - \delta_{p,q+1}\xi_0 a_p + \delta_{p,q}d_p + \delta_{p,q-1}\xi_0 a_p + \delta_{p,q-2}g_p\right), \\ (\mathbf{B})_{p,q} &= \frac{1}{\tau_D}\left(\delta_{p,q+1}a_p - \delta_{p,q-1}a_p\right), \end{aligned} \tag{4.17}$$

Now, the column vector $\mathbf{c}^{(0)}$ can be evaluated via inversion of the system matrix $\mathbf{A}$ as [1]

$$\mathbf{c}^{(0)} = \mathbf{A}^{-1}\begin{pmatrix} \xi_0\tau_D^{-1}a_1 \\ -\tau_D^{-1}c_2 \\ 0 \\ 0 \\ \vdots \end{pmatrix}, \tag{4.18}$$

thereby yielding the initial condition vector $\mathbf{c}_1$ in Eq. (4.14) (we remark in passing that both Eqs. (4.18) and (4.12) yield identical results for $\langle P_n \rangle_0$). Equations (4.14) and (4.15),

which are coupled matrix first-order linear differential equations, may then be solved analytically, yielding the linear response

$$\begin{aligned}\mathbf{c}^{(1)}(t) &= \int_{-\infty}^{t} \xi(t')e^{-\mathbf{A}(t-t')}\mathbf{c}_1 dt' \\ &= \frac{\xi}{2}\int_{-\infty}^{t}\left(e^{i\omega t'}+e^{-i\omega t'}\right)e^{-\mathbf{A}(t-t')}\mathbf{c}_1 dt' \\ &= \frac{\xi}{2}\left[\left(\mathbf{A}+i\omega\mathbf{I}\right)^{-1}\mathbf{c}_1 e^{i\omega t}+\left(\mathbf{A}-i\omega\mathbf{I}\right)^{-1}\mathbf{c}_1 e^{-i\omega t}\right] \\ &= \xi\,\mathrm{Re}\left[\boldsymbol{\varphi}_1^{(1)}(\omega)e^{i\omega t}\right],\end{aligned} \tag{4.19}$$

where the response $\mathbf{c}^{(1)}(t)$ is entirely real so that $\left(\mathbf{A}-i\omega\mathbf{I}\right)^{-1}$ and $\left(\mathbf{A}+i\omega\mathbf{I}\right)^{-1}$ must be a conjugate pair. Similarly we have the second order response $\mathbf{c}^{(2)}(t)$

$$\begin{aligned}\mathbf{c}^{(2)}(t) &= \int_{-\infty}^{t} \xi(t')e^{-\mathbf{A}(t-t')}\mathbf{B}\mathbf{c}^{(1)}(t')dt' \\ &= \int_{-\infty}^{t} \xi(t')e^{-\mathbf{A}(t-t')}\mathbf{B}\int_{-\infty}^{t'} \xi(t'')e^{-\mathbf{A}(t'-t'')}\mathbf{c}_1 dt''dt' \\ &= \frac{\xi^2}{2}\mathrm{Re}\left[\int_{-\infty}^{t}\left(1+e^{2i\omega t'}\right)e^{-\mathbf{A}(t-t')}\mathbf{B}\left(\mathbf{A}+i\omega\mathbf{I}\right)^{-1}\mathbf{c}_1 dt'\right] \\ &= \frac{\xi^2}{2}\mathrm{Re}\left\{\left[\mathbf{A}^{-1}+e^{2i\omega t}\left(\mathbf{A}+2i\omega\mathbf{I}\right)^{-1}\right]\mathbf{B}\left(\mathbf{A}+i\omega\mathbf{I}\right)^{-1}\mathbf{c}_1\right\} \\ &= \frac{\xi^2}{2}\mathrm{Re}\left[\boldsymbol{\varphi}_0^{(2)}(\omega)+\boldsymbol{\Phi}_2^{(2)}(2\omega)\boldsymbol{\varphi}_0^{(2)}(\omega)e^{2i\omega t}\right],\end{aligned} \tag{4.20}$$

the third order response

$$\begin{aligned}\mathbf{c}^{(3)}(t) &= \int_{-\infty}^{t} \xi(t')e^{-\mathbf{A}(t-t')}\mathbf{B}\mathbf{c}^{(2)}(t')dt' \\ &= \int_{-\infty}^{t} \xi(t')e^{-\mathbf{A}(t-t')}\mathbf{B}\int_{-\infty}^{t'} \xi(t'')e^{-\mathbf{A}(t'-t'')}\mathbf{B}\int_{-\infty}^{t''} \xi(t''')e^{-\mathbf{A}(t''-t''')}\mathbf{c}_1 dt'''dt''dt' \\ &= \frac{\xi^3}{4}\int_{-\infty}^{t}\mathrm{Re}\left[\left(e^{i\omega t'}+e^{-i\omega t'}\right)e^{-\mathbf{A}(t-t')}\mathbf{B}\boldsymbol{\varphi}_0^{(2)}(\omega)+\left(e^{3i\omega t'}+e^{i\omega t'}\right)e^{-\mathbf{A}(t-t')}\mathbf{B}\boldsymbol{\Phi}_2^{(2)}(2\omega)\boldsymbol{\varphi}_0^{(2)}(\omega)\right]dt' \\ &= \frac{\xi^3}{4}\mathrm{Re}\left\{\left(2\,\mathrm{Re}\left[\boldsymbol{\Phi}_1^{(3)}(\omega)\right]\boldsymbol{\varphi}_0^{(2)}(\omega)+\boldsymbol{\Phi}_1^{(3)}(\omega)\boldsymbol{\Phi}_2^{(2)}(2\omega)\boldsymbol{\varphi}_0^{(2)}(\omega)\right)e^{i\omega t}\right. \\ &\left.+\boldsymbol{\Phi}_1^{(3)}(3\omega)\boldsymbol{\Phi}_2^{(2)}(2\omega)\boldsymbol{\varphi}_0^{(2)}(\omega)e^{3i\omega t}\right)\Big\},\end{aligned} \tag{4.21}$$

and so on to any desired order in m. Here the column vectors $\boldsymbol{\varphi}_1^{(1)}(\omega)$, $\boldsymbol{\varphi}_0^{(2)}(\omega)$ and matrices $\boldsymbol{\Phi}_2^{(2)}(\omega)$, $\boldsymbol{\Phi}_1^{(3)}(\omega)$ are given by

$$\boldsymbol{\varphi}_1^{(1)}(\omega) = \left(\mathbf{A} + i\omega\mathbf{I}\right)^{-1}\mathbf{c}_1, \tag{4.22}$$

$$\boldsymbol{\varphi}_0^{(2)}(\omega) = \mathbf{A}^{-1}\mathbf{B}\left(\mathbf{A} + i\omega\mathbf{I}\right)^{-1}\mathbf{c}_1, \tag{4.23}$$

$$\boldsymbol{\Phi}_2^{(2)}(\omega) = \left(\mathbf{A} + i\omega\mathbf{I}\right)^{-1}\mathbf{A}, \tag{4.24}$$

$$\boldsymbol{\Phi}_1^{(3)}(\omega) = \left(\mathbf{A} + i\omega\mathbf{I}\right)^{-1}\mathbf{B}, \tag{4.25}$$

where $\mathbf{I}$ is the unit matrix, and we have used the fact that $e^{\mathbf{A}t}\Big|_{t=-\infty} = 0$ (because all the eigenvalues λ_k of $\mathbf{A}$ are positive, i.e., $\lambda_k > 0$). We note that the column vectors $\boldsymbol{\varphi}_1^{(1)}(\omega)$ and $\boldsymbol{\varphi}_0^{(2)}(\omega)$ can also be written as

$$\boldsymbol{\varphi}_1^{(1)}(\omega) = \begin{pmatrix} \chi_{11}X_{11}(\omega) \\ \chi_{21}X_{21}(\omega) \\ \chi_{31}X_{31}(\omega) \\ \vdots \end{pmatrix}, \qquad \boldsymbol{\varphi}_0^{(2)}(\omega) = \begin{pmatrix} \chi_{12}X_{10}^{(2)}(\omega) \\ \chi_{22}X_{20}^{(2)}(\omega) \\ \chi_{32}X_{30}^{(2)}(\omega) \\ \vdots \end{pmatrix}, \tag{4.26}$$

where $X_{n1}(\omega)$ and $X_{n0}^{(2)}(\omega)$ are the normalized (i.e., $X_{n1}(0) = X_{n0}^{(2)}(0) = 1$) linear and second-order nonlinear dc dynamic susceptibilities, respectively, while $\chi_{n1} = \left[\boldsymbol{\varphi}_1^{(1)}(0)\right]_n$ and $\chi_{n2} = \left[\boldsymbol{\Phi}_1^{(3)}(0)\boldsymbol{\varphi}_0^{(2)}(0)\right]_n$ are the corresponding static susceptibilities (which are evaluated in Section 2.7).

These matrix solutions (cf. Eqs. (4.19) - (4.21)) are very useful for computational purposes. As far as the practical calculation is concerned, we approximate all infinite matrices and column vectors involved by the corresponding matrices and column vectors of finite dimensions $N \times N$ and N, respectively. The value of N, depending on the numerical values of the model parameters (ξ_0, σ) as well as on the rank n and the order of perturbation solution m of $f_n^{(m)}(t)$ required, must be chosen according to the desired degree of accuracy. For example, in evaluating $f_1^{(m)}(t)$ and $f_2^{(m)}(t)$ for m = 1, 2, 3 and for σ and ξ_0 up to 20, we found that the matrix dimension N need not exceed 60 for an accuracy of not less than 6 significant digits in most instances. The numerical results obtained using this method are in complete agreement with those from the independent numerical methods developed in Refs. [18, 21, 23, 75] which we have summarized in Section 2.3.

4.3 Approximate Expressions for Linear Response

Although the matrix solutions obtained in the previous section allow us to evaluate nonlinear responses numerically, it does not give us a qualitative understanding of the relaxation dynamics of the system. However, such a qualitative understanding of the dynamical behaviour is provided by the two-mode approximation, which is based on the large separation of the time scales of the fast intrawell and slow overbarrier (interwell) relaxation processes in the double-well mean field potential, Eq. (4.5) [1, 40] (see also Section 2.8). In this section, we shall now show how the two-mode approximation explains the relaxation dynamics in the presence a weak ac field ($\xi << 1$), yielding a simple analytic description of the linear response characteristics of dipolar particles in the potential Eq. (4.5) for all ranges of the model parameters σ and ξ_0. In Sections 4.4 and 4.5, we will extend this method to include nonlinear effects. According to Eq. (4.8), the ac stationary linear response is governed by the response functions $f_n^{(1)}(t) = \left[\mathbf{c}^{(1)}(t)\right]_n$, which are given by the *n*-th element of the column vector $\mathbf{c}^{(1)}(t)$ in Eq. (4.19), so that

$$f_n^{(1)}(t) = \xi \,\mathrm{Re}\left\{\left[\boldsymbol{\varphi}_1^{(1)}(\omega)\right]_n e^{i\omega t}\right\} = \xi \,\mathrm{Re}\left[F_n^{(1)}(\omega) e^{i\omega t}\right], \tag{4.27}$$

where $F_n^{(1)}(\omega) = \chi_{n1} X_{n1}(\omega)$, and $X_{n1}(\omega)$ and $\chi_{n1} = \left[\boldsymbol{\varphi}_1^{(1)}(0)\right]_n$ are the normalized linear dynamic and static susceptibilities, respectively, and are defined by Eq. (4.26). The static susceptibilities χ_{n1} are expressed via the expectation values of the Legendre polynomials at equilibrium as (see Section 2.7, Eq. (2.103))

$$\chi_{n1} = \langle P_n P_1 \rangle_0 - \langle P_n \rangle_0 \langle P_1 \rangle_0 . \tag{4.28}$$

According to linear response theory, the normalized dynamic susceptibility $X_{n1}(\omega)$ is defined by the Kubo equation, as we describe in Section 2.8 [5, 78],

$$X_{n1}(\omega) = 1 - i\omega \int_0^\infty e^{-i\omega t} \Phi_{n1}(t) dt , \tag{4.29}$$

where $\Phi_{n1}(t)$ is the normalized equilibrium correlation function, viz.,

$$\Phi_{n1}(t) = \frac{\langle P_n[\cos\vartheta(0)] P_1[\cos\vartheta(t)]\rangle_0 - \langle P_n\rangle_0 \langle P_1\rangle_0}{\langle P_n P_1\rangle_0 - \langle P_n\rangle_0 \langle P_1\rangle_0}, \tag{4.30}$$

which comprises, in general, an infinity of relaxation modes (decaying exponentials), i.e., [1, 78]

$$\Phi_{n1}(t) = \sum_{k=1}^{\infty} c_k^n e^{-\lambda_k t} \,. \tag{4.31}$$

Here $\lambda_1, \lambda_2, \lambda_3, ...$ are the eigenvalues of the system matrix **A** and, therefore, the eigenvalues of the Fokker–Planck operator L_{FP} defined by Eq. (4.3). These eigenvalues can be evaluated from the characteristic equation [1]

$$\det(\lambda \mathbf{I} - \mathbf{A}) = 0 \,. \tag{4.32}$$

For high potential barriers, $\Delta V = \sigma(1 - \xi_0 / 2\sigma)^2 >> 1$, the relaxation process is dominated by the smallest nonvanishing eigenvalue λ_1, which is much smaller than all other eigenvalues, i.e., $\lambda_1 << \lambda_2, \lambda_3, ...$ [1]. This eigenvalue has an Arrhenius-like behaviour, $\lambda_1 \sim e^{-\Delta V}$, and is associated with the slowest overbarrier relaxation mode (the explicit equations for λ_1 in the low- and high-barrier limits are given by Eqs. (4A.6) and (4A.9), respectively). All other eigenvalues $\lambda_2, \lambda_3, ...$ are associated with the fast "intrawell" relaxation modes and weakly depend on the temperature [1, 40]. Thus one may suppose [1, 37, 40] that $\Phi_{n1}(t)$ may be approximated by two relaxation modes only,

$$\Phi_{n1}(t) \approx \Delta_{n1} e^{-\lambda_1 t} + (1 - \Delta_{n1}) e^{-t/\tau_W^{(n1)}} \,, \tag{4.33}$$

where $\tau_W^{(n1)}$ is the inverse of the characteristic frequency of the near degenerate high-frequency modes, while Δ_{n1} and $1 - \Delta_{n1}$ are amplitudes accounting for the overbarrier and intrawell relaxation processes, respectively. The parameters Δ_{n1} and $\tau_W^{(n1)}$ can be expressed in terms of the characteristic relaxation times of the correlation function $\Phi_{n1}(t)$ [1, 37] (details in Section 2.8). By inserting Eq. (4.33) into Eq. (4.29), the normalized dynamic susceptibility $X_{n1}(\omega)$ can be obtained analytically as the sum of two Lorentzians, viz.,

$$X_{n1}(\omega) \approx \frac{\Delta_{n1}}{1 + i\omega / \lambda_1} + \frac{1 - \Delta_{n1}}{1 + i\omega \tau_W^{(n1)}} \,. \tag{4.34}$$

In particular, both for the linear dielectric and Kerr-effect response, the parameters Δ_{n1} and $\tau_W^{(n1)}$ in Eq. (4.34) are evaluated by letting $n=1$ and $n=2$ in Eqs. (2.125) and (2.126), respectively.

In Fig. 4.2 and Fig. 4.3, we show the real and imaginary parts of $X_{11}(\omega)$ and $X_{12}(\omega)$ calculated using the matrix solution, Eqs. (4.19) and (4.22), and the approximate equation (4.34). These figures indicate that there is no practical difference between the matrix solution and the two-mode approximation (the maximum relative deviation between the corresponding curves does not exceed a few percent). Clearly, two dispersion regions are noticeable in the spectra of the real parts, $\mathrm{Re}\left[X_{11}(\omega)\right]$ and $\mathrm{Re}\left[X_{21}(\omega)\right]$, and two peaks appear in the spectra of the imaginary parts, $-\mathrm{Im}\left[X_{11}(\omega)\right]$ and $-\mathrm{Im}\left[X_{21}(\omega)\right]$. The low-frequency part of the spectra is dominated by the slowest overbarrier relaxation mode.

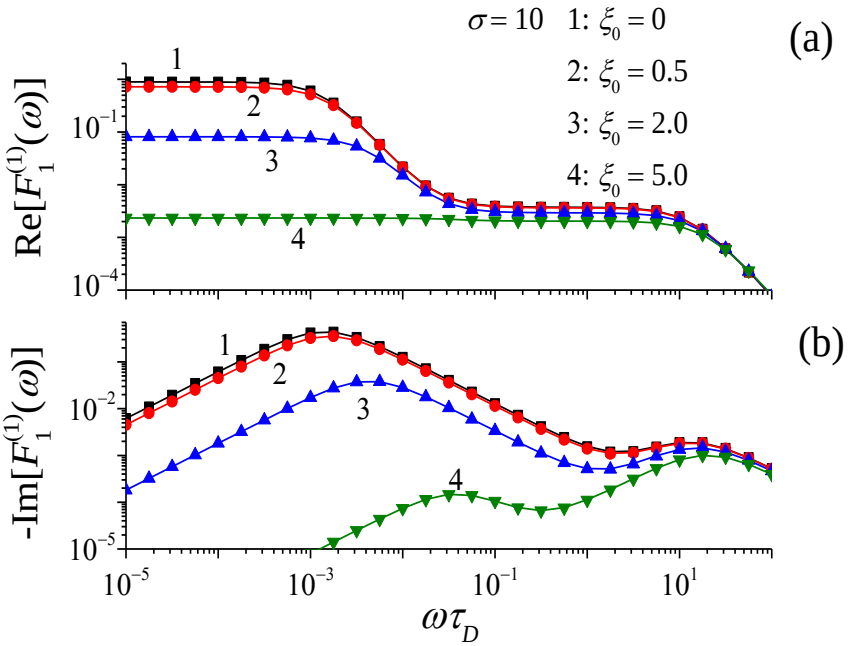

Fig. 4.2. Real (a) and imaginary (b) parts of the linear susceptibility $F_1^{(1)}(\omega)=\chi_{11}X_{11}(\omega)$ vs. the normalized frequency $\omega\tau_D$ for various values of the dc field amplitude ξ_0 with the anisotropy parameter $\sigma=10$. Solid lines: the matrix solution, Eq. (4.19). Symbols: the two-mode approximation Eq. (4.34) with parameters calculated from Eqs. (4.32), (2.121), (2.122), (2.125), and (2.126).

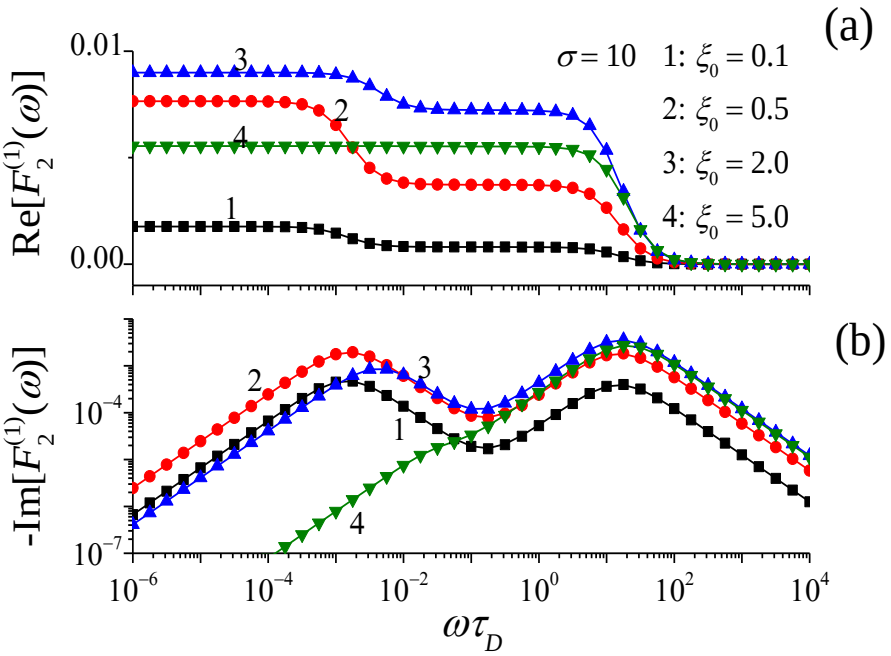

Fig. 4.3. Real (a) and imaginary (b) parts of the linear Kerr-effect response $F_2^{(1)}(\omega) = \chi_{21} X_{21}(\omega)$ vs. $\omega\tau_D$ for various values of the dc field amplitude ξ_0 with the anisotropy parameter $\sigma = 10$. Solid lines: the matrix solution, Eq. (4.19). Symbols: the two-mode approximation Eq. (4.34) with the parameters calculated from Eqs. (4.32), (2.121), (2.122), (2.125), and (2.126).

The characteristic frequency $\omega_{\max}$ and the half-width $\Delta\omega$ of low frequency spectrum are determined by the smallest nonvanishing eigenvalue λ_1. The eigenvalue λ_1 is related to the frequency $\omega_{\max}$ of the low-frequency peak in $-\mathrm{Im}\left[X_{11}(\omega)\right]$ and $-\mathrm{Im}\left[X_{21}(\omega)\right]$, where they attain maxima, and/or the half-width $\Delta\omega$ of the low-frequency dispersion region in $\mathrm{Re}\left[X_{11}(\omega)\right]$ and $\mathrm{Re}\left[X_{21}(\omega)\right]$ via

$$\lambda_1 \approx \omega_{\max} \approx \Delta\omega . \tag{4.35}$$

Here, comparison of λ_1 as extracted from the spectra of $X_{11}(\omega)$ and $X_{12}(\omega)$ via Eq. (4.35), with λ_1 calculated independently via the system matrix **A**, shows that both methods yield identical results. Our calculations indicate that, on increasing the dc field parameter ξ_0, the magnitude of the low-frequency band drastically decreases due to the depletion of the population in the shallower potential well of the potential V [1, 40] which results in the virtual disappearance of the low-frequency peak in the spectra $-\mathrm{Im}\left[X_{11}(\omega)\right]$ and $-\mathrm{Im}\left[X_{21}(\omega)\right]$ (see Fig. 4.2 and Fig. 4.3). Furthermore, the low-

frequency peak shifts monotonically to higher frequencies with increasing ξ_0. The high-frequency peaks of $-\mathrm{Im}\left[X_{11}(\omega)\right]$ and $-\mathrm{Im}\left[X_{21}(\omega)\right]$ are due to the near degenerate high-frequency intrawell modes corresponding to the eigenvalues λ_k ($k \geq 2$). These individual intrawell modes are indistinguishable in the spectra of $-\mathrm{Im}\left[X_{11}(\omega)\right]$ and $-\mathrm{Im}\left[X_{21}(\omega)\right]$, appearing merely as a single high-frequency Lorentzian band (see Fig. 4.2 and Fig. 4.3).

We shall now show that the two-mode approximation also yields an accurate description of the dynamic Kerr effect spectra and nonlinear dielectric relaxation.

4.4 Approximate Expressions for Dynamic Kerr Effect

By inspection of Eq. (4.20), the second-rank response $f_2^{(2)}(t) = \left[\mathbf{c}^{(2)}(t)\right]_2$ governing the dynamic Kerr-effect response can be written as a sum of a dc term and a term depending on $e^{2i\omega t}$, so that

$$f_2^{(2)}(t) = \xi^2 \,\mathrm{Re}\left[F_{2,0}^{(2)}(\omega) + F_{2,2}^{(2)}(\omega) e^{2i\omega t}\right], \tag{4.36}$$

where

$$F_{2,0}^{(2)}(\omega) = \left[\boldsymbol{\varphi}_0^{(2)}(\omega)\right]_2 \Big/ 2 \tag{4.37}$$

and

$$F_{2,2}^{(2)}(\omega) = \left[\boldsymbol{\Phi}_2^{(2)}(2\omega)\boldsymbol{\varphi}_0^{(2)}(\omega)\right]_2 \Big/ 2. \tag{4.38}$$

In the two-mode approximation, the Fourier amplitudes $F_{2,0}^{(2)}(\omega)$ and $F_{2,2}^{(2)}(\omega)$ can be written as

$$F_{2,0}^{(2)}(\omega) \approx \frac{\chi_{22}}{2} X_{20}^{(2)}(\omega), \tag{4.39}$$

and

$$F_{2,2}^{(2)}(\omega) \approx \frac{\chi_{22}}{2} X_{22}(2\omega) X_{20}^{\prime(2)}(\omega), \tag{4.40}$$

where the static susceptibility χ_{22} is given by (see Section 2.7)

$$\chi_{22} = \frac{1}{3}\left(\left\langle P_2^2\right\rangle_0 - \left\langle P_2\right\rangle_0^2\right) - \left\langle P_1\right\rangle_0 \left(\left\langle P_1 P_2\right\rangle_0 - \left\langle P_1\right\rangle_0 \left\langle P_2\right\rangle_0\right), \tag{4.41}$$

and the dynamic susceptibilities $X_{20}^{(2)}(\omega)$, $X_{20}^{\prime(2)}(\omega)$, and $X_{22}(\omega)$ may again be written in the two-mode approximation as

$$X_{20}^{(2)}(\omega) \approx \frac{\Delta_{20}}{1+i\omega/\lambda_1} + \frac{1-\Delta_{20}}{1+i\omega\tau_W^{(20)}}, \tag{4.42}$$

$$X_{20}^{\prime(2)}(\omega) \approx \frac{\Delta'_{20}}{1+i\omega/\lambda_1} + \frac{1-\Delta'_{20}}{1+i\omega\tau_W^{\prime(20)}}, \tag{4.43}$$

and

$$X_{22}(\omega) \approx \frac{\Delta_{22}}{1+i\omega\tau_{22}} + \frac{1-\Delta_{22}}{1+i\omega\tau_W^{(22)}}. \tag{4.44}$$

In the Kerr-effect response, Δ_{20} and $\tau_W^{(20)}$ in Eq. (4.42) can be calculated [3, 67] via Eqs. (2.125) and (2.126), where the time constants τ_{20} and τ_{20}^{eff} are estimated from the low- and high-frequency asymptotes, Eq. (2.120), yielding

$$\tau_{20} = -\lim_{\omega\to 0}\frac{1}{\omega}\,\mathrm{Im}\left\{\frac{1}{\chi_{22}\left[\boldsymbol{\varphi}_0^{(2)}(\omega)\right]_2}\right\} \quad \text{and} \quad \tau_{20}^{\text{eff}} = \lim_{\omega\to\infty}\frac{1}{\omega}\,\mathrm{Im}\left\{\frac{\chi_{22}}{\left[\boldsymbol{\varphi}_0^{(2)}(\omega)\right]_2}\right\}. \tag{4.45}$$

However, analytic equations for the other parameters Δ'_{20}, $\tau_W^{\prime(20)}$, Δ_{22}, τ_{22}, and $\tau_W^{(22)}$ like Eqs. (2.121) and (2.122) no longer exist. Therefore, they are treated as adjustable parameters.

The spectra of the dc component of the 2nd order Kerr effect $\mathrm{Re}\left[F_{2,0}^{(2)}(\omega)\right]$ and the Kerr effect 2nd harmonic component $\mathrm{Re}\left[F_{2,2}^{(2)}(\omega)\right]$ are shown in Fig. 4.4 for various values of the dc field parameter ξ_0 as calculated from the matrix and two-mode approximation solutions. Just as with the linear response, no practical difference exists between the matrix and two-mode approximation solutions.

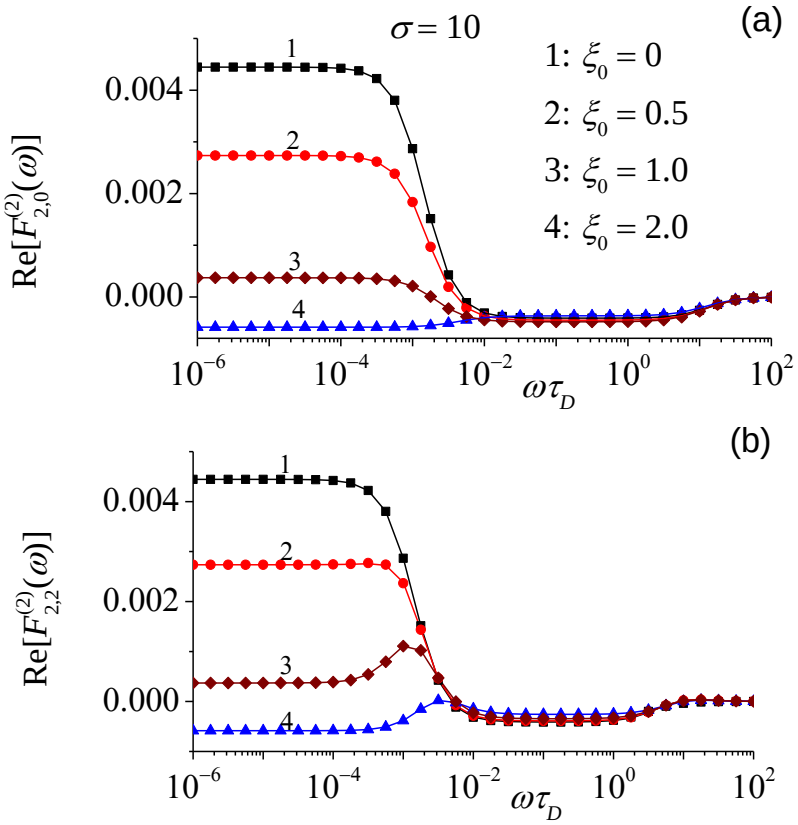

Fig. 4.4. DC component of the 2nd order Kerr effect $\mathrm{Re}\left[F^{(2)}_{2,0}(\omega)\right]$ (a) and the Kerr effect 2nd harmonic component $\mathrm{Re}\left[F^{(2)}_{2,2}(\omega)\right]$ (b) vs. $\omega\tau_D$ for various values of the dc field amplitude ξ_0 with the anisotropy parameter $\sigma = 10$. Solid lines: the matrix solution, Eq. (4.20). Symbols: the two-mode approximation Eq. (4.39) using parameters given by Eq. (4.45), and Eq. (4.40) using fitting parameters.

4.5 Higher Order Dielectric and Kerr-Effect Responses

In the nonlinear dielectric response, where the terms of order ξ^2 and ξ^3 cannot be neglected, the second-rank response function $f^{(2)}_1(t) = \left[\mathbf{c}^{(2)}(t)\right]_1$, which is proportional to ξ^2, can be written, by inspection of Eq. (4.20), as a sum of a dc term and a term depending on $e^{2i\omega t}$, so that

$$f^{(2)}_1(t) = \xi^2\,\mathrm{Re}\left[F^{(2)}_{1,0}(\omega) + F^{(2)}_{1,2}(\omega)e^{2i\omega t}\right], \tag{4.46}$$

where

$$F^{(2)}_{1,0}(\omega) = \frac{1}{2}\left[\boldsymbol{\varphi}^{(2)}_0(\omega)\right]_1 \tag{4.47}$$

and

$$F_{1,2}^{(2)}(\omega)=\frac{1}{2}\left[\boldsymbol{\Phi}_2^{(2)}(2\omega)\boldsymbol{\varphi}_0^{(2)}(\omega)\right]_1. \tag{4.48}$$

Furthermore, the third-order contribution $f_1^{(3)}(t)=\left[\mathbf{c}^{(3)}(t)\right]_1$, which is proportional to ξ^3, can be written, by inspection of Eq. (4.21), as

$$f_1^{(3)}(t)=\xi^3\,\mathrm{Re}\left[F_{1,1}^{(3)}(\omega)e^{i\omega t}+F_{1,3}^{(3)}(\omega)e^{3i\omega t}\right], \tag{4.49}$$

where

$$F_{1,1}^{(3)}(\omega)=\frac{1}{4}\left\{2\left[\mathrm{Re}\left[\boldsymbol{\Phi}_1^{(3)}(\omega)\right]\boldsymbol{\varphi}_0^{(2)}(\omega)\right]_1+\left[\boldsymbol{\Phi}_1^{(3)}(\omega)\boldsymbol{\Phi}_2^{(2)}(2\omega)\boldsymbol{\varphi}_0^{(2)}(\omega)\right]_1\right\}, \tag{4.50}$$

and

$$F_{1,3}^{(3)}(\omega)=\frac{1}{4}\left[\boldsymbol{\Phi}_1^{(3)}(3\omega)\boldsymbol{\Phi}_2^{(2)}(2\omega)\boldsymbol{\varphi}_0^{(2)}(\omega)\right]_1. \tag{4.51}$$

In the two-mode approximation, the Fourier amplitudes $F_{1,0}^{(2)}(\omega)$, $F_{1,2}^{(2)}(\omega)$, $F_{1,1}^{(3)}(\omega)$, and $F_{1,3}^{(3)}(\omega)$ can be written as

$$F_{1,0}^{(2)}(\omega)\approx\frac{\chi_{12}}{2}X_{10}^{(2)}(\omega), \tag{4.52}$$

$$F_{1,2}^{(2)}(\omega)\approx\frac{\chi_{12}}{2}X_{12}(2\omega)X_{10}^{\prime(2)}(\omega), \tag{4.53}$$

$$F_{1,1}^{(3)}(\omega)\approx\frac{\chi_{13}}{4}\left\{2\,\mathrm{Re}\left[X_{13}(\omega)\right]X_{10}^{\prime(2)}(\omega)+X_{13}(\omega)X_{12}(2\omega)X_{10}^{\prime(2)}(\omega)\right\}, \tag{4.54}$$

and

$$F_{1,3}^{(3)}(\omega)\approx\frac{\chi_{13}}{4}X_{13}(3\omega)X_{12}(2\omega)X_{10}^{\prime(2)}(\omega), \tag{4.55}$$

where the generalized dynamic susceptibilities $X_{10}^{(2)}(\omega)$, $X_{10}^{\prime(2)}(\omega)$, $X_{12}(\omega)$ and $X_{13}(\omega)$ are given by

$$X_{10}^{(2)}(\omega)\approx\frac{\Delta_{10}}{1+i\omega/\lambda_1}+\frac{1-\Delta_{10}}{1+i\omega\tau_W^{(10)}}, \tag{4.56}$$

$$X_{10}^{\prime(2)}(\omega)\approx\frac{\Delta_{10}^{\prime}}{1+i\omega/\lambda_1}+\frac{1-\Delta_{10}^{\prime}}{1+i\omega\tau_W^{\prime(10)}}, \tag{4.57}$$

$$X_{12}(\omega)\approx\frac{\Delta_{12}}{1+i\omega\tau_{12}}+\frac{1-\Delta_{12}}{1+i\omega\tau_W^{(12)}}, \tag{4.58}$$

and

$$X_{13}(\omega) \approx \frac{\Delta_{13}}{1+i\omega/\lambda_1} + \frac{1-\Delta_{13}}{1+i\omega\tau_W^{(13)}}, \tag{4.59}$$

and the static susceptibilities χ_{12} and χ_{13} are (see Section 2.7)

$$\chi_{12} = \frac{1}{3}\left(\langle P_2 P_1\rangle_0 - \langle P_2\rangle_0 \langle P_1\rangle_0\right) - \langle P_1\rangle_0 \left(\langle P_1^2\rangle_0 - \langle P_1\rangle_0^2\right), \tag{4.60}$$

and

$$\begin{aligned}\chi_{13} = {} & \frac{1}{6}\left(\langle P_1^4\rangle_0 - \langle P_1^3\rangle_0 \langle P_1\rangle_0\right) - \frac{1}{2}\langle P_1^2\rangle_0 \left(\langle P_1^2\rangle_0 - \langle P_1\rangle_0^2\right) \\ & + \langle P_1\rangle_0^2 \left(\langle P_1^2\rangle_0 - \langle P_1\rangle_0^2\right) - \frac{1}{2}\langle P_1\rangle_0 \left(\langle P_1^3\rangle_0 - \langle P_1\rangle_0 \langle P_1^2\rangle_0\right).\end{aligned} \tag{4.61}$$

Here, Δ_{10} and $\tau_W^{(10)}$ in Eq. (4.56) can be calculated via Eqs. (2.125) and (2.126), where the time constants τ_{10} and τ_{10}^{eff} are estimated from the low- and high-frequency asymptotes, Eq. (2.120), yielding

$$\tau_{10} = -\lim_{\omega\to 0} \frac{1}{\omega} \operatorname{Im}\left\{ \frac{1}{\chi_{12}} \left[\boldsymbol{\varphi}_0^{(2)}(\omega)\right]_1 \right\} \quad \text{and} \quad \tau_{10}^{\text{eff}} = \lim_{\omega\to\infty} \frac{1}{\omega} \operatorname{Im}\left\{ \frac{\chi_{12}}{\left[\boldsymbol{\varphi}_0^{(2)}(\omega)\right]_1} \right\}. \tag{4.62}$$

However, analytic equations for the other parameters Δ_{10}', $\tau_W'^{(10)}$, Δ_{12}, τ_{12}, and $\tau_W^{(12)}$ like Eqs. (2.121) and (2.122) no longer exist. Therefore, they are treated as adjustable parameters.

Similarly, the third order contribution $f_2^{(3)}(t) = \left[\mathbf{c}^{(3)}(t)\right]_2$ to the second-rank response function $f_2(t)$ governing the Kerr-effect relaxation is, by inspection of Eq. (4.21),

$$f_2^{(3)}(t) = \xi^3 \operatorname{Re}\left[F_{2,1}^{(3)}(\omega) e^{i\omega t} + F_{2,3}^{(3)}(\omega) e^{3i\omega t} \right], \tag{4.63}$$

where

$$F_{2,1}^{(3)}(\omega) = \frac{1}{2}\left[\operatorname{Re}\left[\boldsymbol{\Phi}_1^{(3)}(\omega)\right] \boldsymbol{\varphi}_0^{(2)}(\omega) + \frac{1}{2}\boldsymbol{\Phi}_1^{(3)}(\omega)\boldsymbol{\Phi}_2^{(2)}(2\omega)\boldsymbol{\varphi}_0^{(2)}(\omega) \right]_2,$$

and

$$F_{2,3}^{(3)}(\omega) = \frac{1}{4}\left[\boldsymbol{\Phi}_1^{(3)}(3\omega)\boldsymbol{\Phi}_2^{(2)}(2\omega)\boldsymbol{\varphi}_0^{(2)}(\omega)\right]_2.$$

Again, using the two-mode approximation, these Fourier amplitudes are

$$F_{2,1}^{(3)}(\omega) \approx \frac{\chi_{23}}{4}\left\{2\,\mathrm{Re}\left[X_{23}(\omega)\right]X_{20}'^{(2)}(\omega) + X_{23}(\omega)\,X_{22}(2\omega)\,X_{20}'^{(2)}(\omega)\right\}, \quad (4.64)$$

and

$$F_{2,3}^{(3)}(\omega) \approx \frac{\chi_{23}}{4}\,X_{23}(3\omega)\,X_{22}(2\omega)\,X_{20}'^{(2)}(\omega), \quad (4.65)$$

where the dynamic susceptibility $X_{23}(\omega)$ is given by

$$X_{23}(\omega) \approx \frac{\Delta_{23}}{1+i\omega/\lambda_1} + \frac{1-\Delta_{23}}{1+i\omega\tau_W^{(23)}}, \quad (4.66)$$

and the static susceptibility χ_{23} is (Section 2.7)

$$\begin{aligned}\chi_{23} = {} & \frac{1}{6}\left(\left\langle P_1^3 P_2\right\rangle_0 - \left\langle P_1^3\right\rangle_0\left\langle P_2\right\rangle_0\right) - \frac{1}{2}\left\langle P_1 P_2\right\rangle_0\left(\left\langle P_1^2\right\rangle_0 - \left\langle P_1\right\rangle_0^2\right) \\ & + \left\langle P_1\right\rangle_0\left\langle P_2\right\rangle_0\left(\left\langle P_1^2\right\rangle_0 - \left\langle P_1\right\rangle_0^2\right) - \frac{1}{2}\left\langle P_1\right\rangle_0\left(\left\langle P_1^2 P_2\right\rangle_0 - \left\langle P_1\right\rangle_0\left\langle P_1 P_2\right\rangle_0\right).\end{aligned} \quad (4.67)$$

Again, Δ_{23} and $\tau_W^{(23)}$ are treated as adjustable parameters.

The frequency spectra of the dc component $\mathrm{Re}\left[F_{1,0}^{(2)}(\omega)\right]$ and the 2nd harmonic component $\mathrm{Re}\left[F_{1,2}^{(2)}(\omega)\right]$ of the second order nonlinear dielectric response, the fundamental component $\mathrm{Re}\left[F_{1,1}^{(3)}(\omega)\right]$ and the 3rd harmonic component $\mathrm{Re}\left[F_{1,3}^{(3)}(\omega)\right]$ of the third order nonlinear dielectric response, and the fundamental component $\mathrm{Re}\left[F_{2,1}^{(3)}(\omega)\right]$ and the third harmonic component $\mathrm{Re}\left[F_{2,3}^{(3)}(\omega)\right]$ of the third order nonlinear Kerr-effect response are shown in Fig. 4.5 and Fig. 4.6 for various values of the dc field parameter ξ_0, which are calculated using the matrix (see Section 4.2) and two-mode approximation solutions. Just as with the other responses, the matrix and two-mode approximation solutions are in complete agreement.

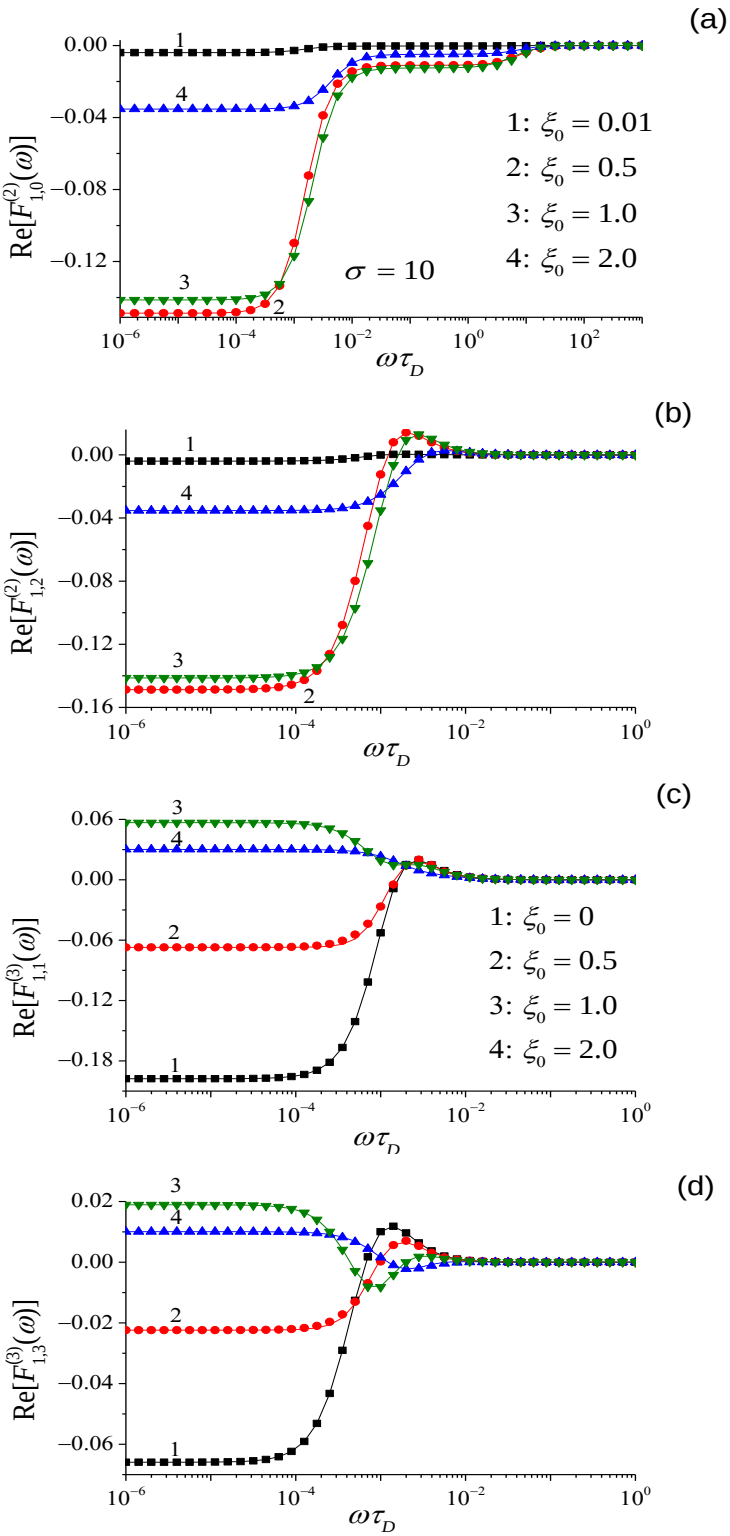

Fig. 4.5. DC component $\mathrm{Re}\left[F^{(2)}_{1,0}(\omega)\right]$ (a), the 2nd harmonic component $\mathrm{Re}\left[F^{(2)}_{1,2}(\omega)\right]$ (b), the fundamental component $\mathrm{Re}\left[F^{(3)}_{1,1}(\omega)\right]$ (c), and the 3rd harmonic component $\mathrm{Re}\left[F^{(3)}_{1,3}(\omega)\right]$ (d) of the nonlinear dielectric response vs. $\omega\tau_D$ for various values of the dc field amplitude ξ_0 with $\sigma = 10$. Solid lines: the matrix solution, Eqs. (4.20) and (4.21). Symbols: the two-mode approximation, Eqs. (4.52), (4.53), (4.54), and (4.55), using fitting parameters.

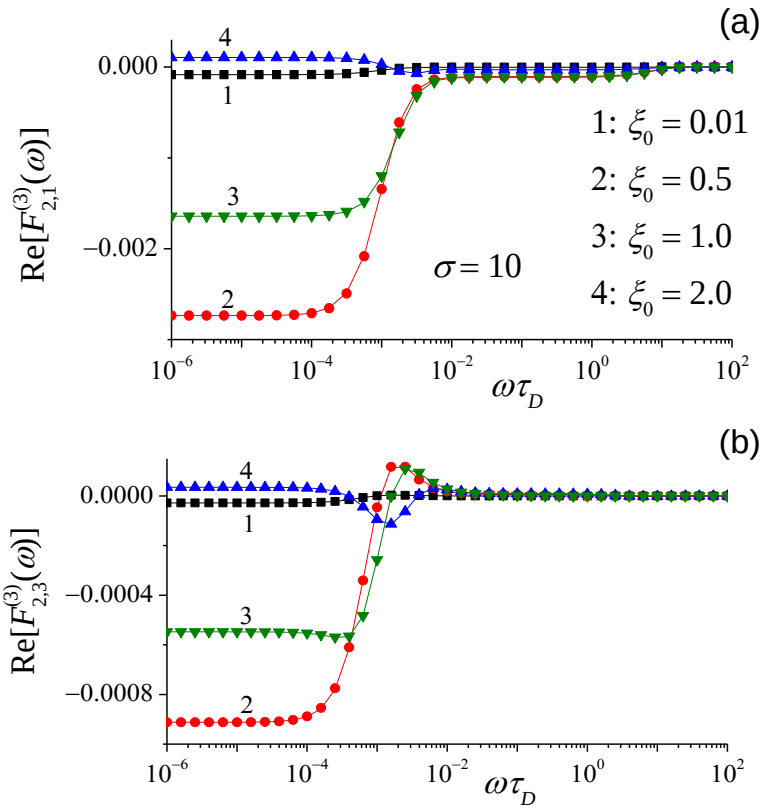

Fig. 4.6. Fundamental component $\mathrm{Re}\left[F^{(3)}_{2,1}(\omega)\right]$ (a) and the third harmonic component $\mathrm{Re}\left[F^{(3)}_{2,3}(\omega)\right]$ (b) of the 3rd order Kerr effect vs. $\omega\tau_D$ for various values of the dc field amplitude ξ_0 with the anisotropy parameter $\sigma = 10$. Solid lines: the matrix solution, Eq. (4.21). Symbols: the two-mode approximation, Eqs. (4.64) and (4.65), using fitting parameters.

For the particular case of zero anisotropy $\sigma = 0$, the equations we have obtained above for the dielectric and Kerr-effect response functions $f_1(t)$ and $f_2(t)$ subjected to combined ac and dc fields, by evaluating $f_1^m(t)$ and $f_2^m(t)$ for $m \le 3$ in Eqs. (4.19) - (4.21) explicitly, reduce to Eqs. (3.28) and (3.29), respectively. Similarly, if we consider the particular case of both zero anisotropy $\sigma = 0$ and zero dc bias field $\xi_0 = 0$, our equations of $f_1(t)$ and $f_2(t)$ obtained in this chapter will reduce to the known results of Ref. [2], namely,

$$f_1(t) = \frac{\xi}{3}\frac{\cos\omega t + \omega\tau_D \sin\omega t}{1+\omega^2{\tau_D}^2} - \frac{\xi^3}{45}\left[\frac{\left(27-13{\tau_D}^2\omega^2\right)\cos\omega t}{4\left(1+{\tau_D}^2\omega^2\right)^2\left(9+4{\tau_D}^2\omega^2\right)} + \frac{\omega\tau_D\left(21+{\tau_D}^2\omega^2\right)\sin\omega t}{2\left(1+{\tau_D}^2\omega^2\right)^2\left(9+4{\tau_D}^2\omega^2\right)}\right. \\ \left. +3\frac{\left(3-17{\tau_D}^2\omega^2\right)\cos 3\omega t + 2\omega\tau_D\left(3{\tau_D}^2\omega^2-7\right)\sin 3\omega t}{4\left(9+4{\tau_D}^2\omega^2\right)\left(1+{\tau_D}^2\omega^2\right)\left(1+9{\tau_D}^2\omega^2\right)}\right] + o(\xi^3), \quad (4.68)$$

and

$$f_2(t) = \frac{\xi^2}{30\left(1+\omega^2{\tau_D}^2\right)}\left[1+\frac{\left(3-2\omega^2{\tau_D}^2\right)\cos 2\omega t + 5\omega\tau_D \sin 2\omega t}{3\left(1+4\omega^2{\tau_D}^2/9\right)}\right] + o\left(\xi^2\right). \quad (4.69)$$

4.6 DC Component of the Dielectric and Kerr-Effect AC Stationary Responses

Now we consider in detail the time-independent but frequency-dependent components of the dielectric and Kerr-effect ac stationary responses $\overline{f_1}(\omega)$, and $\overline{f_2}(\omega)$, defined as the time averages over a period of the ac field:

$$\overline{f_n}(\omega) = \frac{\omega}{2\pi}\int_0^{2\pi/\omega} f_n(t)\,dt = \langle P_n\rangle_0 + \xi^2\,\mathrm{Re}\left[F_{n,0}^{(2)}(\omega)\right] + o\left(\xi^2\right), \quad n = 1,\ 2. \quad (4.70)$$

First, in contrast to the Kerr-effect response, the dc component of the dielectric response $\overline{f_1}(\omega)$ is nonzero only when an external dc bias field is superimposed on the ac field. The nonlinear ac field contributions to $\overline{f_1}(\omega)$ and $\overline{f_2}(\omega)$ are of order ξ^2 and both strongly depend on the dc bias field ξ_0 and the anisotropy parameter σ. According to the results of Sections 4.4 and 4.5, namely Eqs. (4.39), (4.42), (4.52) and (4.56), in the two-mode approximation both $\overline{f_1}(\omega)$ and $\overline{f_2}(\omega)$ may be approximated by a sum of two Lorentzians, viz.,

$$\overline{f_n}(\omega) \approx \langle P_n\rangle_0 + \frac{\chi_{n2}\xi^2}{2}\left(\frac{\Delta_{n0}}{1+(\omega/\lambda_1)^2} + \frac{1-\Delta_{n0}}{1+(\omega\tau_W^{(n0)})^2}\right), \quad n = 1,\ 2, \quad (4.71)$$

where χ_{12} and χ_{22} are given by Eqs. (4.60) and (4.41), respectively, while Δ_{n0} and $\tau_W^{(n0)}$ can be calculated via Eqs. (2.125) and (2.126), respectively, in the manner we treated the dynamic Kerr effect in Section 4.4.

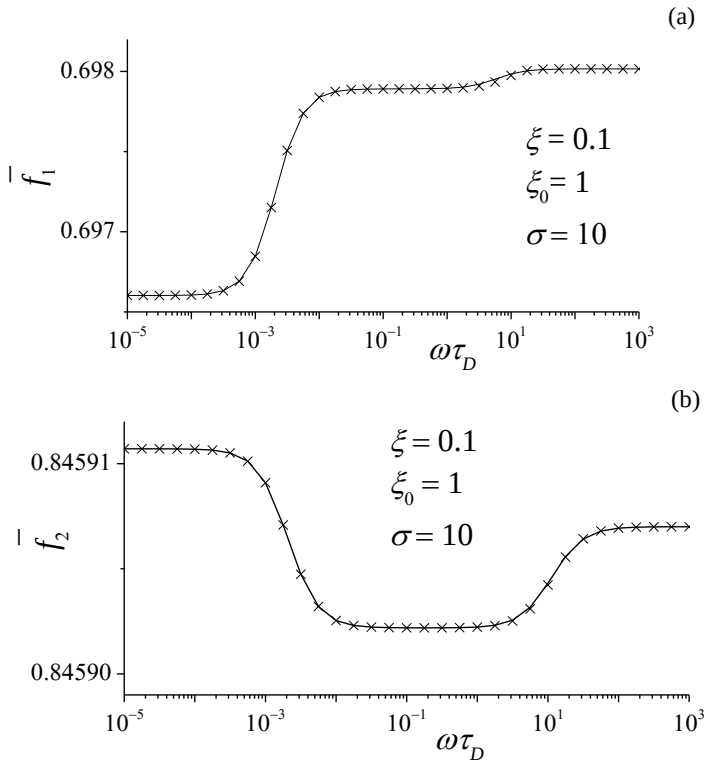

Fig. 4.7. DC components $\overline{f_1}(\omega)$ (a) and $\overline{f_2}(\omega)$ (b) vs. $\omega\tau_D$ with $\sigma = 10$, $\xi = 0.1$, and $\xi_0 = 1$ showing pronounced frequency-dependence including two distinct dispersion regions caused by the entanglement of the dc and ac responses. Solid lines: the matrix solution of Section 4.2. Crosses: the two-mode approximation, Eq. (4.71).

In Fig. 4.7, we plot $\overline{f_1}(\omega)$ and $\overline{f_2}(\omega)$ as functions of frequency in order to illustrate the nonlinear effects induced by the ac field in the dc components $\overline{f_1}(\omega)$ and $\overline{f_2}(\omega)$, which exhibit a pronounced frequency dependence. Clearly, the approximate equation (4.71) is in agreement with the numerical calculations. By inspection of Fig. 4.7, two distinct low- and high-frequency dispersion regions appear in the spectra of $\overline{f_1}(\omega)$ and $\overline{f_2}(\omega)$, just as with the real part of the dynamic susceptibilities $\mathrm{Re}\left[X_{11}(\omega)\right]$ (cf. Fig. 4.2). The low-frequency dispersion region of each of the two functions $\overline{f_1}(\omega)$ and $\overline{f_2}(\omega)$ is clearly governed by the barrier crossing relaxation modes with the *same* characteristic frequency ω_1 *indicating that the overbarrier relaxation time may be determined directly from measurements of the dc responses* $\overline{f_1}(\omega)$ and $\overline{f_2}(\omega)$. In addition, for weak ac fields, the characteristic frequency ω_1 of this low-frequency band is associated with the overbarrier relaxation processes and may be determined as $\omega_1 = \lambda_1$.

Now, at the opposite end of the spectrum, the high-frequency band is due to "intrawell" relaxation modes. These individual near-degenerate high frequency modes are, however, virtually indistinguishable in the frequency spectra of $\overline{f_1}(\omega)$ and $\overline{f_2}(\omega)$, appearing merely as a single high-frequency relaxation band, just as with $\mathrm{Re}\left[X_{11}(\omega)\right]$ (see Fig. 4.2). The results clearly demonstrate that the dc components of the ac stationary nonlinear dielectric and Kerr-effect responses *contain* the *same* information about the *relaxation processes* as the linear and nonlinear dynamic susceptibilities. This fact suggests that a *new* method of measurement of the overbarrier relaxation time is possible via the *dc* component of dielectric (or magnetic) relaxation and birefringence.

4.7 Generalization to Anomalous Relaxation

The nonlinear dielectric and Kerr-effect relaxation, treated in this chapter via the rotational diffusion model, may be extended to anomalous relaxation by using the fractional kinetic equation approach of Section 2.9, just like we have done for the noninteracting dipoles in Section 3.5. Here we consider, as an example, the Cole-Cole relaxation mechanism given by Eqs. (2.130) and (2.134) and characterized by the anomalous exponent α (other relaxation mechanisms can be treated in like manner). The generalization of the theory, based on a fractional version of the Smoluchowski equation, namely,

$$(\tau_D)^{\alpha-1}\,{}_{-\infty}D_t^{\alpha}W = \mathrm{L}_{FP}W + \mathrm{L}_t W, \tag{4.72}$$

has been fully explained in Section 2.9 and Refs. [1, 25] and ${}_{-\infty}D_t^{\alpha}$ is defined by Eq. (2.135). Here the general solution of Eq. (4.72) is of the form of the Fourier series, Eq. (2.23), so that, just as for the normal diffusion, we can obtain from Eq. (4.72) the fractional analogue of the differential-recurrence equation (4.7) for the response functions $f_n(t) = \langle P_n(\cos\vartheta)\rangle(t)$,

$$\begin{aligned}&\left[(\tau_D)^{\alpha}\,{}_{-\infty}D_t^{\alpha} + d_n\right] f_n(t) + c_n f_{n-2}(t) + g_n f_{n+2}(t)\\ &= a_n\left(\xi_0 + \xi\cos\omega t\right)\left[f_{n-1}(t) - f_{n+1}(t)\right].\end{aligned} \tag{4.73}$$

Under linear response conditions, $\xi << 1$, and σ, $\xi_0 = 0$, Eq. (4.73) yields the linear susceptibility from Eq. (2.130). Moreover, just as for the normal diffusion, Eq. (4.73) also allows one to evaluate the nonlinear ac stationary responses via a generalization of the two-mode approximation (see Ref. [78] for details). In the time domain, such a two-mode

approximation is equivalent to assuming that the relaxation function $\Phi_{nm}(t)$ may be approximated by *two* Mittag-Leffler functions only (cf. Eq. (4.33)),

$$\Phi_{nm}(t) \approx \Delta_{nm} E_\alpha \left[-(t/\tau_D)^\alpha \tau_D \lambda_1 \right] + (1-\Delta_{nm}) E_\alpha \left[-(t/\tau_D)^\alpha \tau_D / \tau_W^{(nm)} \right]. \quad (4.74)$$

In general, $\Phi_{nm}(t)$ comprises an *infinite number* of Mittag-Leffler functions $E_\alpha(z)$ [25] which are defined by Eq. (2.136). Noting that [1]

$$\int_0^\infty E_\alpha \left[-(t/\tau)^\alpha \right] e^{-st} dt = \frac{1}{s + \tau^{-\alpha} s^{1-\alpha}}, \quad (4.75)$$

the corresponding normalized dynamic susceptibility $X_{nm}(\omega)$ may now be approximated by a sum of two Cole-Cole functions, viz.,

$$X_{nm}(\omega) \approx \frac{\Delta_{nm}}{1+(i\omega/\omega_c)^\alpha} + \frac{1-\Delta_{nm}}{1+(i\omega/\omega_W^{(nm)})^\alpha}, \quad (4.76)$$

where $\omega_c = \tau_D^{-1}(\tau_D \lambda_1)^{1/\alpha}$ and $\omega_W^{(n1)} = \tau_D^{-1}(\tau_D / \tau_W^{(n1)})^{1/\alpha}$ are the characteristic frequencies. In particular, we have the generalization of Eqs. (4.71) for the dc component of the dielectric or Kerr-effect response, viz.,

$$\overline{f_n}(\omega) \approx \langle P_n \rangle_0 + \frac{\chi_{n2}\xi^2}{2} \mathrm{Re}\left(\frac{\Delta_{n0}}{1+(i\omega/\omega_c)^\alpha} + \frac{1-\Delta_{n0}}{1+(i\omega/\omega_W^{(n0)})^\alpha} \right), \quad (4.77)$$

All other nonlinear response equations obtained can be readily generalized in like manner. Such a generalization is likely to be important as the Cole-Cole relaxation behaviour has proved useful in the analysis of magnetic and dielectric relaxation data.

4.8 Discussion and Conclusion

We have presented two complementary approaches for treating the effects of an external dc bias field on the nonlinear ac stationary response of permanent dipoles in a uniaxial mean field potential to any desired order of the ac field amplitude with arbitrary dc field strength. The first approach (Section 4.2) is based on perturbation theory, allowing one to calculate numerically the nonlinear ac stationary responses using powerful matrix methods. For weak ac fields, $\xi << 1$, the results obtained from these numerical calculations are in complete agreement with the independent numerical matrix continued fraction solution of Ref. [18] which we introduced in Section 2.3. The second, semi-analytic approach (Sections 4.3-4.5), based on the two-mode approximation, originally proposed to model linear response functions of dipolar systems [27, 40], effectively

generalizes the existing results to treat the nonlinear response of dipolar particles over wide ranges of the anisotropy and external field parameters. Our results apply both to nonlinear dielectric and Kerr-effect relaxation of nematic liquid crystals and to nonlinear magnetization relaxation and magnetic birefringence relaxation of axially symmetric magnetic nanoparticles. In particular, one may explain the successful application of the known frequency dependence of the Kerr-effect response for free rotational diffusion to the analysis of experimental spectra of electric birefringence of nematics, which was previously done without any theoretical justification (see, for example, Ref. [79]). Furthermore, the analytic solution for the Kerr-effect response (e.g., Fig. 4.3 and Fig. 4.4) clearly demonstrates that this response contains information about the longest relaxation time of the system, which is due to the overbarrier relaxation processes. This fact suggests that new methods of measurement of the overbarrier (longest) relaxation time are possible via the electric or magnetic birefringence. We remark that, until now, two kinds of nonlinear response experiments have usually been carried out, namely: where either (i) a strong ac field alone (e.g., [52-54]) or (ii) a weak ac field superimposed on a strong dc bias field (e.g., [10, 11, 55-57]) were applied to the dielectric liquids. In polar dielectrics, although the applied fields in these experiments were high enough ($\geq 10^6$ V/m) to observe nonlinear effects, their strengths were sufficiently weak to allow one to use the nonlinear response equations obtained using perturbation theory. Comparison of experimental data [10, 11, 52-57] with the perturbation theory results demonstrated that they are in agreement. However, as the theory presented here is also applicable for arbitrary dc field strengths, it provides a theoretical basis for comparison with nonlinear response experiments in high *dc* fields. Note that some molecular and Brownian dynamics simulation data for systems of dipolar molecules in strong ac fields are also available (e.g., [80-83]). Furthermore, the use of computer simulation data is preferable to experimental data for testing a nonlinear theory as it is much easier to achieve high values of the dc field parameter $\xi_0 \geq 1$.

It is worth mentioning the experimental results of Wandersman *et al*. [84] in the context of the present work. In particular, these authors measured the magnetic birefringence in two dense ferrofluids. Their experimental data is fitted by the birefringence function

$$K(t) = ae^{-t/\tau_1} + (1-a)e^{-(t/\tau_2)^{\alpha}}, \tag{4.78}$$

where a is the normalized amplitude of the short-time decay mode and τ_1 is the associated time scale, while the τ_2 time scale describes the stretched exponentially long time decay of the magnetic birefringence. Bearing in mind that this stretched exponential behaviour is the short time expansion of the Mittag-Leffler function, one may say that anomalous diffusion manifests itself at long times only. Equation (4.33) is then formally a special case of Eq. (4.78) with $\alpha = 1$. Equation (4.78) in turn suggests a straightforward generalization to fractional birefringence dynamics, which has been alluded to in Section 4.7 (see, for example, Eqs. (4.74) and (4.76)).

Now, as mentioned to at the beginning of this chapter, Ladieu *et al*. [77] have recently suggested a model of nonlinear dielectric relaxation of supercooled liquids that has been compared with experimental data. The work presented here may be of importance in order to accurately represent their so-called "trivial" component (the term "trivial" component, used by Ladieu and coworkers refers to the monotonic frequency behaviour of the nonlinear response modulus, similar to the "ideal gas" behaviour of the Coffey-Paranjape formulas [2], so that the nonlinear polarization response consists of this "trivial" component augmented by a "singular" component which must definitely be associated with intermolecular dynamical correlations). The formulas obtained in this chapter cannot describe all the features of the experimental spectrum because dynamical correlations are not accounted for in the mean field approximation. This is clearly illustrated by the quasi-monotonic behaviour of the moduli of the Fourier amplitudes for the nonlinear dielectric response, as can be seen in Fig. 4.8 (conversely, the moduli of the Fourier amplitudes for the Kerr-effect response have nonmonotonic behaviour; see Fig. 4.9). However, the formulas presented here can be used to calculate the quasi-static nonlinear properties of the polarization of glass-forming liquids, and can therefore be included in Ladieu's model [77] as a first approximation.

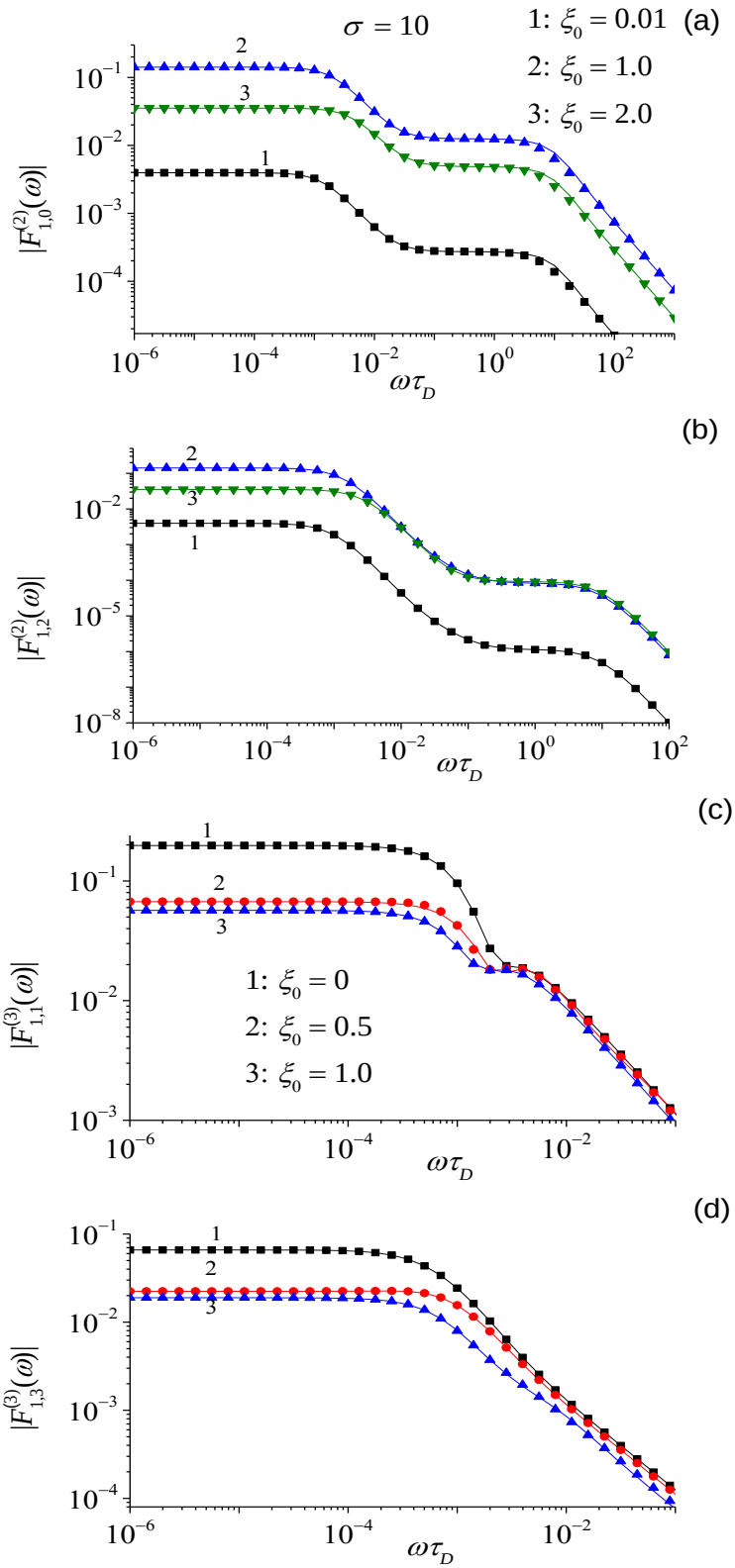

Fig. 4.8. Moduli of the dc component $\left|F_{1,0}^{(2)}(\omega)\right|$ (a), the 2nd harmonic component $\left|F_{1,2}^{(2)}(\omega)\right|$ (b), the fundamental component $\left|F_{1,1}^{(3)}(\omega)\right|$ (c), and the 3rd harmonic component $\left|F_{1,3}^{(3)}(\omega)\right|$ (d) of the nonlinear dielectric response vs. $\omega\tau_D$ for various values of the dc field amplitude ξ_0 with $\sigma = 10$. Solid lines: the matrix solution of Section 4.2. Symbols: the two-mode approximation, Eqs. (4.52), (4.53), (4.54), and (4.55), using fitting parameters.

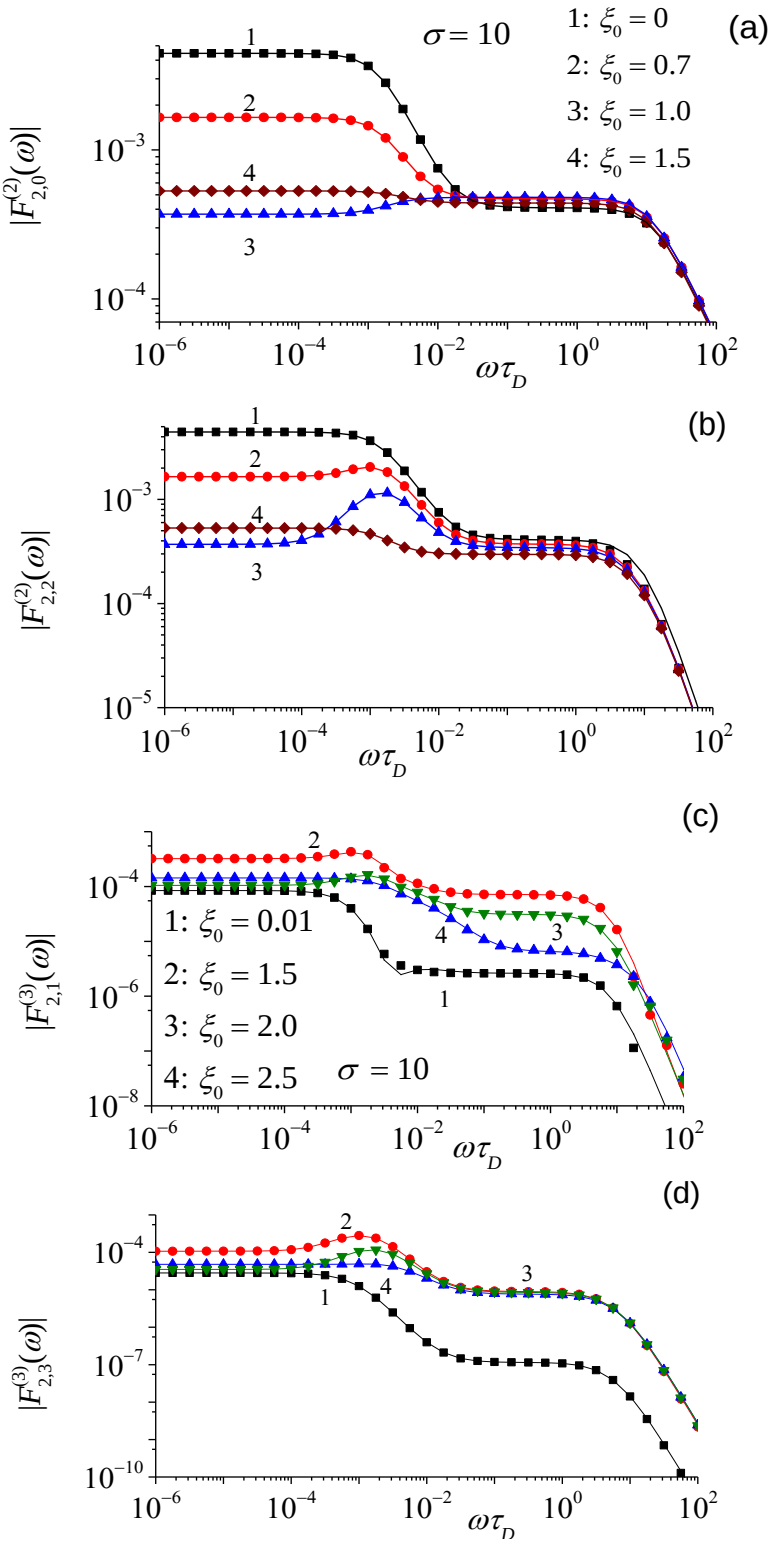

Fig. 4.9. Moduli of dc component $\left|F^{(2)}_{2,0}(\omega)\right|$ (a) and 2nd harmonic component $\left|F^{(2)}_{2,2}(\omega)\right|$ (b) of the 2nd order Kerr effect, the fundamental component $\left|F^{(3)}_{2,1}(\omega)\right|$ (c) and the third harmonic component $\left|F^{(3)}_{2,3}(\omega)\right|$ (d) of the 3rd order Kerr effect vs. $\omega\tau_D$ for various values of the dc field amplitude ξ_0 with the anisotropy parameter $\sigma = 10$. Solid lines: the matrix solution of Section 4.2. Symbols: the two-mode approximation, Eqs. (4.39), (4.40), (4.64) and (4.65), using fitting parameters.

The given methods of the solution of infinite hierarchies of *multi-term* recurrence relations are quite general and can be applied to analogous nonlinear response problems where time-dependent stimuli in high ac external fields are considered. In particular, our methods can also be used for the nonlinear dielectric and Kerr-effect ac stationary responses of polar and *anisotropically polarizable* molecules [50, 58-60]. Furthermore, they may be extended to nonstationary responses and to other mean field potentials. Moreover, they can be applied (with small modifications) to the nonlinear magnetic response of uniaxial magnetic nanoparticles, which we will discuss in the next chapter (see Eqs. (5.26)). Here the magnetization dynamics are governed by equations very similar to the Smoluchowski equation (4.2) [1, 6, 75]. Finally, the range of applicability of the rotational diffusion model in the mean field potential is restricted to the low-frequencies range ($\omega\tau_D \leq 1$), because the model does not include inertial effects. A consistent treatment of these effects must be carried out using the Fokker-Planck equation for the probability density function in configuration-angular velocity space. The inertia corrected rotational diffusion model in the uniaxial potential was used in Ref. [85] to determine the linear complex dielectric susceptibility tensor of polar liquid crystals in the entire frequency range of orientational polarization (up to 5 THz).

Appendix 4A: Parameters for the Two-Mode Approximation of the Linear Dielectric and Kerr-Effect Responses

We calculate explicitly the parameters appearing in Eq. (4.34) for the linear dielectric and Kerr-effect responses. For the dielectric response, the equations for τ_1 and τ_1^{eff} required for the calculation of Δ_{11} and $\tau_W^{(11)}$ in Eq. (4.34) can be evaluated by letting $n=1$ in Eqs. (2.121) and (2.122), which yields after simplifications

$$\tau_1 = \frac{2\tau_D}{Z\left(\left\langle P_1^2\right\rangle_0 - \left\langle P_1\right\rangle_0^2\right)} \int_{-1}^{1} \frac{\psi_1^2(z) e^{\sigma(z^2+2hz)}}{1-z^2}\, dz\,, \tag{4A.1}$$

and

$$\tau_1^{\text{eff}} = -\frac{1}{\dot{\Phi}_{11}(0)} = 2\tau_D \frac{\left\langle P_1^2\right\rangle_0 - \left\langle P_1\right\rangle_0^2}{1-\left\langle P_1^2\right\rangle_0}\,. \tag{4A.2}$$

Here the equilibrium averages $\langle P_1\rangle_0$ and $\langle P_1^2\rangle_0$, according to Eqs. (2.99)-(2.101), are

$$\langle P_1 \rangle_0 = \frac{1}{Z}\int_{-1}^{1} x e^{\sigma(x^2+2hx)} dx = \frac{e^{\sigma}\sinh(2\sigma h)}{\sigma Z} - h\,, \tag{4A.3}$$

and

$$\langle P_1^2 \rangle_0 = \frac{1}{Z}\int_{-1}^{1} x^2 e^{\sigma(x^2+2hx)} dx = \frac{e^{\sigma}[\cosh(2\sigma h) - h\sinh(2\sigma h)]}{\sigma Z} + h^2 - \frac{1}{2\sigma}\,, \tag{4A.4}$$

where $h = \xi_0 / 2\sigma$ is the dimensionless dc bias field parameter, Z is the partition function given by

$$Z = \int_{-1}^{1} e^{\sigma(x^2+2hx)} dx = \sqrt{\frac{\pi}{4\sigma}} e^{-\sigma h^2} \left\{ \text{erfi}[(1+h)\sqrt{\sigma}] + \text{erfi}[(1-h)\sqrt{\sigma}] \right\}, \tag{4A.5}$$

and

$$\text{erfi}(z) = \frac{2}{\sqrt{\pi}}\int_0^z e^{t^2} dt\,,$$

is the error function of imaginary argument [32]. Now, in the low barrier case, $\sigma, h << 1$, the behaviour of λ_1 , Δ_{11}, and $\tau_W^{(11)}$ is [1]

$$\lambda_1 \tau_D = 1 - \frac{2}{5}\sigma + \frac{48}{875}\sigma^2 - \frac{32}{21875}\sigma^3 + 4h^2\left(\frac{1}{10}\sigma^2 + \frac{1}{875}\sigma^3 + \ldots\right) + \ldots, \tag{4A.6}$$

$$\frac{\tau_W^{(11)}}{\tau_D} = \frac{1}{6} + \frac{1}{135}\sigma + \left(\frac{175}{108} + \frac{1739}{486}\sigma + \ldots\right)h^2 + \ldots, \tag{4A.7}$$

and

$$\Delta_{11} = 1 - \frac{12}{4375}\sigma^2 - \frac{22}{375}\sigma^2 h^2 + \ldots, \tag{4A.8}$$

respectively. Equation. (4A.6) is related to the smallest nonvanishing eigenvalue of the Fokker Planck operator, while Eqs. (4A.7) and (4A.8) may be evaluated by taking the Taylor series expansions of Eqs. (4A.1) and (4A.2) and then substituting the results into Eqs. (2.125) and (2.126). In the high barrier case, $\sigma(1-h)^2 >> 1$ and $h < 1$, the behaviour of λ_1 , Δ_{11}, and $\tau_W^{(11)}$ is given by [40]

$$\lambda_1 \tau_D \approx \frac{(1-h^2)\sigma^{3/2}}{\sqrt{\pi}}\left[(1-h)\,\mathrm{e}^{-(1-h)^2\sigma} + (1+h)\,\mathrm{e}^{-(1+h)^2\sigma}\right] + \ldots, \tag{4A.9}$$

$$\frac{\tau_D}{\tau_W^{(11)}} \approx 2(1+h)\sigma - \frac{5+h}{1+h} + \ldots, \tag{4A.10}$$

and

$$\Delta_{11} \approx \frac{1}{1+\dfrac{(1-h)\cosh^2(2\sigma h)}{4\sigma^2\left(1+h\right)^3}} + \ldots, \tag{4A.11}$$

where Eq. (4A.9) follows from asymptotic expansions of the mean first-passage time [7], while Eqs. (4A.10) and (4A.11) follow from Eqs. (4.15) and (3.15) of Ref. [40] respectively.

For the Kerr-effect response, the parameters Δ_{21} and $\tau_W^{(21)}$ are again expressed via three characteristic time constants, namely, the inverse of the smallest nonvanishing eigenvalue $1/\lambda_1$, the integral relaxation time τ_2 defined by Eq. (2.121), and the effective relaxation time τ_2^{eff} defined by Eq. (2.122). The relaxation times τ_2 and τ_2^{eff} are now given by Eqs. (2.121) and (2.122) for n = 2. In the low barrier case, $\sigma, h << 1$, the behaviour of Δ_{21}, and $\tau_W^{(21)}$ are given by, following the method for calculating Δ_{11} and $\tau_W^{(11)}$ (Eqs. (4A.7) and (4A.8)),

$$\frac{\tau_W^{(21)}}{\tau_D} = \frac{1}{3} + \frac{1}{315}\sigma - \frac{1252}{165375}\sigma^2 - \frac{16}{315}\sigma^2 h^2 + \ldots, \tag{4A.12}$$

and

$$\Delta_{21} = \frac{3}{4} - \frac{23}{280}\sigma + \frac{1149}{98000}\sigma^2 - \frac{11}{140}\sigma^2 h^2 + \ldots, \tag{4A.13}$$

while for the high barrier case, $\sigma\left(1-h\right)^2 >> 1$, we have the following relaxation times τ_2 and τ_2^{eff}:

$$\frac{\tau_2}{\tau_D} = \frac{8e^{\sigma(1-h)^2}\sqrt{\dfrac{\pi}{\sigma}}\left[1+\dfrac{\sinh\left(4\sigma h\right)}{4\sigma h}\right]^{-1}}{\left[1-h+e^{-4\sigma h}\right]\left\{2+4\sigma\left(1-h^2\right)^2 - e^{-\sigma(1-h)^2}\left[1+2\sigma\left(1+h\right)^2\right]\right\}}, \tag{4A.14}$$

and

$$\begin{aligned}\frac{\tau_2^{\text{eff}}}{\tau_D} &= 6h^2\frac{\cosh\left(4\sigma h\right)}{\sinh^2\left(4\sigma h\right)} + h\frac{64+28\sigma-7\cosh\left(4\sigma h\right)}{32\sigma\sinh\left(4\sigma h\right)} \\ &\quad + \left(85+28\sigma\right)\frac{224\sigma^2h^2\cosh\left(8\sigma h\right)-1}{112\sigma^2\sinh^2\left(4\sigma h\right)}.\end{aligned} \tag{4A.15}$$

Equations (4A.14) and (4A.15) can be used to evaluate $\tau_W^{(21)}$ and Δ_{21} by Eqs. (2.125) and (2.126), respectively, for large σ in the range $h \leq 0.17$, since outside this range Eq. (4A.14) diverges exponentially from λ_1^{-1}.

5 DC Response of Uniaxial Magnetic Nanoparticles

In the previous chapters, the model of the Brownian motion was used to study the behaviour of the electric dipoles under the influence of the ac and dc bias field. Since the motion of the uniaxial magnetic nanoparticles can also be described by a similar Fokker-Planck equation, in this chapter we are going to investigate the nonlinear frequency-dependent effects in the dc magnetization in superimposed strong ac and dc fields.

A fine ferromagnetic particle is characterized by an internal magnetocrystalline anisotropy potential with several local states of equilibrium and potential barriers between them, the heights of which depend on the size of the particle. If the particles are small (~10 nm) so that the energy barriers are comparable to the thermal energy, the magnetization vector **M** may cross over from one potential well to another and vice versa due to the thermal agitation, with a relaxation time which depends exponentially on the volume of a particle. The ensuing thermal instability of the magnetization of fine particles results in superparamagnetism and magnetic after-effect. The thermal fluctuations and relaxation of the magnetization of such particles play a central role in information storage, rock magnetism, magnetic hyperthermia, etc. [86, 87]. In addition, the Zeeman energy is relatively large even in moderate external magnetic fields due to the large magnitude of the particles' magnetic dipole moment (~10^4–10^5 μ_B). Hence we expect that their magnetization dynamics will exhibit a pronounced dependence on the strength, frequency and orientation of these fields [75], which is significant because the nonlinear response of fine particles driven by a strong ac field occurs in diverse physical applications. These include nonlinear dynamic susceptibilities and field induced birefringence [75, 88-90], nonlinear stochastic resonance [91], dynamic hysteresis [17, 33], and microwave field effects [92].

The calculation of the nonlinear magnetic response of nanomagnets in the presence of thermal agitation originating in a heat bath usually commences with the magnetic Langevin equation (2.52). This is Gilbert's (or the Landau-Lifshitz) equation augmented by a random magnetic field $\mathbf{h}(t)$ with Gaussian white noise properties, Eq. (2.53), accounting for the thermal fluctuations of the magnetization $\mathbf{M}(t)$ of an individual

particle [29]. The stochastic differential equation (2.52) is then used to derive the accompanying Fokker-Planck equation governing the time evolution of the probability density function $W(\mathbf{u},t)$ of the magnetization orientations on the surface of a sphere of constant radius M_S ($\mathbf{u}$ is a unit vector along $\mathbf{M}$) (see Fig. 2.2), where the relevant Fokker-Planck equation is [29]

$$2\tau_N \frac{\partial W}{\partial t} = \nabla^2 W + \frac{\beta}{\alpha}\left(\mathbf{u}\cdot\left[\nabla V \times \nabla W\right]\right) + \beta\left(\nabla \cdot W \nabla V\right). \tag{5.1}$$

Here $\nabla = \partial/\partial\mathbf{u}$ is the gradient operator on the unit sphere, $\alpha = \gamma\eta M_S$ is the dimensionless damping constant, $\tau_N = \tau_0(\alpha + \alpha^{-1})$ is the characteristic free diffusion time of $\mathbf{M}(t)$ with $\tau_0 = \beta\mu_0 M_S/(2\gamma)$, $\beta = v/(kT)$, v is the volume of a typical particle, k is Boltzmann's constant, T is the absolute temperature, and μ_0 is the permeability of free space. A general method of solving the Fokker-Planck equation (5.1) for *arbitrary* magnetocrystalline anisotropy energy density has been given in Chapter 2 (see also Refs. [1, 15]). We remark that Eq. (5.1), omitting the second (precessional) term on the right hand side, is essentially similar to the Smoluchowski equation (2.16) describing the dielectric and Kerr-effect relaxation in polar liquids [1], as discussed in the previous chapters. However, the precessional term has a profound effect on the magnetization dynamics, especially in the nonlinear case, because it may couple, depending on the *direction* of the applied field, the longitudinal and transverse modes in Eq. (5.1) as we shall presently see.

Now, in the most basic model used to study nonlinear relaxation processes, the free-energy density V (Fig. 5.1) of a single-domain nanoparticle with uniaxial anisotropy in superimposed homogeneous external dc bias and ac magnetic fields $\mathbf{H}_0 + \mathbf{H}\cos\omega t$ of arbitrary strengths and orientations relative to the easy axis of the particle is given by

$$\beta V = \sigma \sin^2\vartheta - \xi_0\left(\mathbf{u}\cdot\mathbf{H}_0\right)/H_0 - \xi\cos\omega t\left(\mathbf{u}\cdot\mathbf{H}\right)/H, \tag{5.2}$$

where $\sigma = \beta K$, $\xi_0 = \beta H_0 M_S$, $\xi = \beta H M_S$ are the dimensionless anisotropy and external field parameters, and K is the anisotropy constant.

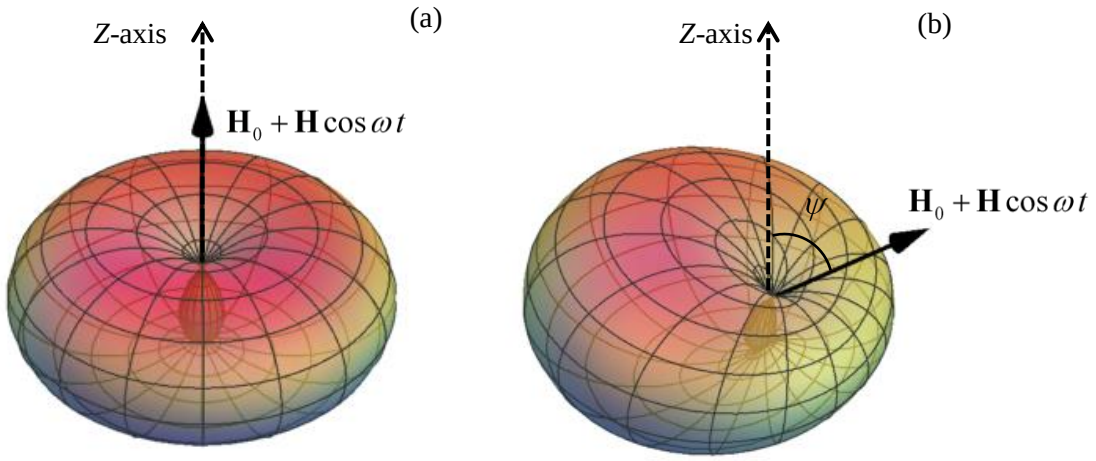

Fig. 5.1. Uniaxial anisotropy with the dc bias and ac magnetic fields applied along the easy axis (Z-axis) (a) and at an oblique angle ψ (b) as used in this chapter.

Various treatments of the nonlinear ac stationary response have been effected by means of numerical solutions of the governing dynamical equations (2.52) and/or (5.1). In particular, efficient numerical algorithms for the calculation of the nonlinear ac stationary response of the magnetization of *uniaxial* magnetic nanoparticles have been proposed [16-18] by assuming that the dc bias and ac driving fields *are directed along the easy axis* of the particle. However, in the *axially symmetric* configuration, many interesting nonlinear effects are suppressed because no dynamical coupling between the longitudinal and transverse precessional modes of motion exists. These mode coupling effects in the *nonlinear* ac stationary response can only be modelled for uniaxial particles driven by a strong ac field applied at *an angle* to the easy axis of the particle, so that the axial symmetry is broken by the Zeeman energy [19-22]. Now, building on the axially symmetric solutions described in Refs. [16, 18], an exact nonperturbative method for the determination of the Fourier amplitudes (see Eq. (5.9)) and so the nonlinear magnetization of magnetic nanoparticles with an *arbitrary* anisotropy potential and subjected to a strong ac driving field superimposed on a strong dc bias field has recently been given by Titov *et al*. [23]. The method is rooted in posing the solution of the averaged magnetic Langevin equation for the statistical moments (expectation values of the spherical harmonics) in terms of matrix continued fractions in the frequency domain, which can be applied to the Fokker-Planck equation approach as fully explained in Chapter 2. So far this method has been used to determine the dynamic susceptibilities (linear, cubic, etc.) and dynamic hysteresis loops in uniaxial magnetic nanoparticles in Refs. [21, 23]. Here, we focus for the first time on nonlinear frequency-dependent effects in the *time-independent* dc

component of the magnetization in superimposed external dc bias and ac magnetic fields, which were not sufficiently investigated in previous studies. Thus we shall demonstrate that under such conditions, the dc magnetization of a magnetic nanoparticle drastically alters leading to pronounced nonlinear effects including three dispersion bands at low, intermediate and high frequencies in the dc magnetization spectrum. We shall also evaluate the dc magnetization of *an assembly* of noninteracting uniaxial nanoparticles with *randomly* oriented easy axes in space which display similar nonlinear phenomena.

5.1 Exact AC Stationary Solution of DC Magnetization

Henceforth, we shall assume for simplicity that the easy axis of the particles coincides with the *Z*-axis (see Fig. 5.1) and that $\mathbf{H}_0$ and $\mathbf{H}$ are parallel. Now, due to cylindrical symmetry about the *Z*-axis, the component of the magnetization in the direction of $\mathbf{H}_0$ and $\mathbf{H}$ depends only on the oblique angle ψ between $\mathbf{H}_0$ and the *Z*-axis. In Chapter 2 we extended the method of Titov *et al.* [23] to determine the magnetization in the direction of the ac field when the system was subjected to ac and dc magnetic fields. First, the magnetic Langevin equation (2.52) is used to derive the accompanying Fokker-Planck equation (2.57). Then the Fokker-Planck equation (2.57) instead of using (ϑ, φ) as variables, is transformed to an infinite hierarchy of differential-recurrence relations for the statistical moments (the averages of the spherical harmonics) $\langle Y_{l,m} \rangle (t)$ (see Eq. (2.80)). Here, without loss of generality, we may suppose that both $\mathbf{H}_0$ and $\mathbf{H}$ lie in the *XZ* plane of the laboratory coordinate system (see Fig. 2.2). Thus, by replacing the direction cosines of the fields with $(\gamma_1, \gamma_2, \gamma_3) = (\sin\psi, 0, \cos\psi)$, Eq. (2.80) becomes

$$\tau_N \frac{d}{dt}\langle Y_{l,m}\rangle(t)+\left[\frac{l(l+1)}{2}+\frac{im}{2\alpha}(\xi_0+\xi\cos\omega t)\cos\psi-\sigma\frac{l(l+1)-3m^2}{(2l-1)(2l+3)}\right]\langle Y_{l,m}\rangle(t)$$
$$=\frac{\sigma(l+1)}{2l-1}\sqrt{\frac{(l^2-m^2)[(l-1)^2-m^2]}{(2l-3)(2l+1)}}\langle Y_{l-2,m}\rangle(t)$$
$$-\frac{\sigma l}{2l+3}\sqrt{\frac{[(l+2)^2-m^2][(l+1)^2-m^2]}{(2l+5)(2l+1)}}\langle Y_{l+2,m}\rangle(t)$$
$$+\left[(\xi_0+\xi\cos\omega t)\frac{l+1}{2}\cos\psi-\frac{im\sigma}{\alpha}\right]\sqrt{\frac{l^2-m^2}{4l^2-1}}\langle Y_{l-1,m}\rangle(t)$$
$$-\left[(\xi_0+\xi\cos\omega t)\frac{l}{2}\cos\psi+\frac{im\sigma}{\alpha}\right]\sqrt{\frac{(l+1)^2-m^2}{(2l+3)(2l+1)}}\langle Y_{l+1,m}\rangle(t)$$
$$-\frac{(\xi_0+\xi\cos\omega t)\sin\psi}{4}\left[\frac{i}{\alpha}\sqrt{(l-m+1)(l+m)}\langle Y_{l,m-1}\rangle(t)-\frac{i}{\alpha}\sqrt{(l+m+1)(l-m)}\langle Y_{l,m+1}\rangle(t)\right.$$
$$+(l+1)\sqrt{\frac{(l+m)(l+m-1)}{4l^2-1}}\langle Y_{l-1,m-1}\rangle(t)+(l+1)\sqrt{\frac{(l-m)(l-m-1)}{4l^2-1}}\langle Y_{l-1,m+1}\rangle(t)$$
$$\left.+l\sqrt{\frac{(l-m+1)(l-m+2)}{(2l+3)(2l+1)}}\langle Y_{l+1,m-1}\rangle(t)+l\sqrt{\frac{(l+m+1)(l+m+2)}{(2l+3)(2l+1)}}\langle Y_{l+1,m+1}\rangle(t)\right], \tag{5.3}$$

where the angular brackets $\langle\ \ \rangle$ denote the ensemble averaging in the presence of the ac field. Now, by confining ourselves to the stationary solution for the magnetization in the direction of the ac driving field $m(t)=M_S\langle\cos\Theta\rangle(t)$, where Θ is the angle between the vectors $\mathbf{M}$ and $\mathbf{H}$ so that

$$\begin{aligned} m(t)&=\langle\mathbf{M}\cdot\mathbf{H}\rangle(t)/H=M_S\langle\cos\Theta\rangle(t)\\ &=M_S\langle\sin\psi\sin\vartheta\cos\varphi+\cos\psi\cos\vartheta\rangle(t), \end{aligned} \tag{5.4}$$

and, using the known definitions of the spherical harmonics of the first rank, viz., [36]

$$Y_{1,0}=\sqrt{\frac{3}{4\pi}}\cos\vartheta,\quad Y_{1,\pm1}=\mp\sqrt{\frac{3}{8\pi}}\sin\vartheta e^{\pm i\varphi}, \tag{5.5}$$

we see that the magnetization $m(t)$ can be expressed via the statistical moments $\langle Y_{1,0}\rangle(t)$ and $\langle Y_{1,\pm1}\rangle(t)$ as

$$m(t)=M_S\sqrt{\frac{2\pi}{3}}\left\{\sqrt{2}\cos\psi\langle Y_{1,0}\rangle(t)+\sin\psi\left[\langle Y_{1,-1}\rangle(t)-\langle Y_{1,1}\rangle(t)\right]\right\}. \tag{5.6}$$

Since, as in Section 2.6, the averaged spherical harmonics can be written as a Fourier series in the time,

$$\left\langle Y_{l,m}\right\rangle(t)=\sum_{k=-\infty}^{\infty}c_{l,m}^{k}(\omega)\,e^{ik\omega t}\,, \tag{5.7}$$

Eq. (5.6) can be written as

$$m(t)=\sqrt{\frac{4\pi}{3}}M_S\sum_{k=-\infty}^{\infty}\left[\cos\psi c_{1,0}^{k}(\omega)+\sin\psi\,\frac{c_{1,-1}^{k}(\omega)-c_{1,1}^{k}(\omega)}{\sqrt{2}}\right]e^{ik\omega t}\,, \tag{5.8}$$

which we write in the compact form

$$m(t)=M_S\sum_{k=-\infty}^{\infty}m_1^{k}(\omega)\,e^{ik\omega t}\,, \tag{5.9}$$

where $m_1^{k}(\omega)$ is the amplitude of the k^{th} harmonic in the nonlinear response given by [23] (cf. Eq. (8) of that paper specialized to cylindrical symmetry)

$$m_1^{k}(\omega)=\sqrt{\frac{4\pi}{3}}\left[\cos\psi c_{1,0}^{k}(\omega)+\sin\psi\,\frac{c_{1,-1}^{k}(\omega)-c_{1,1}^{k}(\omega)}{\sqrt{2}}\right]. \tag{5.10}$$

Therefore the magnetization $m(t)$ can be determined exactly using the method of Section 2.6. The $c_{l,m}^{k}(\omega)$ are themselves the Fourier coefficients in a Fourier series development in the time of the average spherical harmonics governed by the evolution Eq. (5.3), viz. Eq. (5.7). However, the Fourier coefficients $c_{l,m}^{k}(\omega)$ of the k^{th} harmonic component in Eq. (5.7) of the average first rank spherical harmonics, $\left\langle Y_{1,0}\right\rangle(t)$ and $\left\langle Y_{1,\pm1}\right\rangle(t)$, underpinning the magnetization nonlinear response, are connected to *all other* Fourier coefficients $c_{l,m}^{k}(\omega)$ of spherical harmonics of different ranks via the differential-recurrence relation, Eq. (5.3). Nevertheless, despite this entanglement, the particular coefficients $c_{1,m}^{k}(\omega)$ pertaining to Eq. (5.10) can be calculated numerically via matrix continued fractions [23] (details in Section 2.6). Here, we focus on the *time-independent* or dc component of the magnetization $M_{\xi}(\omega)$, defined by the mean value

$$M_{\xi}(\omega)=\frac{\omega}{2\pi M_S}\int_{0}^{2\pi/\omega}m(t)\,dt=m_1^{0}(\omega)\,, \tag{5.11}$$

which, we note, is entirely real.

5.2 Limit Values of DC Magnetization

In Section 5.1 we developed an exact solution for the dc magnetization (cf. Eqs. (5.10) and (5.11)) using matrix continued fractions (Section 2.6) which is valid for all strengths, orientations, and frequencies of the applied fields. In the cases of a vanishing ac field, very high driving frequency or very low frequency, however, we can derive asymptotic solutions for the dc magnetization.

First, we note that Eqs. (5.10) and (5.11) yield two limiting values for the dc magnetization in the limits of *vanishing ac field*, $\xi \to 0$, and/or of *very high frequency field*, $\omega \to \infty$, which are

$$\lim_{\xi \to 0} M_{\xi}(\omega) = M_0 \quad \text{and} \quad \lim_{\omega \to \infty} M_{\xi}(\omega) = M_{\xi}(\infty),$$

respectively. However, both of the foregoing limits are equal, i.e., $M_{\xi}(\infty) = M_0 = M_0(\sigma, \xi_0, \psi)$, and can be expressed simply in terms of the stationary average $\langle \cos\Theta \rangle_0$ as

$$M_{\xi}(\infty) = M_0 = \langle \cos\Theta \rangle_0, \tag{5.12}$$

where the angular brackets $\langle \quad \rangle_0$ denote *stationary* ensemble averaging, namely,

$$\langle \cos\Theta \rangle_0 = \frac{1}{Z} \int_0^{2\pi} \int_0^{\pi} \cos\Theta \, e^{\sigma \cos^2 \vartheta + \xi_0 \cos\Theta} \sin\vartheta \, d\vartheta \, d\varphi, \tag{5.13}$$

where Z is the partition function given by

$$Z = \int_0^{2\pi} \int_0^{\pi} e^{\sigma \cos^2 \vartheta + \xi_0 \cos\Theta} \sin\vartheta \, d\vartheta \, d\varphi. \tag{5.14}$$

In the *very low frequency* limit, $\omega \to 0$, the mean value $M_{\xi}(0)$ can also be evaluated by using a quasistatic Boltzmann distribution in Eqs. (5.13) and (5.14) as

$$M_{\xi}(0) = \lim_{\omega \to 0} \frac{\omega}{2\pi} \int_0^{2\pi/\omega} M_0(\sigma, \xi_0 + \xi \cos\omega t, \psi) dt, \tag{5.15}$$

which can be rewritten as

$$M_{\xi}(0) \approx \lim_{\omega \to 0} \frac{\omega}{2\pi} \int_0^{2\pi/\omega} \frac{\displaystyle\int_0^{2\pi} \int_0^{\pi} \cos\Theta \, e^{\sigma \cos^2 \vartheta + \xi_0 \cos\Theta + \xi \cos\omega t \cos\Theta} \sin\vartheta \, d\vartheta \, d\varphi}{\displaystyle\int_0^{2\pi} \int_0^{\pi} e^{\sigma \cos^2 \vartheta + \xi_0 \cos\Theta + \xi \cos\omega t \cos\Theta} \sin\vartheta \, d\vartheta \, d\varphi} dt. \tag{5.16}$$

Moreover, if we consider the response to a *weak* ac field $\xi << 1$, perturbation theory will be valid (which we used to find the static susceptibilities for electric dipoles in Section 2.7). Thus, using the expansion of the functions in the limit of $x \ll 1$ [32],

$$e^x = 1 + x + \frac{x^2}{2!} + \cdots, \qquad \frac{1}{1+x} = 1 - x + x^2 - \cdots, \tag{5.17}$$

Eq. (5.16) to the second order of ξ becomes

$$M_\xi(0) = \lim_{\omega\to 0} \frac{\omega}{2\pi} \int_0^{2\pi/\omega} \left[\frac{\int_0^{2\pi}\int_0^{\pi} \cos\Theta e^{\sigma\cos^2\vartheta + \xi_0\cos\Theta} \left(1 + \xi\cos\omega t\cos\Theta + \frac{(\xi\cos\omega t\cos\Theta)^2}{2!}\right)\sin\vartheta d\vartheta d\varphi}{\int_0^{2\pi}\int_0^{\pi} e^{\sigma\cos^2\vartheta + \xi_0\cos\Theta} \left(1 + \xi\cos\omega t\cos\Theta + \frac{(\xi\cos\omega t\cos\Theta)^2}{2!}\right)\sin\vartheta d\vartheta d\varphi} \right] dt, \tag{5.18}$$

which we can write in terms of the stationary averages,

$$M_\xi(0) = \lim_{\omega\to 0} \frac{\omega}{2\pi} \int_0^{2\pi/\omega} \left[\frac{\langle\cos\Theta\rangle_0 + \xi\cos\omega t\langle\cos^2\Theta\rangle_0 + \frac{1}{2}\xi^2\cos^2\omega t\langle\cos^3\Theta\rangle_0}{1 + \xi\cos\omega t\langle\cos\Theta\rangle_0 + \frac{1}{2}\xi^2\cos^2\omega t\langle\cos^2\Theta\rangle_0} \right] dt. \tag{5.19}$$

Using Eq. (5.17) then gives us

$$\begin{aligned} M_\xi(0) &= \lim_{\omega\to 0} \frac{\omega}{2\pi} \int_0^{2\pi/\omega} \left[\left(\langle\cos\Theta\rangle_0 + \xi\cos\omega t\langle\cos^2\Theta\rangle_0 + \frac{1}{2}\xi^2\cos^2\omega t\langle\cos^3\Theta\rangle_0 \right) \right. \\ &\quad \left. \left(1 - \xi\cos\omega t\langle\cos\Theta\rangle_0 - \frac{1}{2}\xi^2\cos^2\omega t\langle\cos^2\Theta\rangle_0 + \xi^2\cos^2\omega t\langle\cos\Theta\rangle_0^2 \right) \right] dt \\ &= \lim_{\omega\to 0} \frac{\omega}{2\pi} \int_0^{2\pi/\omega} \left[\langle\cos\Theta\rangle_0 + \xi\cos\omega t\left(\langle\cos^2\Theta\rangle_0 - \langle\cos\Theta\rangle_0^2\right) \right. \\ &\quad \left. + \frac{1}{2}\xi^2\cos^2\omega t\left(\langle\cos^3\Theta\rangle_0 - 3\langle\cos^2\Theta\rangle_0\langle\cos\Theta\rangle_0 + 2\langle\cos\Theta\rangle_0^3\right) \right] dt, \end{aligned} \tag{5.20}$$

which reduces to

$$M_\xi(0) = \langle\cos\Theta\rangle_0 + \frac{1}{4}\xi^2\left(\langle\cos^3\Theta\rangle_0 - 3\langle\cos^2\Theta\rangle_0\langle\cos\Theta\rangle_0 + 2\langle\cos\Theta\rangle_0^3\right). \tag{5.21}$$

Thus, the dispersion amplitude $M_\xi(\infty) - M_\xi(0)$ can be evaluated from Eqs. (5.12) and (5.21) via the stationary averages $\langle\cos\Theta\rangle_0$, $\langle\cos^2\Theta\rangle_0$, and $\langle\cos^3\Theta\rangle_0$, viz.,

$$M_\xi(0) - M_\xi(\infty) = \frac{\xi^2}{4}\left(\langle\cos^3\Theta\rangle_0 - 3\langle\cos^2\Theta\rangle_0\langle\cos\Theta\rangle_0 + 2\langle\cos\Theta\rangle_0^3\right) + o\left(\xi^2\right) \tag{5.22}$$

Furthermore, for axial symmetry (i.e., where both the dc bias and ac fields are applied along the easy axis) we have $\psi = 0$ and $\Theta = \vartheta$, so that Eqs. (5.12) - (5.14) become known integrals, viz.,

$$M_0(\sigma, \xi_0, 0) = \langle \cos\vartheta \rangle_0 = \frac{1}{Z}\int_{-1}^{1} x e^{\sigma x^2 + \xi_0 x} dx = \frac{e^{\sigma}\sinh\xi_0}{\sigma Z} - \frac{\xi_0}{2\sigma}, \qquad (5.23)$$

where the partition function Z is given by

$$Z = \int_{-1}^{1} e^{\sigma x^2 + \xi_0 x} dx = \frac{1}{2}\sqrt{\frac{\pi}{\sigma}} e^{-\frac{\xi_0^2}{4\sigma}} \left\{ \mathrm{erfi}\left[\sqrt{\sigma}\left(1 + \frac{\xi_0}{2\sigma}\right)\right] + \mathrm{erfi}\left[\sqrt{\sigma}\left(1 - \frac{\xi_0}{2\sigma}\right)\right]\right\}, \qquad (5.24)$$

and

$$\mathrm{erfi}(z) = \frac{2}{\sqrt{\pi}}\int_0^z e^{t^2} dt\,,$$

is the error function of imaginary argument. Hence, in all the foregoing limits, only a knowledge of the equilibrium averages is required.

Now regarding the behaviour of $M_{\xi}(\omega)$ as a function of the ac field amplitude, we remark that strong nonlinear effects in the dc magnetization are expected for $\xi > 1$. For example, for cobalt nanoparticles with mean diameter a ~10 nm and saturation magnetization $M_S \approx 1.4 \cdot 10^6$ A m^{-1}, the field parameter ξ has order unity for $H \sim 6kT/(\pi a^3 \mu_0 M_S) \sim 4.5 \cdot 10^3$ A m^{-1} at $T \sim 30$ K [16]. Moreover, an ac field of this order of magnitude is easily attainable in practical measurements of the nonlinear response of magnetic nanoparticles [88]. On the other hand, the condition $\xi << 1$ corresponds to the response to a weak ac field, where we have stated that perturbation theory is valid. Here, because the nonlinear contribution to the dc magnetization has order ξ^2, $M_{\xi}(\omega)$ is itself only weakly dependent upon ξ. Nevertheless, $M_{\xi}(\omega)$ strongly depends on the angle ψ, dc bias field ξ_0, barrier height σ, and damping α.

5.3 DC Magnetization for $\psi = 0$

In order to illustrate the nonlinear effects in the time-independent but frequency-dependent magnetization $M_{\xi}(\omega)$ induced by the ac field, which in general exhibits a pronounced frequency dependence due to the ac field acting in conjunction with the bias field, we plot

$M_\xi(\omega)$ as a function of the dc field ξ_0, frequency ω, and inverse temperature σ for various values of the ac field magnitude ξ, damping α, and lastly (in Section 5.3) the oblique angle ψ between the bias field and easy axis.

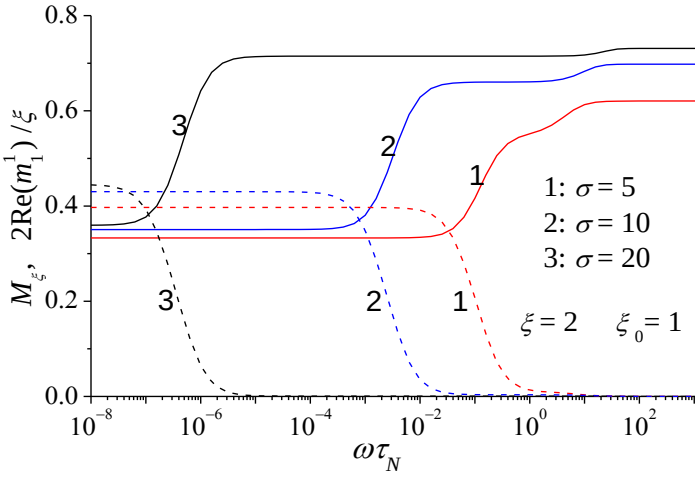

Fig. 5.2 Comparison of the dc magnetization M_ξ, Eq. (5.11), (solid lines) and real part of the fundamental component of the nonlinear dynamic susceptibility $2\,\mathrm{Re}(m_1^1)/\xi$ (dashed lines) vs. normalized frequency $\omega\tau_N$ for $\xi_0 = 1$, $\xi = 2$, $\alpha = 1$, and various values of the anisotropy parameter $\sigma = vK/(kT)$.

We first present results for the dc magnetization of an assembly of *aligned* nanoparticles with the angle $\psi = 0$ so that axial symmetry prevails. Then, in the small ac field limit, $\xi << 1$, the dc component $M_\xi(\omega)$ can be evaluated analytically via perturbation theory (see Section 4.6) while, in strong ac driving fields, $\xi > 1$, $M_\xi(\omega)$ can be determined using the matrix continued fraction method as applied to axially symmetric problems [18] (see Section 5.1). To facilitate our discussion, plots of both $M_\xi(\omega)$ and the real part of the *fundamental* component (i.e., the term prefixed by $e^{i\omega t}$ in Eq. (5.9)) of the nonlinear dynamic susceptibility $\chi(\omega) = 2m_1^1/\xi$ [1] as a function of the normalized frequency $\omega\tau_N$ for various values of the anisotropy (or inverse temperature) parameter $\sigma = vK/(kT)$ are shown in Fig. 5.2. By inspection of that figure, two distinct low- and high-frequency dispersion bands appear in the spectrum of $M_\xi(\omega)$ just as with the susceptibility $\chi(\omega)$ (in the latter, the high-frequency dispersion region would be visible on the logarithmic scale [1, 18]). Moreover, the low-frequency dispersion of each of the two functions $M_\xi(\omega)$ and $\chi(\omega)$ are clearly governed by the barrier crossing relaxation

modes with the *same* characteristic frequency *indicating that the magnetization reversal time may be directly determined from measurements of the dc response* $M_\xi(\omega)$.

In addition, for weak ac fields, the characteristic frequency ω_1 of this low-frequency band may be determined explicitly as $\omega_1 = \lambda_1$ via the smallest nonvanishing eigenvalue λ_1 of the Fokker-Planck operator in Eq. (5.1) associated with the overbarrier relaxation processes. We recall that, subject to $\xi << 1$, λ_1 for the potential given by Eq. (5.2) with $\psi = 0$, corresponding to axial symmetry, is given by Brown's asymptotic high barrier formula [6, 29]

$$\lambda_1 \sim \frac{(1-h^2)\sqrt{\sigma^3}}{\tau_N \sqrt{\pi}}\left[(1+h)e^{-\sigma(1+h)^2} + (1-h)e^{-\sigma(1-h)^2}\right], \tag{5.25}$$

where $h = \xi_0/(2\sigma) = \mu_0 M_S H_0/(2K)$. Equation (5.25), because it relates to an axially symmetric system governed by a scalar differential-recurrence relation for the observables in the time domain, is valid for all values of the damping α. Now, for cobalt nanoparticles with anisotropy constant $K \sim 10^5$ J/m^3 and $\alpha \sim 0.1$, the free diffusion relaxation time is $\tau_N \sim 4\cdot 10^{-10}$ s (with $\gamma = 2.2\cdot 10^5$ mA^{-1}s^{-1}). Furthermore, considering the critical value [1] of the dimensionless parameter $h = \mu_0 M_S H_0/(2K) = 1$ at which the double well structure of the magnetocrystalline/Zeeman energy $\sigma \sin^2\vartheta - \xi_0 \cos\Theta$ disappears, one may infer that the low-frequency overbarrier relaxation processes vanish for a dc bias field $H_0 \approx 1.14\cdot 10^5$ Am^{-1}. Now, at the opposite end of the spectrum, the high-frequency band is due to "intrawell" relaxation modes. These individual near-degenerate high frequency modes are, however, virtually indistinguishable in the frequency spectrum of $M_\xi(\omega)$, appearing merely as a single high-frequency dispersion band, just as with the magnetic dynamic susceptibility. Thus, like the susceptibility $\chi(\omega)$, the spectrum of $M_\xi(\omega)$ may in practice be approximated by a sum of two Lorentzians, viz.,

$$M_\xi(\omega) \approx M_\xi(\infty) + \left[M_\xi(0) - M_\xi(\infty)\right]\left(\frac{\Delta}{1+(\omega/\omega_1)^2} + \frac{1-\Delta}{1+(\omega/\omega_2)^2}\right). \tag{5.26}$$

Here ω_1 and ω_2 are, respectively, the characteristic frequencies of the overbarrier relaxation modes, which are related to the Kramers escape rate $\Gamma \sim \lambda_1$, and the near-

degenerate high frequency "intrawell" relaxation modes (both in the presence of an ac external field), and Δ is an adjustable amplitude parameter.

The dc magnetization $M_\xi(\omega)$, obtained via the matrix continued fraction method [1], is shown as a function of the normalized frequency $\omega\tau_N$ and as a function of the dc field ξ_0 in Fig. 5.3 and Fig. 5.4, respectively for various values of the ac driving field amplitude ξ. Furthermore, M_ξ is shown as a function of the inverse temperature parameter σ for the particular dc field amplitude $\xi_0 = 1$ in Fig. 5.5. As shown in Fig. 5.3 - Fig. 5.5, the approximate equation (5.26) accurately fits the numerical matrix continued fraction results. The corresponding fitting parameters ω_1, ω_2, and Δ are exhibited in Fig. 5.6 as functions of the ac field amplitude ξ, dc field amplitude ξ_0, and inverse temperature parameter σ. In Fig. 5.2 and Fig. 5.3, the limiting value of $M_\xi(\omega)$ as $\omega \to \infty$ is $M_\xi(\infty) = M_0(\sigma, \xi_0, 0)$, calculated from Eq. (5.23) with $\psi = 0$, and the limiting value of $M_\xi(\omega)$ as $\omega \to 0$ is $M_\xi(0)$, calculated from Eq. (5.15) with $\psi = 0$. We remark that for weak ac fields $\xi << 1$ and high barriers $\sigma(1-h^2) >> 1$, ω_1 can be evaluated explicitly from Brown's asymptotic lowest nonvanishing eigenvalue expression Eq. (5.25) as then $\omega_1 = \lambda_1$. Furthermore, for both $\xi, \xi_0 << 1$ with $\sigma = 0$ (i.e., zero anisotropy), the approximate equation (5.26) concurs with the known perturbation solution of the Fokker-Planck equation (5.1) for axial symmetry, Eq. (3.33) in Chapter 3 with appropriate changes of variables (see also Fig. 3.1(a)), namely,

$$M_\xi(\omega) = \frac{\xi_0}{3} - \frac{\xi_0^3}{45} - \frac{\xi_0 \xi^2}{180}\left(\frac{5}{1+\omega^2\tau_N^2} + \frac{1}{1+\omega^2\tau_N^2/9}\right) + \ldots . \qquad (5.27)$$

Here the first two terms on the right hand side constitute the expansion of the Langevin function in the dc field alone while the last term refers to the frequency-dependent combined effect of the strong dc and ac fields. Moreover, comparing Eq. (5.27) to Eq. (5.26), now $\omega_1 = \tau_N^{-1}$, where the free diffusion time τ_N is a characteristic time of the first rank relaxation function $\langle Y_{1,0} \rangle(t)$ (see Eq. (3.13)), while the frequency $\omega_2 = 3\tau_N^{-1}$ characterizes the contribution of the second rank relaxation function $\langle Y_{2,0} \rangle(t)$ (see Eq. (3.14)) to the dc magnetization.

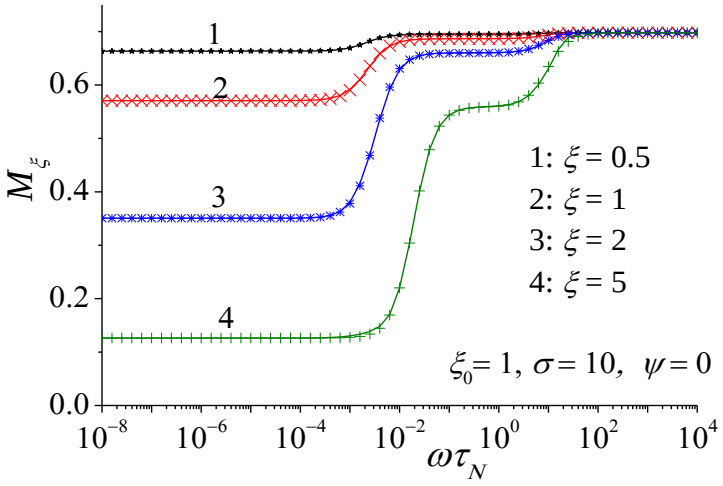

Fig. 5.3. DC magnetization M_ξ vs. normalized frequency $\omega\tau_N$ for $\sigma = 10$, $\xi_0 = 1$, and various values of the ac field amplitude ξ showing pronounced frequency-dependence including two distinct dispersion regions caused by entanglement of the dc and ac responses. Solid lines: exact matrix continued fraction solution, Eq. (5.11). Symbols: the approximate fitting equation (5.26).

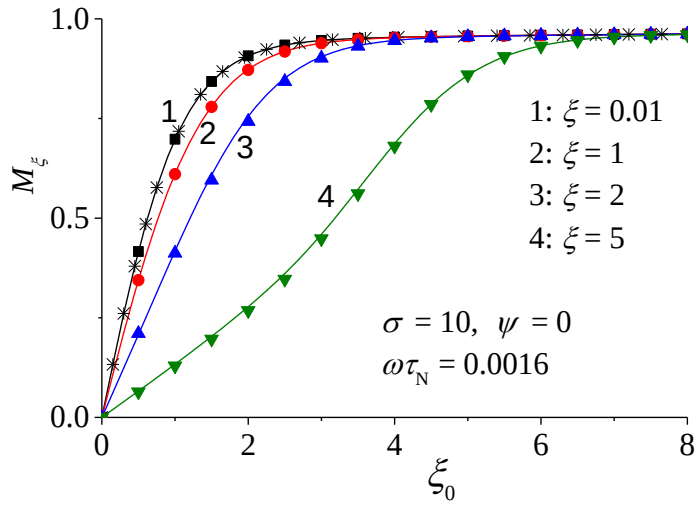

Fig. 5.4. DC magnetization M_ξ vs. dc field $\xi_0 = \nu\mu_0 M_S H_0 / (kT)$ for $\omega\tau_N = 0.0016$, $\sigma = 10$, and various values of the ac field ξ ($\xi = 0.01$ represents linear response conditions, where the ac and dc field responses do not entangle). Solid lines: exact matrix continued fraction solution, Eq. (5.11). Asterisks: the weak ac field solution rendered by Eq. (5.23). Other symbols: the approximate equation (5.26). All curves display more or less monotonic increase to the asymptotic value.

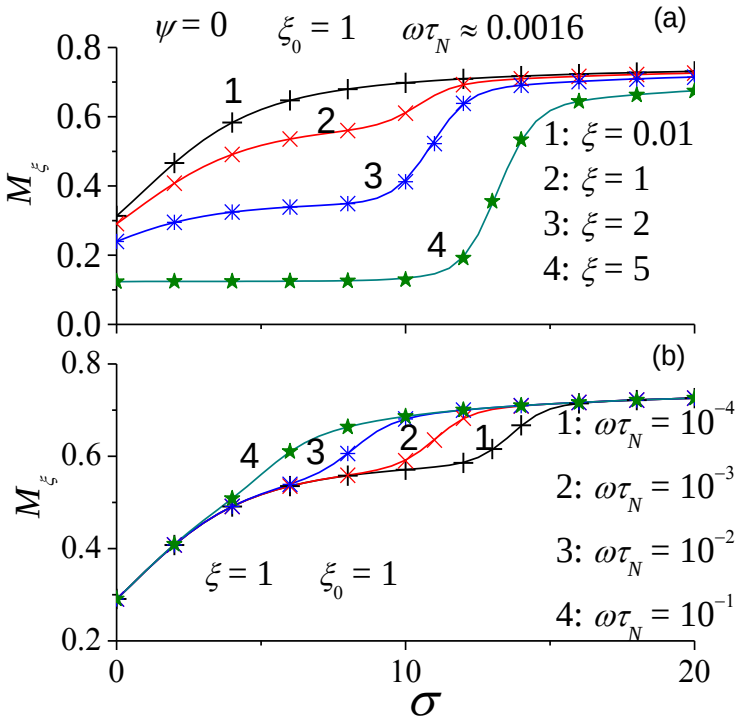

Fig. 5.5. DC magnetization M_ξ vs. inverse temperature parameter $\sigma = vK/(kT)$ with dc field parameter $\xi_0 = 1$ for various values of the ac parameter ξ at $\omega\tau_N = 0.0016$ (a) and for various values of $\omega\tau_N$ at $\xi = 1$ (b). Solid lines: exact matrix continued fraction solution, Eq. (5.11). Symbols: the approximate fitting equation (5.26). Notice the pronounced field strength and frequency dependence.

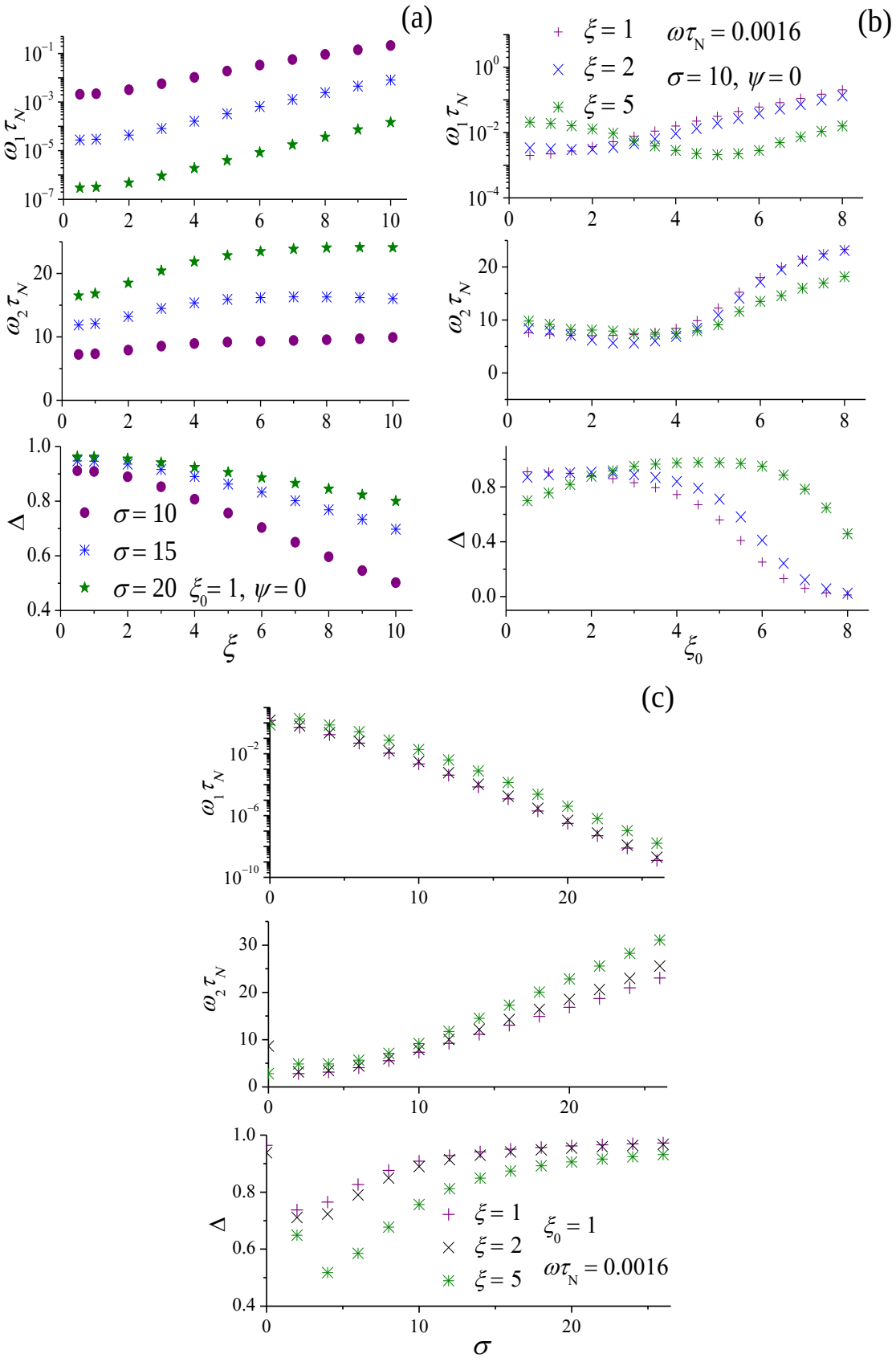

Fig. 5.6. Characteristic fitting parameters ω_1, ω_2, and Δ vs. (a) the ac field parameter ξ, (b) the dc field parameter ξ_0, and (c) the inverse temperature parameter σ. These parameter values were used in Fig. 5.3, Fig. 5.4 and Fig. 5.5.

5.4 DC Magnetization for $\psi \neq 0$

The results of Section 5.3 pertain to the case where both dc bias and ac fields are applied *parallel* to the easy axis of a uniaxial particle. Thus the inherent coupling between the longitudinal relaxational and transverse precessional modes implied by the magnetic Langevin equation (2.52) is automatically suppressed due to axial symmetry, where the orders $m \neq 0$ of the spherical harmonics in Eq. (5.3) are not involved. Hence the important precessional and mode coupling effects, which are present in nonaxially symmetric potentials, cannot be detected if one is so restricted. If, in contrast, the external fields are applied at an oblique angle ψ to the easy axis, so breaking the axial symmetry (meaning that the differential-recurrence relation (5.3) involves averages of spherical harmonics of different orders *m* besides those of different rank *l*), pronounced precessional and longitudinal mode coupling effects will occur in the frequency-dependent dc magnetization. These nonlinear frequency-dependent effects due to the loss of axial symmetry principally comprise a new high-frequency dispersion of resonant character in the vicinity of the frequency ω_{pr} of the ferromagnetic resonance (FMR), which also exhibits parametric resonance (see Fig. 5.7), and angular dependence of the dc magnetization curves (see Fig. 5.8). Both effects arise from the coupling of the slow thermally activated magnetization reversal mode with the fast precessional modes via the driving ac field acting in conjunction with the dc bias field, which is inherent in Eq. (5.3)

The high-frequency resonance dispersion in the spectrum of $M_{\xi}(\omega)$, originating in the excitation of transverse modes, having frequencies close to the precession frequency ω_{pr} of the magnetization, appears only at low damping and $\psi \neq 0$, i.e., when the axial symmetry is broken. In contrast, for axial symmetry $\psi = 0$, the high-frequency dispersion disappears altogether because the transverse modes no longer take part in the relaxation process (see Fig. 5.7 and Eq. (5.3)). Furthermore, just as with the nonlinear dynamic susceptibility for low damping [23], a subharmonic weak resonance dispersion appears at frequencies $\sim \omega_{pr}/2$ (Fig. 5.7), due to parametric resonance of the nonlinear oscillatory (precessional) motion of the magnetization $\mathbf{M}(t)$. In Fig. 5.7, the limiting values of $M_{\xi}(\omega)$ as $\omega \to 0$ and $\omega \to \infty$ are given by Eqs. (5.15) and (5.12), respectively. Notice that the appearance of a high-frequency dispersion region of resonant character is entirely consistent with the concept [1] of the role of the coupling between transverse and

longitudinal modes in the magnetization problem as being, in certain ways, analogous to that played by inertia in mechanical problems with separable and additive Hamiltonians [8, 93]. For example, in the escape rate problem for both mechanical and magnetic systems, the role of inertia and mode-coupling, respectively, is to give rise to the limiting cases of spatially and energy-controlled diffusion identified by Kramers [63] with a turnover region between them [94, 95]. This is true regardless of the fact that the physical origin of the various diffusion regimes is, in each case, entirely different. In the magnetic situation, the diffusion regimes spring from the lack of axial symmetry and so are geometric in origin, while in the mechanical one, they stem from including the inertia of the particles. However, the common feature that unites the two systems is that very similar differential-recurrence relations in the time domain are involved in both. For example, in the magnetic case, the recurrence relation is in the recurring numbers l and m of the spherical harmonics, while in the mechanical case, the recurrence relation is in the order n of the orthogonal Hermite polynomials, describing the variation of the phase space density function with momentum, while the second recurring number m is that associated with the variation of the phase space density function with position [1].

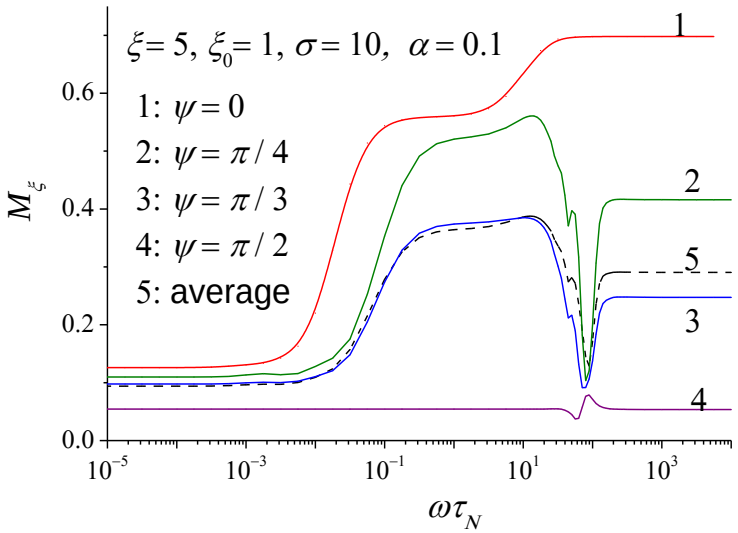

Fig. 5.7. DC magnetization M_ξ vs. normalized frequency $\omega\tau_N$ for $\sigma = 10$, $\xi_0 = 1$, $\xi = 5$, and various values of the oblique angle ψ between the bias field and easy axis showing pronounced frequency dependence, now comprising three distinct dispersion regions. Solid lines (1-4): exact matrix continued fraction solution, Eq. (5.11). Dashed line 5: the average dc magnetization $\overline{M_\xi}$ from Eq. (5.30) below. Notice the much weaker frequency dependence for a purely transverse applied field $\psi = \pi/2$.

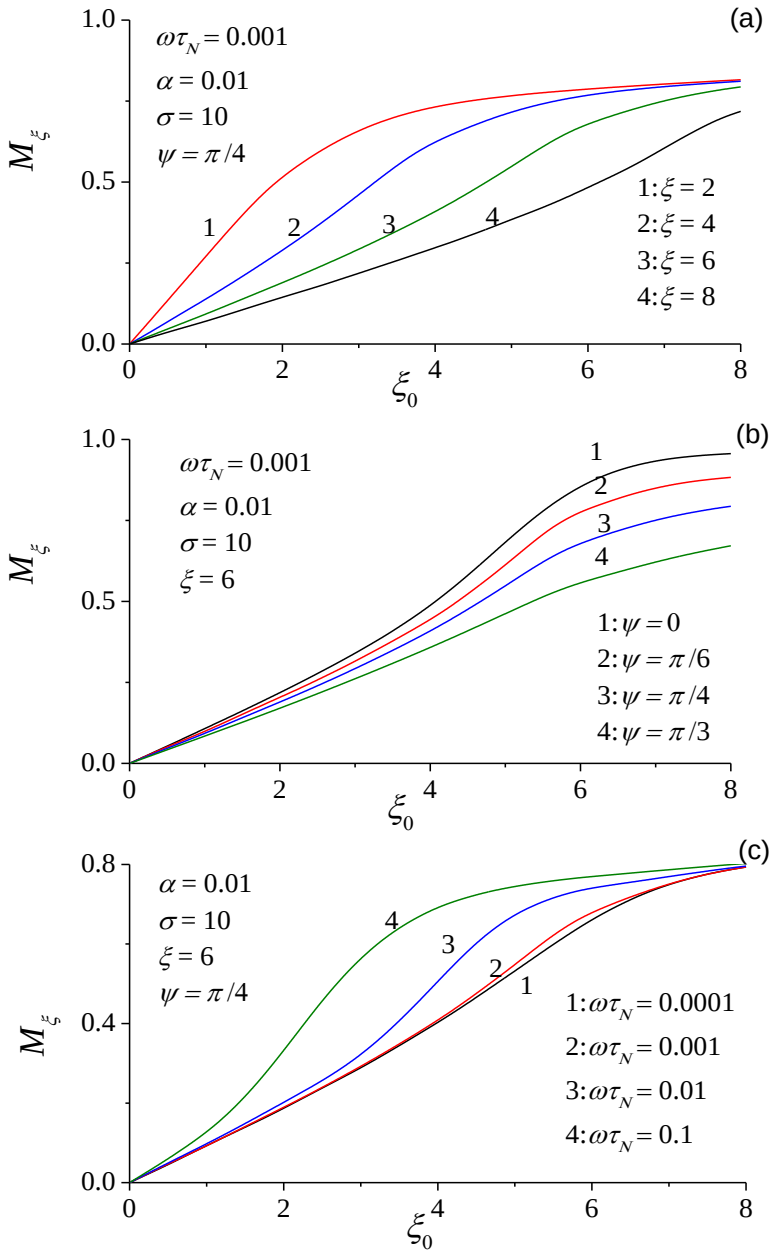

Fig. 5.8. M_ξ vs. normalized dc field $\xi_0 = vM_S H_0/(kT)$ for various values of the ac field amplitude ξ (a), oblique angles ψ (b), and normalized frequencies $\omega\tau_N$ (c).

For the oblique field configuration, just as with $\psi = 0$, the low-frequency dispersion of $M_\xi(\omega)$ is governed by slow barrier crossing relaxation modes with the characteristic frequency ω_1. Therefore, for relatively weak ac driving fields, $\xi << 1$, ω_1 may again be associated with the smallest nonvanishing eigenvalue λ_1 for the potential given by Eq. (5.2) with $\xi = 0$ as $\omega_1 = \lambda_1$. Now, the high barrier (or low temperature) asymptote for λ_1 for nonaxially symmetric potentials, valid for all damping regimes, has

been obtained by Coffey *et al.* [8, 93]. This was accomplished by extending the Kramers theory [63], as generalized by Mel'nikov and Meshkov [94, 95], of thermally activated escape of point particles over a potential barrier to the magnetization reversal, so as to include the turnover region between the transition state theory and the very low damping or energy-controlled diffusion regime (see Ref. [4] for a review of the application of Kramers theory to magnetic nanoparticles). Therefore, since in the weak ac field case we are effectively treating a *nonaxially symmetric* double-well potential with *nonequivalent* wells, as is evident from Eq. (5.2), λ_1 is formally given by [96]

$$\lambda_1(\sigma,\alpha,\xi_0,\psi) \sim \left(\Gamma_1^{IHD}+\Gamma_2^{IHD}\right)\frac{A(\alpha S_1)A(\alpha S_2)}{A(\alpha S_1+\alpha S_2)}. \tag{5.28}$$

Despite being *formally* similar to that for point particles, Eq. (5.28) is rooted in the lack of axial symmetry rather than in inertial effects. Here $A(\delta)$ and S_i are, respectively, the depopulation factor and the action calculated at the saddle point of the *i*th well, $\Gamma_i^{IHD}=\Omega_0\omega_i e^{-\Delta V_i}/\left(2\pi\omega_0\right)$ is the Kramers escape rate in the so-called intermediate-to-high damping (IHD) limit, where ΔV_i is the dimensionless barrier height, ω_i and ω_0 are the well and saddle angular frequencies, respectively, and Ω_0 is the damped saddle angular frequency. Explicit equations for all quantities appearing in the asymptotic smallest nonvanishing eigenvalue equation (5.28) are given in Refs. [4, 96]. The simple analytic equation (5.28) then allows one to accurately estimate [1] the damping dependence of the relaxation time of the magnetization for values of the angle ψ and the field parameter $h=\xi_0/(2\sigma)$ such that

$$h\sin\psi > 0.03 \text{ and } h < h_c(\psi)=\left(\cos^{2/3}\psi+\sin^{2/3}\psi\right)^{-3/2}. \tag{5.29}$$

5.5 DC Magnetization for Assemblies

All the previous frequency-dependent nonlinear dc response results concern either a *single* particle or an assembly of noninteracting particles with *aligned* easy axes. However, we can also calculate the dc magnetization $\overline{M_\xi}$ of an assembly of noninteracting uniaxial particles with *randomly* oriented easy axes, where the overbar denotes averaging over the angle ψ. Averaging over the particle easy axis orientations can be accomplished

numerically. In the calculation of $\overline{M_\xi}$ for randomly oriented easy axes using Gaussian quadratures [36], we only require [36]

$$\overline{M_\xi} = \int_0^{\pi/2} m_1^0(\omega,\psi)\sin\psi d\psi = \frac{\pi}{4}\sum_{i=1}^{n} w_i m_1^0(\omega,\psi_i)\sin\psi_i\,, \tag{5.30}$$

where

$$w_i = \frac{2(1-x_i^2)}{n^2\left[P_{n-1}(x_i)-x_iP_n(x_i)\right]^2}, \quad \psi_i = \frac{\pi}{4}(x_i+1),$$

and x_i is the ith root of the Legendre polynomial $P_n(x)$ (here we have noted that $m_1^0(\psi) = m_1^0(\pi-\psi)$) and the usual recursion relations for the Legendre polynomials [36] , e.g., Eq. (2.26), have been used.

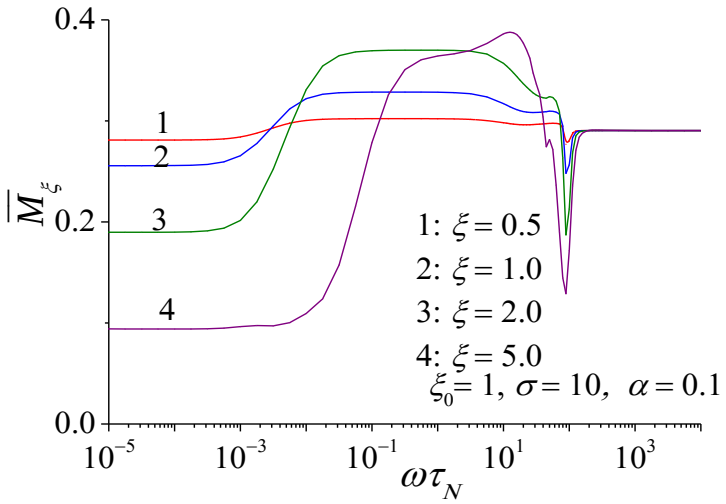

Fig. 5.9. Average dc magnetization $\overline{M_\xi}$ vs. normalized frequency $\omega\tau_N$ for $\sigma = 10$, $\alpha = 0.1$, $\xi_0 = 1$, and various values of the ac field amplitude ξ. Notice the parametric resonance behaviour in the high frequency dispersion in curve 4 (a subharmonic weak resonance dispersion at frequencies $\sim \omega_{pr}/2$).

First of all, referring to Fig. 5.7 alone, $\overline{M_\xi}$ of an assembly for noninteracting uniaxial particles with randomly oriented easy axes is compared with M_ξ for an individual particle as a function of the normalized frequency $\omega\tau_N$ for the particular values $\psi = 0$, $\pi/6$, $\pi/4$, and $\pi/2$. Here, three distinct dispersion bands again appear in the spectrum of $\overline{M_\xi}$, just as with the average dynamic susceptibility [1, 18]. In Fig. 5.9, plots

of $\overline{M_\xi}$ as a function of $\omega\tau_N$ for various values of the ac driving field amplitude ξ are shown. As seen in Fig. 5.9, with increasing ξ, the magnitude of the dispersion in the vicinity of the precession frequency ω_{pr} increases, showing pronounced nonlinear effects including parametric resonance.

5.6 Conclusion

We have treated the time-independent but frequency-dependent dc magnetization for an ensemble of fully aligned noninteracting particles, as well as that of an ensemble of particles with randomly oriented easy axes, driven by strong dc and ac fields using a nonperturbative approach. We have shown, owing to the coupling between the fast precession of the magnetization and its slow thermally activated reversal, that the *average* magnetization (with a strong ac field applied in conjunction with a strong dc bias field at an angle to the easy axis of the particle so that the axial symmetry is broken) is very sensitive to the ac field orientation, amplitude, and frequency. The influence of the field orientation and magnitude seems particularly obvious in retrospect by inspection of the equation of motion of an average spherical harmonic explicitly in the time domain, Eq. (5.3). All our calculations, since they are valid for ac fields of arbitrary strengths and orientations, allow one to predict and interpret quantitatively nonlinear phenomena in magnetic nanoparticles, where perturbation theory and the assumption that axial symmetry is preserved are no longer valid. In general, from a theoretical point of view, the nonlinear behaviour of the *frequency-dependent* dc component of the magnetization of nanomagnets driven by an ac external magnetic field closely resembles that of the frequency-dependent dc component of the dynamic Kerr effect in both polar liquids and liquid crystals [97, 98] insofar as it has a *frequency-dependent* dc response (e.g., Eq. (4.69)). A nonlinear frequency-dependent dc response due to the combined effect of strong ac and dc fields can also be observed in the dielectric response for noninteracting dipoles as considered in Chapter 3 (see Eq. (3.28)), as well as the dielectric response and Kerr effect for permanent dipoles in a mean-field potential, as considered in Chapter 4 (see Fig. 4.7). This is because, from a physical point of view, the stochastic magnetization dynamics of single-domain ferromagnetic particles (magnetic dipoles) in magnetic fields are analogous to the rotational Brownian motion of polar molecules (electric dipoles) in electric fields [1]. The results we have obtained suggest that the existing experimental measurements of nonlinear susceptibilities of fine particles, e.g., Refs. [88-90], should be repeated for the frequency-

dependent dc component of the magnetization in a strong bias-field configuration to show pronounced nonlinear effects which were not sufficiently investigated in previous measurements.

For simplicity, only uniaxial particles have been treated in this chapter. Particles with non-axially symmetric anisotropies (cubic, biaxial, etc.) can be considered in like manner. We have assumed throughout that all the particles are identical and that interparticle interactions are negligible. In order to account for polydispersity, it is necessary to average over the appropriate distribution function, e.g., over the particle volumes, cf. Ref. [75]. The assumption in the present model suggests that the results apply only to systems where interparticle interactions are ignored, such as individual nanoparticles and dilute solid suspensions of nanoparticles.

6 Conclusions

In this thesis, the nonlinear effects in the ac stationary response of both electric and magnetic dipoles are studied under the influence of combined ac and dc fields via the noninertial rotational diffusion model. In particular, the approximate analytical formulas are obtained using perturbation theory and the two-mode approximation. Additionaly, the matrix continued fraction methods to generate numerical solutions as the comparisons of analytical formulas are very useful. They can be used to determine the nonlinear ac stationary responses of electric and magnetic dipoles with an arbitrary anisotropy potential and subjected to a strong ac driving field superimposed on a strong dc bias field applied with a tilted angle from the easy axis. In the case of permanent electric dipoles in a symmetric potential, the perturbative matrix solution allows one to calculate numerically the nonlinear ac stationary responses in high dc fields using powerful matrix methods. Moreover, the generalisations of the results of the normal diffusion to the anomalous relaxation behaviour via the fractional diffusion equation have also been investigated.

In Chapter 3, we have emphasised the rectifying effect of a strong bias field superimposed on a strong ac field on the electric polarization (or magnetization) of an assembly of noninteracting dipolar particles. We suggested that experiments should be designed to detect the frequency-dependent dc nonlinear response introduced by the bias field, as well as the nonlinear fundamental and third harmonic frequency components (cf. Eq. (3.28)). Furthermore, we demonstrated how the anomalous nonlinear dielectric and magnetic relaxation can be treated using fractional kinetic equations (Eq.(3.34)). The results obtained can explain the anomalous nonlinear relaxation of complex dipolar systems, where the relaxation process is characterized by a broad distribution of relaxation times. Since the perturbation method of the calculation of nonlinear ac responses is quite general, we also applied this method to the calculation of the dynamic Kerr-effect ac response of polar and anisotropically polarizable molecules, and to nonlinear dielectric and Kerr-effect relaxation of molecules under the influence of a mean-field potential as considered in the next chapter.

In Chapter 4, we have developed two complementary approaches for treating the nonlinear ac stationary responses of permanent dipoles in a uniaxial mean field potential to any desired order in the ac field amplitude and for arbitrary dc field. The first is based

on perturbation theory, allowing one to calculate numerically the nonlinear ac stationary responses using powerful matrix methods, with results that agree with the independent numerical solution in Ref. [18] for weak ac fields, $\xi << 1$ (see Eqs. (4.19) - (4.21)). The second semi-analytic approach (see Eqs. (4.34), (4.27), (4.36) and (4.46)), based on the two-mode approximation [27, 40], effectively generalizes the existing analytic results for dipolar systems in superimposed ac and dc fields to a mean field potential. The results apply both to nonlinear dielectric relaxation and dynamic Kerr effect of nematics and also to magnetic birefringence relaxation of ferrofluids. However, the applicability of the rotational diffusion model in the mean field potential is restricted to the low-frequency range $(\omega\tau_D \leq 1)$, because the model does not include inertial effects. Furthermore, these methods can be applied (with small modifications) to the nonlinear magnetic response of uniaxial magnetic nanoparticles which are governed by equations very similar to the Smoluchowski equation used here. This motivates the investigation of the dc magnetization case discussed in the next chapter.

In Chapter 5, we have treated the time-independent but frequency-dependent dc component of the magnetization for an ensemble of fully aligned noninteracting particles, as well as that of an ensemble of particles with randomly oriented easy axes, driven by strong dc and ac fields using a nonperturbative approach. We have shown that, owing to the coupling between the fast precession of the magnetization and its slow thermally activated reversal, the *average* magnetization (with a strong ac field applied in conjunction with a strong dc bias field at an angle to the easy axis of the particle, so that the axial symmetry is broken) is very sensitive to both the ac field orientation, amplitude, and frequency. All our calculations, since they are valid for ac fields of arbitrary strengths and orientations, allow one to predict and interpret quantitatively nonlinear phenomena in magnetic nanoparticles, where perturbation theory and the assumption that axial symmetry is preserved are no longer valid. The results we have obtained suggest that experimental measurements of nonlinear susceptibilities of fine particles, e.g., Refs. [88-90], should be carried out to measure the frequency-dependent dc component of the magnetization in a strong bias-field configuration to show pronounced nonlinear effects. We also remark that similar nonlinear effects should be observed in the dc polarization of polar liquids in superimposed external dc bias and ac electric fields, because from a physical point of view the stochastic magnetization dynamics of single-domain ferromagnetic particles (magnetic dipoles) in magnetic fields is analogous to the rotational Brownian motion of

polar molecules (electric dipoles) in electric fields as we mentioned in Chapter 4. For simplicity, only uniaxial particles have been treated here. Particles with non-axially symmetric anisotropies (cubic, biaxial, etc.) can be considered in like manner. We have assumed throughout that all the particles are identical and that interparticle interactions are negligible. In order to account for polydispersity, it is necessary to average over the appropriate distribution function, e.g., over the particle volumes, cf. Ref. [75]. The assumptions in the present model suggests that the results apply only to systems, where interparticle interactions can be ignored, such as individual nanoparticles and dilute solid suspensions of nanoparticles.

The treatment of the dielectric and Kerr-effect responses studied in this thesis can be extended to include inertial effects using the Fokker-Planck equation for the probability density function in configuration-angular velocity space. The inertia corrected rotational diffusion model in the uniaxial potential was used in Ref. [85] to determine the linear complex dielectric susceptibility tensor of polar liquid crystals in the entire frequency range of orientational polarization (up to 5 THz). In the future, work can also be carried out on the calculations of nonstationary responses, inspired by the methods used here for the ac stationary response. Moreover, our model in this thesis only focuses on a simple uniaxial anisotropy potential where the amplitude of the potential is a constant. In order to accurately explain more complex systems, other mean-field potentials, e.g., time-dependent ones, should be taken into consideration, while our formulas may still be used as a starting point of the calculation.

7 References

[1] W.T. Coffey and Y.P. Kalmykov, *The Langevin Equation*, 3rd edition, World Scientific, Singapore, 2012.

[2] W.T. Coffey and B.V. Paranjape, Dielectric and Kerr Effect Relaxation in Alternating Electric Fields, *Proc. R. Ir. Acad., Sect. A.* **78**, 17-25 (1978).

[3] W. Coffey, D. Crothers, Y. Kalmykov, and P. Déjardin, Nonlinear response of permanent dipoles in a uniaxial potential to alternating fields, *Phys. Rev. E*. **71**, 062102 (2005).

[4] W.T. Coffey and Y.P. Kalmykov, Thermal fluctuations of magnetic nanoparticles: Fifty years after Brown, *J. Appl. Phys.* **112**, 121301 (2012).

[5] H. Risken, *The Fokker-Planck Equation*, 2nd edition, Springer-Verlag, Berlin 1989.

[6] W.F. Brown, Thermal Fluctuations of a Single-Domain Particle, *Phys. Rev.* **130**, 1677-1686 (1963).

[7] P. Debye, *Polar Molecules*, Chemical Catalog Co., New York, 1929.

[8] W.T. Coffey, D.A. Garanin, and D.J. McCarthy, Crossover formulae in the Kramers theory of thermally activated escape rates - application to spin systems, *Adv. Chem. Phys.* **117**, 483-765 (2001).

[9] A. Aharoni, *Introduction to the Theory of Ferromagnetism*, Clarendon Press, 2000.

[10] K. De Smet, L. Hellemans, J.F. Rouleau, R. Courteau, and T.K. Bose, Rotational relaxation of rigid dipolar molecules in nonlinear dielectric spectra, *Phys. Rev. E*. **57**, 1384-1387 (1998).

[11] P. Kdziora, J. Jadżyn, K. De Smet, and L. Hellemans, Nonlinear dielectric relaxation in non-interacting dipolar systems, *Chem. Phys. Lett.* **289**, 541-545 (1998).

[12] J.L. Déjardin and Y.P. Kalmykov, Nonlinear dielectric relaxation of polar molecules in a strong ac electric field: steady state response, *Phys. Rev. E*. **61**, 1211-1217 (2000).

[13] J.L. Déjardin and Y.P. Kalmykov, Steady state response of the nonlinear dielectric relaxation and birefringence in strong superimposed ac and dc bias electric fields: Polar and polarizable molecules, *J. Chem. Phys.* **112**, 2916-2923 (2000).

[14] J.L. Déjardin, G. Debiais, and A. Ouadjou, On the nonlinear behavior of dielectric relaxation in alternating fields. II. Analytic expressions of the nonlinear susceptibilities, *J. Chem. Phys.* **98**, 8149-8153 (1993).

[15] Y.P. Kalmykov and S.V. Titov, Matrix Elements of the System of Moment Equations Governing the Kinetics of Superparamagnetic Particles, *Phys. Rev. Lett.* **82**, 2967-2970 (1999).

[16] Y.L. Raikher and V.I. Stepanov, Dynamic hysteresis of a superparamagnetic nanoparticle at low-to-intermediate frequencies, *J. Magn. Magn. Mater*. **300**, e311-e314 (2006).

[17] Y.L. Raikher, V.I. Stepanov, and R. Perzynski, Dynamic hysteresis of a superparamagnetic nanoparticle, *Physica B: Condensed Matter*. **343**, 262-266 (2004).

[18] P.-M. Déjardin and Y.P. Kalmykov, Relaxation of the magnetization in uniaxial single-domain ferromagnetic particles driven by a strong ac magnetic field, *J. Appl. Phys.* **106**, 123908 (2009).

[19] J.L. García-Palacios and P. Svedlindh, Large Nonlinear Dynamical Response of Superparamagnets: Interplay between Precession and Thermoactivation in the Stochastic Landau-Lifshitz Equation, *Phys. Rev. Lett.* **85**, 3724-3727 (2000).

[20] I.S. Poperechny, Y.L. Raikher, and V.I. Stepanov, Dynamic magnetic hysteresis in single-domain particles with uniaxial anisotropy, *Phys. Rev. B.* **82**, 174423 (2010).

[21] H.E. Mrabti, S.V. Titov, P.-M. Déjardin, and Y.P. Kalmykov, Nonlinear stationary ac response of the magnetization of uniaxial superparamagnetic nanoparticles, *J. Appl. Phys.* **110**, 023901 (2011).

[22] G.T. Landi, Dynamic symmetry loss of high-frequency hysteresis loops in single-domain particles with uniaxial anisotropy, *J. Magn. Magn. Mater.* **324**, 466-470 (2012).

[23] S.V. Titov, P.-M. Déjardin, H. El Mrabti, and Y.P. Kalmykov, Nonlinear magnetization relaxation of superparamagnetic nanoparticles in superimposed ac and dc magnetic bias fields, *Phys. Rev. B.* **82**, 100413 (2010).

[24] I. Goychuk, Anomalous relaxation and dielectric response, *Phys. Rev. E*. **76**, 040102 (2007).

[25] W.T. Coffey, Y.P. Kalmykov, and S.V. Titov, Fractional Rotational Diffusion and Anomalous Dielectric Relaxation in Dipole Systems, *Adv. Chem. Phys.* **133B**, 285-437 (2006).

[26] W.T. Coffey, Y.P. Kalmykov, and S.V. Titov, Anomalous nonlinear dielectric and Kerr effect relaxation steady state responses in superimposed ac and dc electric fields, *J. Chem. Phys.* **126**, 084502 (2007).

[27] W.T. Coffey, Y.P. Kalmykov, and N. Wei, Nonlinear normal and anomalous response of non-interacting electric and magnetic dipoles subjected to strong AC and DC bias fields, *Nonlinear Dyn*. **80**, 1861-1867 (2015).

[28] N. Wei, P.-M. Déjardin, Y.P. Kalmykov, and W.T. Coffey, External dc bias-field effects in the nonlinear ac stationary response of dipolar particles in a mean-field potential, *Phys. Rev. E*. **93**, 042208 (2016).

[29] W. Brown, Jr., Thermal fluctuations of fine ferromagnetic particles, *IEEE Trans. Mag.* . **15**, 1196-1208 (1979).

[30] N. Wei, D. Byrne, W.T. Coffey, Y.P. Kalmykov, and S.V. Titov, Nonlinear frequency-dependent effects in the dc magnetization of uniaxial magnetic

nanoparticles in superimposed strong alternating current and direct current fields, *J. Appl. Phys.* **116**, 173903 (2014).

[31] J.T. Lewis, J.R. McConnell, and B.K.P. Scaife, Relaxation effects in rotational Brownian motion, *Proc. R. Ir. Acad. A.* **76**, 43-69 (1976).

[32] M. Abramowitz and I.A. Stegun, *Handbook of Mathematical Functions: with Formulas, Graphs, and Mathematical Tables*, Dover Publications, 2012.

[33] P.M. Déjardin, Y.P. Kalmykov, B.E. Kashevsky, H. El Mrabti, I.S. Poperechny, Y.L. Raikher, and S.V. Titov, Effect of a dc bias field on the dynamic hysteresis of single-domain ferromagnetic particles, *J. Appl. Phys.* **107**, 073914 (2010).

[34] E.C. Stoner and E.P. Wohlfarth, A Mechanism of Magnetic Hysteresis in Heterogeneous Alloys, *Philosophical Transactions of the Royal Society of London A: Mathematical, Physical and Engineering Sciences*. **240**, 599-642 (1948).

[35] D.J. Griffiths, *Introduction to Quantum Mechanics*, Pearson, 2013.

[36] D.A. Varshalovich, A.N. Moskalev, and V.K. Khersonskii, *Quantum Theory of Angular Momentum*, World Scientific Pub., 1988.

[37] Y.P. Kalmykov, W.T. Coffey, and S.V. Titov, Analytic calculation of the longitudinal dynamic susceptibility of uniaxial superparamagnetic particles in a strong uniform DC magnetic field, *J. Magn. Magn. Mater.* **265**, 44-53 (2003).

[38] A. Morita and H. Watanabe, Nonlinear response and its behavior in transient and stationary processes, *Phys. Rev. A.* **35**, 2690-2696 (1987).

[39] A. Morita, Theory of nonlinear response, *Phys. Rev. A.* **34**, 1499-1504 (1986).

[40] D.A. Garanin, Integral relaxation time of single-domain ferromagnetic particles, *Phys. Rev. E*. **54**, 3250-3256 (1996).

[41] S. Havriliak and S. Negami, A complex plane representation of dielectric and mechanical relaxation processes in some polymers, *Polymer*. **8**, 161-210 (1967).

[42] K.S. Cole and R.H. Cole, Dispersion and Absorption in Dielectrics I. Alternating Current Characteristics, *J. Chem. Phys.* **9**, 341-351 (1941).

[43] D.W. Davidson and R.H. Cole, Dielectric Relaxation in Glycerol, Propylene Glycol, and n‐Propanol, *J. Chem. Phys.* **19**, 1484-1490 (1951).

[44] R. Metzler and J. Klafter, The random walk's guide to anomalous diffusion: a fractional dynamics approach, *Physics Reports*. **339**, 1-77 (2000).

[45] V.V. Novikov and V.P. Privalko, Temporal fractal model for the anomalous dielectric relaxation of inhomogeneous media with chaotic structure, *Phys. Rev. E*. **64**, 031504 (2001).

[46] W.T. Coffey, Y.P. Kalmykov, and S.V. Titov, Anomalous dielectric relaxation in the context of the Debye model of noninertial rotational diffusion, *J. Chem. Phys.* **116**, 6422-6426 (2002).

[47] Y.P. Kalmykov, W.T. Coffey, D.S.F. Crothers, and S.V. Titov, Microscopic models for dielectric relaxation in disordered systems, *Phys. Rev. E*. **70**, 041103 (2004).

[48] H. Fröhlich, *Theory of dielectrics : dielectric constant and dielectric loss*, Clarendon Press, Oxford, 1958.

[49] R.R. Nigmatullin and Y.A. Ryabov, Cole–Davidson dielectric relaxation and self-similar relaxation process, *Phys. Solid State*. **39**, 87-90 (1997).

[50] H. Watanabe and A. Morita, Kerr effect relaxation in high electric fields, *Adv. Chem. Phys.* **56**, 255 (1984).

[51] A. Morita, On nonlinear dielectric relaxation, *J. Phys. D: Appl. Phys.* **11**, 1357-1367 (1978).

[52] C. Crauste-Thibierge, C. Brun, F. Ladieu, D. L'Hôte, G. Biroli, and J.P. Bouchaud, Evidence of Growing Spatial Correlations at the Glass Transition from Nonlinear Response Experiments, *Phys. Rev. Lett.* **104**, 165703 (2010).

[53] F. Takeo, T. Masahiro, N. Kenji, and S. Iwao, Nonlinear Dielectric Relaxations in a Vinylidene Cyanide / Vinyl Acetate Copolymer, *Jpn. J. Appl. Phys.* **27**, 200-204 (1988).

[54] C. Brun, F. Ladieu, D. L'Hôte, M. Tarzia, G. Biroli, and J.P. Bouchaud, Nonlinear dielectric susceptibilities: Accurate determination of the growing correlation volume in a supercooled liquid, *Phys. Rev. B.* **84**, 104204 (2011).

[55] H. Block and E.F. Hayes, Dielectric behaviour of stiff polymers in solution when subjected to high voltage gradients, *Trans. Faraday Society*. **66**, 2512-2525 (1970).

[56] J. Jadzyn, P. Kędziora, and L. Hellemans, Frequency dependence of the nonlinear dielectric effect in diluted dipolar solutions, *Phys. Lett. A.* **251**, 49-53 (1999).

[57] P. Kdziora, J. Jadżyn, K. DeSmet, and L. Hellemans, Linear and nonlinear dipolar relaxation of 4,4′ -n-hexylcyanobiphenyl, *J. Mol. Liq.* **80**, 19-25 (1999).

[58] R.B. Jones, Transient and steady linear response of dielectric particles in a high bias field subject to a weak AC probe field, *J. Phys.: Condens. Matter*. **14**, 7719-7736 (2002).

[59] B.U. Felderhof and R.B. Jones, Mean field theory of the nonlinear response of an interacting dipolar system with rotational diffusion to an oscillating field, *J. Phys.: Condens. Matter*. **15**, 4011-4024 (2003).

[60] B.U. Felderhof and R.B. Jones, Nonlinear response of a dipolar system with rotational diffusion to an oscillating field, *J. Phys.: Condens. Matter*. **15**, S1363-S1378 (2003).

[61] P.C. Fannin, B.K.P. Scaife, and S.W. Charles, A study of the complex ac susceptibility of magnetic fluids subjected to a constant polarizing magnetic field, *J. Magn. Magn. Mater.* **85**, 54-56 (1990).

[62] P.C. Fannin and A.T. Giannitsis, Investigation of the field dependence of magnetic fluids exhibiting aggregation, *J. Mol. Liq.* **114**, 89-96 (2004).

[63] H.A. Kramers, Brownian motion in a field of force and the diffusion model of chemical reactions, *Physica*. **7**, 284-304 (1940).

[64] G.B. Arfken, H.J. Weber, and F.E. Harris, *Mathematical Methods for Physicists: A Comprehensive Guide*, Elsevier, 2012.

[65] R.L. Fulton, On the theory of nonlinear dielectrics, *J. Chem. Phys.* **78**, 6865-6876 (1983).

[66] P.C. Fannin, S.W. Charles, C. Mac Oireachtaigh, and S. Odenbach, Investigation of possible hysteresis effects arising from frequency- and field-dependent complex susceptibility measurements of magnetic fluids, *J. Magn. Magn. Mater.* **302**, 147-152 (2006).

[67] W.T. Coffey, D.S.F. Crothers, and Y.P. Kalmykov, Nonlinear response of permanent dipoles in a mean-field potential to alternating fields, *J. Non·Cryst. Solids*. **352**, 4710-4717 (2006).

[68] P.M. Déjardin and F. Ladieu, Nonlinear susceptibilities of interacting polar molecules in the self-consistent field approximation, *J. Chem. Phys.* **140**, 034506 (2014).

[69] P.-M. Déjardin, Magnetic relaxation of a system of superparamagnetic particles weakly coupled by dipole-dipole interactions, *J. Appl. Phys.* **110**, 113921 (2011).

[70] A. Kozak, J.K. Moscicki, and G. Williams, On Dielectric Relaxation in Liquid Crystals, *Mol. Cryst. Liq. Cryst.* **201**, 1-12 (1991).

[71] W.T. Coffey, D.S.F. Crothers, Y.P. Kalmykov, and J.T. Waldron, Exact solution for the extended Debye theory of dielectric relaxation of nematic liquid crystals, *Physica A: Statistical Mechanics and its Applications*. **213**, 551-575 (1995).

[72] W.T. Coffey and Y.P. Kalmykov, Rotational Diffusion and Dielectric Relaxation in Nematic Liquid Crystals, *Adv. Chem. Phys.*, 487-551 (2007).

[73] S. Urban, B. Gestblom, W. Kuczynski, S. Pawlus, and A. Wurflinger, Nematic order parameter as determined from dielectric relaxation data and other methods, *PCCP*. **5**, 924-928 (2003).

[74] K. Merkel, A. Kocot, J.K. Vij, G.H. Mehl, and T. Meyer, Orientational order and dynamics of the dendritic liquid crystal organo-siloxane tetrapodes determined using dielectric spectroscopy, *Phys. Rev. E*. **73**, 051702 (2006).

[75] Y.L. Raikher and V.I. Stepanov, Nonlinear Dynamic Susceptibilities and Field-Induced Birefringence in Magnetic Particle Assemblies, *Adv. Chem. Phys.* **129**, 419-588 (2004).

[76] D. L'Hôte, R. Tourbot, F. Ladieu, and P. Gadige, Control parameter for the glass transition of glycerol evidenced by the static-field-induced nonlinear response, *Phys. Rev. B.* **90**, 104202 (2014).

[77] F. Ladieu, C. Brun, and D. L'Hôte, Nonlinear dielectric susceptibilities in supercooled liquids: A toy model, *Phys. Rev. B.* **85**, 184207 (2012).

[78] R. Kubo, M. Toda, and N. Hashitsume, *Statistical Physics II, Non-Equilibrium Statistical Mechanics*, 2nd edition, Springer-Verlag, Berlin, 1991.

[79] M. Schadt, Kerr effect and orientation relaxation of pretransitional domains and individual molecules in positive dielectric liquid crystals, *J. Chem. Phys.* **67**, 210-216 (1977).

[80] M.W. Evans, Computer simulation of some field-induced phenomena of molecular liquids, *J. Mol. Liq.* **26**, 49-61 (1983).

[81] M.X. Fernandes and J.G. de la Torre, Brownian Dynamics Simulation of Rigid Particles of Arbitrary Shape in External Fields, *Biophys. J.* **83**, 3039-3048 (2002).

[82] J. García de la Torre, Dynamic electro-optic properties of macromolecules and nanoparticles in solution: A review of computational and simulation methodologies, *Colloids and Surfaces B: Biointerfaces*. **56**, 4-15 (2007).

[83] T.R. Evensen, S.N. Naess, and A. Elgsaeter, Use of the Rotation Vector in Brownian Dynamics Simulation of Transient Electro-Optical Properties, *Macromol. Theory Simul.* **18**, 50-60 (2009).

[84] E. Wandersman, V. Dupuis, E. Dubois, and R. Perzynski, Rotational dynamics and aging in a magnetic colloidal glass, *Phys. Rev. E.* **80**, 041504 (2009).

[85] Y.P. Kalmykov, S.V. Titov, and W.T. Coffey, Inertial and bias effects in the rotational Brownian motion of rodlike molecules in a uniaxial potential, *J. Chem. Phys.* **134**, 044530 (2011).

[86] A.P. Guimarães, *Principles of Nanomagnetism*, Springer Berlin Heidelberg, 2009.

[87] Q.A. Pankhurst, N.T.K. Thanh, S.K. Jones, and J. Dobson, Progress in applications of magnetic nanoparticles in biomedicine, *J. Phys. D: Appl. Phys.* **42**, 224001 (2009).

[88] T. Bitoh, K. Ohba, M. Takamatsu, T. Shirane, and S. Chikazawa, Comparative study of linear and nonlinear susceptibilities of fine-particle and spin-glass systems: quantitative analysis based on the superparamagnetic blocking model, *J. Magn. Magn. Mater.* **154**, 59-65 (1996).

[89] P. Jönsson, T. Jonsson, J.L. García-Palacios, and P. Svedlindh, Nonlinear dynamic susceptibilities of interacting and noninteracting magnetic nanoparticles, *J. Magn. Magn. Mater.* **222**, 219-226 (2000).

[90] L. Spinu, D. Fiorani, H. Srikanth, F. Lucari, F. D'Orazio, E. Tronc, and M. Noguès, Dynamic studies of γ-Fe2O3 nanoparticle systems, *J. Magn. Magn. Mater.* **226–230, Part 2**, 1927-1929 (2001).

[91] Y.L. Raikher, V.I. Stepanov, A.N. Grigorenko, and P.I. Nikitin, Nonlinear magnetic stochastic resonance: Noise-strength-constant-force diagrams, *Phys. Rev. E*. **56**, 6400-6409 (1997).

[92] G. Bertotti, I.D. Mayergoyz, C. Serpico, M. d'Aquino, and R. Bonin, Nonlinear-dynamical-system approach to microwave-assisted magnetization dynamics (invited), *J. Appl. Phys.* **105**, 07B712 (2009).

[93] P.M. Déjardin, D.S.F. Crothers, W.T. Coffey, and D.J. McCarthy, Interpolation formula between very low and intermediate-to-high damping Kramers escape rates for single-domain ferromagnetic particles, *Phys. Rev. E*. **63**, 021102 (2001).

[94] V.I. Mel'nikov, The Kramers problem: Fifty years of development, *Physics Reports*. **209**, 1-71 (1991).

[95] V.I. Mel'nikov and S.V. Meshkov, Theory of activated rate processes: Exact solution of the Kramers problem, *J. Chem. Phys.* **85**, 1018-1027 (1986).

[96] Y.P. Kalmykov, The relaxation time of the magnetization of uniaxial single-domain ferromagnetic particles in the presence of a uniform magnetic field, *J. Appl. Phys.* **96**, 1138-1145 (2004).

[97] G.B. Thurston and D.I. Bowling, The frequency dependence of the Kerr effect for suspensions of rigid particles, *J. Coll. Interface Sci.* **30**, 34-45 (1969).

[98] K. Hosokawa, T. Shimomura, H. Frusawa, Y. Kimura, K. Ito, and R. Hayakawa, Two-dimensional spectroscopy of electric birefringence relaxation in frequency domain: Measurement method for second-order nonlinear after-effect function, *J. Chem. Phys.* **110**, 4101-4108 (1999).